HAMILTONIAN FORMULATION FOR SINGLE/FEW PHOTON DETECTION

by

SAUMYA BISWAS

A DISSERTATION

Presented to the Department of Physics
and the Division of Graduate Studies of the University of Oregon
in partial fulfillment of the requirements
for the degree of
Doctor of Philosophy

December 2021

DISSERTATION APPROVAL PAGE

Student: Saumya Biswas

Title: Hamiltonian Formulation for Single/Few Photon Detection

This dissertation has been accepted and approved in partial fulfillment of the requirements for the Doctor of Philosophy degree in the Department of Physics by:

Jens Noeckel	Chairperson
Steven J van Enk	Advisor
Jayson Paulose	Core Member
Brittany Erickson	Institutional Representative

and

Krista Chronister	Vice Provost for Graduate Studies

Original approval signatures are on file with the University of Oregon Division of Graduate Studies.

Degree awarded December 2021

DISSERTATION ABSTRACT

Saumya Biswas

Doctor of Philosophy

Department of Physics

December 2021

Title: Hamiltonian Formulation for Single/Few Photon Detection

Fully quantum mechanical models for device models of single photon detectors have recently been developed. Detection of single/few photons in both inanimate devices and biological eyes have the universal structure of absorption, amplification and measurement stages. Previous models succeeded in developing definite models for all stages but the amplification stage. We write out explicit Hamiltonians that can describe such irreversible changes and also measurement induced decoherence. The time evolutions created by these Hamiltonians are solved in the discrete part of the Hilbert space and the desired dynamics are verified. Previous proposals of minimum noise amplification schemes are completed with specific Hamiltonians presented in this dissertation. A new kind of problem where a molecule absorbs two photons sequentially is investigated. The proposed Hamiltonian method is matched with a classic method in the field called

"generalized density matrix operator method" to calculate the probabilities for such sequential absorption of photons.

This dissertation contains previously published and unpublished material.

CURRICULUM VITAE

NAME OF AUTHOR: Saumya Biswas

GRADUATE AND UNDERGRADUATE SCHOOLS ATTENDED:
> University of Oregon, Eugene, Oregon
> University of California, Riverside, California
> Bangladesh University of Engineering and Technology, Dhaka, Bangladesh

DEGREES AWARDED:
> Doctor of Philosophy, 2021, University of Oregon
> Master of Science, 2019, University of Oregon
> Master of Science, 2016, University of California Riverside
> Bachelor of Science, 2012, Bangladesh University of Engineering and
>   Technology, Dhaka, Bangladesh

AREAS OF SPECIAL INTEREST:
> Theoretical Atomic, Molecular and Optical Physics, Condensed Matter
>   Physics, and Quantum Information Theory

PROFESSIONAL EXPERIENCE:

> Graduate Teaching/Research Assistant, University of California Riverside,
>   2013-2017

> Graduate Employee, University of Oregon, 2017-2021

> Summer Intern, NumFocus/QuTiP (Google Summer of Code'19),
>   Summer'2019

GRANTS, AWARDS AND HONORS:

> Emanuel Optical, Molecular, and Quantum Sciences Scholarship,
>   Summer'2021, University of Oregon

> Jhamandas Watumull Scholarship, University of Oregon, 2018-19

> Dean's Distinguished Fellowship, University of California Riverside, 2013-14

> Dean's List, Level-2,3,4; Bangladesh University of Engineering and
>   Technology

PUBLICATIONS:

Biswas, Saumya, and S. J. van Enk. "Heisenberg picture of photodetection." Physical Review A 102.3 (2020): 033705.

Biswas, Saumya, and S. J. van Enk. "Detecting two photons with one molecule." Physical Review A 104 (2021): 043703.

ACKNOWLEDGEMENTS

I dedicate this dissertation to my parents.

TABLE OF CONTENTS

Chapter   Page

LIST OF FIGURES

LIST OF TABLES

CHAPTER I

INTRODUCTION

> Everything we call real is made of
> things that cannot be regarded as
> real.
> If quantum mechanics hasn't
> profoundly shocked you, you
> haven't understood it yet.
>
> ——————————————————
>   Niels Bohr

> Are not rays of light very small
> bodies emitted from shining
> substances?
>
> ——————————————————
>   Sir Isaac Newton

1.1. Overview and Glossary

Chapter 1 explains the motivation behind writing the entire photodetection process with the help of a Hamiltonian. The discussion has been kept mostly nontechnical.

Chapter 2 reviews some of the theoretical formalisms used in the dissertation. The discussion is technical and is helpful for a smooth read of chapter 3 and 4.

Chapter 3 presents a simple Hamiltonian that embodies the physics of a typical single photon detector in its entirety. The evolution problem is solved in the Heisenberg picture for elucidation of the magnitude of gain and noise.

Chapter 4 presents the problem of two photon detection with one absorber molecule.

Chapter 5 presents some novel schemes for amplifying weak signals, computations of operator evolution in Heisenberg picture with time dependent Hamiltonians.

Appendix A discusses the general structure of an operator evolution in the Heisenberg picture. Appendix B discusses further Hamiltonian models that can facilitate amplification and connect with available measurement theories.

A glossary of terms is presented in the table 1.1 that are not necessarily technical, but have special meanings in the context of single photon detection.

1.2. What happens in a quantum measurement?

The trademark of nature's departure from classical behaviour is undoubtedly quantum superposition. Our perception or knowledge of the physical world is subject to the measurement induced wavefunction collapse. Knowledge is limited to the instant of measurement. And the quantum world meets the classical one through the measurement. Erwin Schrödinger's gedanken experiment of a cat simultaneously alive and dead inside a box is a cliché, far too well known to be repeated here. It has invited interesting accounts from physicists and authors in the field. Maximilian Schlosshauer ([2]) in his book "Decoherence: and the quantum-to-classical transition", writes "no other example has illustrated this problem of the quantum-to-classical transition more poignantly and drastically than Schrödinger's infamous cat, which appears, by the verdict of quantum theory, to be doomed into a netherworldy superposition of being alive and dead". It is widely accepted that measurement yields classical readout results from a

Term	Meaning
Amplification (non-unitary)	The irreversible growth of a microscopic signal into a classical macroscopic signal.
Amplification (unitary quantum amplification)	The unitary evolution (between final and initial time) equation for a quantum mechanical "signal" operator where it is magnified by some gain and corrupted by the addition of noise operators during the evolution.
Continuous measurement	Monitoring of the "meter" through a coupling to a bath of large degrees of freedom. Information flows from the "meter" to the bath.
Continuum	Solutions of the Schrödinger equation (without any imposed boundaries) that carry a nonzero probability current are continuum states.
Decay Rate	The uniform (Markovian) coupling of discrete states to the continuum. The rate at which a discrete state decays into a continuum.
Discrete State	Solutions of the Schrödinger equation confined by a boundary (higher potential than energy eigenvalue) that carry zero probability current.
Electron Shelving	A method where macroscopic fluorescence is created with laser from a molecule when it is in a particular state (shelving state).
Filtering (frequency)	Sifting through the optical scatterers. Reflection and transmission coefficient dictates whether a particular frequency of electromagnetic wave passes through or not.
Minimum noise amplification	Quantum mechanical amplification of an operator with addition of minimal noise [1].
POVM	Positive Operator Valued Measure: A set of operators that completely specify a quantum measurement process.
Reflection coefficient	Ratio of the reflected probability current and incident probability current by a scatterer.
Shelving state	The particular state of the absorber molecule that drives the amplification mechanism.

TABLE 1.1. Glossary of terms.

quantum observable. The dephasing that follows through measurement eats away the quantum attributes of a system and can render the state completely classical. Since any measurement device we use such as a photodetector can itself be considered a quantum object, it is in turn performed a measurement on by the circuity it has. The circuitry, in turn, is measured by the dial or display of the device and our eyes perform a measurement of the dial/display. This series or chain of measurement devices is referred to as the "von Neumann chain" and we can cut it off ("Heisenberg's cut") at the final link (of our choice) to the measurement device whose measurement readout we consider to be classical. The chain can extend at best to the human mind which records the information gained from neurological impulses from our eyes. A subsequent observer cannot be imagined which can find our brain to be in a quantum superposition state. Human consciousness is not subject to quantum superposition ambiguity, our minds have an unambiguous idea about what we saw, and no subsequent observer can be defined that measures our brains. Human consciousness is unique in a world of quantum objects since it can possess classical knowledge and make up its "mind" about some observed quantity. Physicist Sean Carroll finds it quite remarkable, "We are part of the universe that has developed a remarkable ability: We can hold an image of the world in our minds. We are matter contemplating itself." Since measurement process always ends with a human mind learning some new numbers or images, consciousness based quantum measurement theories have been propounded. Eugene Wigner, a pioneer of consciousness based quantum measurement theories adds a twist to the Schrödinger's cat experiment. Dubbed as "Wigner's friend" experiment, the cat is replaced by a (lady)friend of Wigner who is asked upon opening the box if at a given point in time, the vial was intact

4

or broken. In her mind, she has no doubts about one certain state of the vial at that point in time (and she will relay that) and we cannot agree with the idea of the vial being in a superposition state prior to opening the box anymore.

The separateness of soul/mind/consciousness from the physical world gives rare common ground to major religions and scientific minds. In fact, the validation or confirmation of some observational fact (such as the Moon orbits our planet Earth) is not made until some human mind observed and recorded the information. It is the inspiration behind Einstein's famous quip, " Is the moon there when nobody looks?". In fact, some thinkers have invoked "God" or an omnipresent observer with eyes set on all of the universe for the continuation of matter left unobserved by all humans at any given point in time. In certain quantum information theories, laws of physics are valid for all of the universe but the assumed non-physical human consciousness. The other extreme theory uses many worlds interpretation to preserve the universality of physical laws at the expense of branching out of universes at every single measurement event that happens. See ref. [3] for a comprehensive overview.

If we are dead set on preserving the universality of quantum laws and are economical about the number of universes (many world theoy is a little extravagant in terms of necessary number of universes), we need a closer look on why the measuring device can produce classical results measuring a quantum observable/system and are themselves somewhat distinct from the quantum system under study. Firstly, a measurement device like galvanometer is made up of a massive number of atoms (and in turn subatomic particles) whereas quantum systems are typically a few atoms (or photons or some other particles) at most. Secondly, the working principle of a measurement device can be explained

with classical laws exclusively (laws of electromagnetism for a galvanometer for example). A proposition called "spontaneous collapse" has been used in some theories to describe the collapse of the superposition when a macroscopic object is used in the measurement chain or von Neumann chain. Despite being explainable by macroscopic classical rule, the origin of the behaviour of a macroscopic object can come from microscopic components. The bulk ("classical") resistances of metals and insulators are to be calculated from microscopic quantum mechanical description of band theories. The heat conductivity or capacity is also calculated from microscopic quantum mechanical models before the values can be used in classical laws. Therefore in a sense, macroscopic objects are quantum mechanical as well. How could they be different from the few atom quantum system we investigate?

One possible answer is the presence of cooperative/collective motion of a large number of particles that indicate the measurement result. The pointer that moves across the dial in a galvanometer is made up of an enormous number of atoms which move in unison that human eye can observe. The "avalanche" of particles in a avalanche photodiode is also a collective motion of a massive number of particles. Does such cooperative/collective motion result in a collape of quantum superposition spontaneously? Although macroscopic quantum states have been realized in superposition, no confirmation of spontaneous collapse of collective states like superconducting current (in Superconducting Quantum Interference Devices (SQUIDS)) has ever been observed. However, it is yet not possible to rule out the spontaneous collapse theory [3].

To distinguish between a quantum process (reversible) and measurement process (seems to be irreversible), a third category of theory distinguishes

between the quantum systems isolated from external disturbance and quantum systems affected by thermal noise. It also requires the mechanism for a collapse, where some of the measurement outcome would be actualised. If a detector or measurement device is coupled to external degrees of freedom, it can make a tangible measurement record like with a flash of light, pulse or current or movement of a pointer. This will be a "measurement process". If it does couple to numerous degrees of freedom, there is a minuscule chance of avoiding making a mark, some telling sign of some change is almost guaranteed. In an effort to not leave a mark, in an experiment, horizontal/vertical polarized photon may pass through a H/V polariser and the record and everything associated with it may be erased and the photon may be reconstructed in the original state; only we know doing this is prohibitively difficult if not impossible, so postulating it to be impossible is not illogical. So, a quantum process is reversible, but measurement process is absolutely irreversible.

And we need not look hard to find theories of irreversibility, since thermodynamics pre-dates quantum mechanics by years. Irreversibility is predicted to occur with high likelihood by the second law of thermodynamics in the relevant timescale. There also exists the ergodic principle which predicts that a thermodynamic system touches upon every possible (allowed by conservation laws) configurations if left to evolve on itself. Therefore there will be recurrences of any given configuration after waiting long enough times– a phenomena known as Poincaré recurrence. The postulate that works for quantum measurement problem now becomes one that assumes ergodic principle is incorrect and Poincaré recurrence does not occur. Important distinctions between reversible quantum processes and irreversible quantum measurements were discussed by Ilya Prigogine.

It is well known that future dynamics of a system can be very sensitive to small changes in the initial conditions, which is referred to as "strong mixing". Prigogine solves the measurement problem with the basic idea that a measurement chain is broken whenever strong mixing is involved and the second law takes precedence over quantum mechanical rules. It necessarily implies pure quantum behaviour is observed only when strong mixing is negligible. This perspective makes irreversible changes fundamental entities and reversible dynamics are considered an approximation.

There exists recent theories for explaining quantum measurement without necessarily falling back on irreversibility, such as "consistent histories" where the most faithful representation or map of a physical process is constructed [3]. The modern update of the theory, however, is based on quantum decoherece. As such, most theories, do work with a premise of irreversibility in the measurement process. A modern contribution, "Quantum Darwinism" by Wojciech Zurek is gaining ground, even passing initial experimental tests [4]. Quantum Darwinism explains emergence of classical reality with an environment "watching" over. Since, we are interested in irreversibility based approaches and so we simply sum them up with two simple conclusions. First, quantum measurement devices will have intrinsic irreversibility as a fundamental attribute. Second, our eyes are the final conceivable measurement device (the latest link in the chain where the cut can be taken) before the signal is imparted to our consciousness. Naturally, we should take a closer look at what happens in a human eye in converting optical rays into neurological pulses.

1.3. Are our eyes special? Like our minds?

The process responsible for human perception through vision is of fundamental importance. Seeing with own eyes has been considered the fail-safe method for acquiring reliable information – in all adages across all societies. Efforts to understand the mechanism of light transmission and human vision also originated in ancient times, notably by Euclid and Ptolemy. Ibn al-Haytham aka Alhazen, Sir Isaac Newton and Johannes Kepler made crucial contributions fractions of millennia apart. The 20th century, however, witnessed a revolution where our knowledge of light and knowledge of quantum theory complemented each other's growth. The biggest debates and celebrated problems in the history of quantum mechanics have been starred by photon, the fundamental quanta of light. The EPR paradox and the photo-electric effect have revolved around photons, which originally marked the coming of age of quantum mechanics. Feynman resolved the enigma of interference pattern created by light in Young's double slit experiment, showing that they simultaneously take every possible path from point A to point B. Photon has enjoyed a unique attention in major conceptual breakthroughs in physics. All in all, we have come to peace with the wave and particle dual nature of light/photon and quantum theory has become the most successful and meaningful theory of our universe. Naturally, scientists are getting more interested in the response of our eyes to photons, and not just electromagnetic waves. It is still impressive that, such efforts originated as early as 1942, with the seminal work by Hecht et al. [5]. Previously, physicist Hendrik Lorentz had given the problem a fair shake in 1911 freshly equipped with the knowledge of photons or particles of light [6].

Quantum measurement problem and theories ultimately separate mind from matter. We have measurement devices that can produce numbers as measures of a physical quantum mechanical observable. If nature is indeed quantum mechanical, so would be the measurement device itself. So, in effect, our minds perform a measurement on the measurement device itself, be it a photodetector display or the interference pattern out of an interferometer. Since the human observer uses their eyes to read that display, the eye counts as a "quantum" measurement device as well. In the end, a neurological impulse from the eyes take the information to the brain or human mind. A mathematical description of the process would hold clues for the mathematical description of a general single photon detection that can be applied to photon detection devices as well.

Ref. [7] reports a recent convincing experiment establishing the ability of human eye for detecting single photons. The ideas originally are credited to Hecht et al.[5] (see also [8] for a review). Experiments characterizing single photon responses in mammalian eyes have been reported for a while now [9, 10, 11]. With the advent of modern quantum optics techniques, modern experiments are employing state of the art quantum optics capabilities (such as heralded single photons) for measuring attributes of human eye response to single photon signals [12, 13, 14, 15]. To be fair, the basic mechanism of single photon detection by the human eye had been "disentangled" at least two decades earlier [6].

Human eyes have two distinct (in shape and functionality) kind of photoreceptors, rods (approximately 100 million in a retina) and cones (approximately 3 million in a retina). Cones respond to bright light and facilitates colour vision. Rods are functional in dim lights and can detect single photons. Seeing a flash involves less than 10 of these rods. The chain of events in seeing
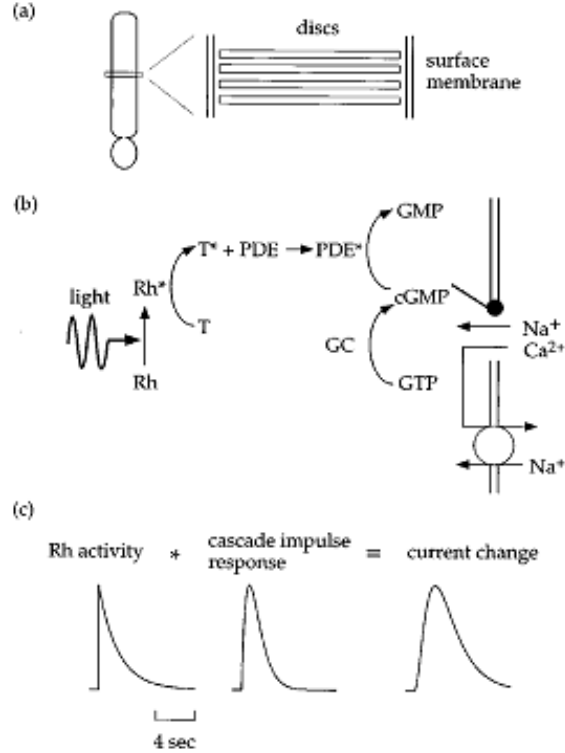
FIGURE 1.1. Phototransduction cascade.
(a) Outer-segment discs (a stack of about 1000) are specialized for photoreception. In the absence of light, Ca^{2+} and Na^+ ions flow into the outer segment through a channel gated by cGMP. The photosensitive molecule (called rhodopsin) in the rods have a prosthetic group 11-cis retinal (light absorbing chromophore) and a protein component opsin linked together. (b) Schematic of transduction cascade. Absorption of light causes an isomerization of the 11-cis-retinal group to a all-trans form. In dim light, an incident photon activates rhodopsin (Rh) as a catalyst which activates transducin (T), in turn T activates a cGMP phosphodiesterase (PDE), next activated PDE causes cGMP concentration to fall. (c) The rod current, I(t) calculated from eq.1.1. Rhodopsin activity, R(t) is taken to be a decaying exponential. The parameter values and other equations can be found in [6] (reproduced with permmission from [6])

a dim light, commonly referred to as "phototransduction" in vertebrate rods

can be summarised from the review [16]. The photopigment molecule rhodopsin

changes its structure upon absorption of a photon and becomes active as a catalyst

(fig. (1.1)). In response to a photon, the isomerization from cis to trans of the

11

prosthetic group in the rod is characterized by a 5Ådisplacement of Schiff-base nitrogen atom [17]. This is a characteristc of bio-based photodetectors. Photon transduction brings about structural-chemical changes in their bond structure. The current in the rods, was modelled with a linear filter system, where the rhodopsin response function, R(t) acts an an input. The filter function (impulse response), F(t) can be estimated [6]. I_D is the current in the dark, k is a constant, G_D is the cGMP concentration in the dark.

$$I(t) = I_D - 3kG_D^2 \int_0^t d\tau F(\tau) R(t - \tau) \qquad (1.1)$$

The electrical signal change manifests as a closure of some channels in the outer segment and a dip in the circulating current. The names of the compounds or types of compounds (in Fig. 1.1(b), see also [17]) are less important for the purpose here, so they are mentioned briefly in the caption of Fig. 1.1 without much details. What is more important is the structure of the equation 1.1. The filtering function acts a temporal and frequency filtering operation. In effect, the input photon undergoes filtering in passage through the eye lens as well as in the internal mechanism of eye's response into the output macroscopic current signal. The production of a macroscopic signal through the closing and opening of a gate is equivalent of an amplification process. Modern idea of a general quantum mechanical model for photodetector resorts to same "filtering+amplification" strategy as we shall shortly see. A structural change in the photoreceptive molecule is responsible for initiating the amplification mechanism. We later discuss how this irreversible change in the structure is a feature of device based photodetectors as well. Single photon detection in a device has the same working

principle. A single photon wavepacket is filtered in, creates a structural change and incurs a macroscopic signal.

1.3.1. Two-photon detection in a human eye

An interesting question to contemplate would be if human or animal eyes can do Photon Number Resoling (PNR) detection. Can our eyes tell a single photon excitation from two photons? We have known for awhile, the toad rods produce distinct signals in response to 0,1,2 photons and can thus differentiate between the three possibilities for number of absorbed photons [6]. And very recently Two Photon Absorption (TPA) has been reported in human vision as well, with the added intrigue that we have learnt that human eye may be sensitive outside the visible range. Previously, Rods were believed to have a sensitivity range from 300 to 700nm of wavelength. Recent works have found rods to be sensitive at wavelengths longer than 800nm and some authors have purportedly perceived 1060nm of infrared light as pale green. [18] The physical mechanism behind it were suspected to be either Second Harmonic Generation (SHG) or Two Photon Absorption (2PO). We can be safe in assuming that human eyes have capabilities far exceeding our previous expectations, also physics that confounds current theory.

1.4. How are quantum observables (classically) measured?

Einstein and Bohr faced off ("officiated" by mutual friend Ehrenfrest) a number of rounds (Solvay conferences) in, perhaps, the most consequential mano a mano in the history of science. A particular bone of contention was Bohr's complementarity principle. It refers to the dual nature of the behaviour of the

13

photon (particle and wave) observed, depending on the particular setup of the experiment. In fig. 1.2, the first or left-most screen has a slit small enough for the wavelength of the light so as to create single slit diffraction. If the size of the slit were large, the diffraction pattern would disappear. The second screen (middle) has two slits that the photon deflected through the first screen's slit can take if unobserved. And on the third screen the interference pattern of the two states (one each for the photon passing through each slit) shows up as alternate bright and dark spots. If the photon is not observed (through which slit it passes) the wave nature wins and an interference fringe is observed. If it is observed the particle nature takes over and interference fringe is lost (Heisenberg's statement, "the particle trajectory is created by our act of observing it."). Bohr's complementarity principle proclaims mutual exclusivity of the two natures. Fig. 1.3 shows a modification of the first screen that Einstein proposed. The slit is suspended by a spring and can be deflected vertically up or down while the photon passes through. Einstein argued that from the deflection observed of the first slit and conservation of momentum principle we can deduce the direction the photon was deflected when it passed the first screen which in turn gives away whichever slit the photon went through on the second screen (a piece of information referred to as "which-path" information). Since the interference is the result of the two wavefronts created from the two slits, it will not be disturbed by whatever happens before the second screen. Thus we can obtain both which-path information and the interference pattern in direct contradiction of Bohr's complementarity principle. Bohr successfully countered pointing out that the precise measurement of the momentum of the first slit would smudge its position (due to Heisenberg's indeterminacy principle) and effectively increase the size of the slit making the

14

diffraction from it disappear and destroy the interference pattern on the third screen.
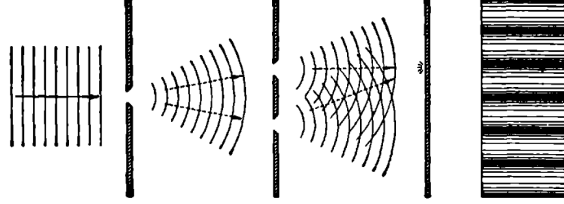
FIGURE 1.2. Schematic for the double slit experiment for light.
The first slit can deflect the photon towards the top or bottom slit in the middle screen. An interference pattern emerges on the third screen.
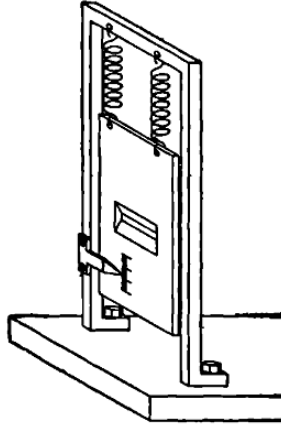
FIGURE 1.3. Bohr's original drawing for the thought experiment behind Bohr-Einstein debate.
If the screen has a recoil upward or downward, the "which-path" information namely the path taken by the photon can be learned.

The round went to Bohr (in fact the match eventually as well), needless to say. It also serves to warn us against treating macroscopic objects as completely classical, because if we did then atomic scale measurements that violate the uncertainty principle may become a possibility. However, later theorists (Wootters, Zurek, Scully, and Drühl) have shown in certain cases if the which-path information is partial (and not complete), we can have interference pattern that

is partially smudged ([2]). This is the mechanism through which environment can monitor a system and gain which-path information without completely destroying the quantum attributes of the system. The system is affected in a way that quantum phase relationship between certain states is partially lost, a process called decoherence. The solutions derived in this thesis utilizes the method of employing an environment to watch the quantum system and absorb "which-path" information. Before discussing decoherence and strategies of learning which-path information from the environment, a segment of Bohr's account of the events is worth remembering.

From Bohr's reminiscence, "Discussions with Einstein on Epistemological Problems in Atomic Physics" (1949), "all unambiguous use of space-time concepts in the description of atomic phenomena is confined to the recording of observations which refer to marks on a photographic plate or to similar practically irreversible amplification effects like the building of a water drop around an ion in a cloud-chamber." Niels Bohr might have inadvertently outlined the methodology for amplification of a quantum observable long before quantum theory received wide acceptance. The amplification mechanism he alluded to is still the method to obtain classical measurement record from quantum observables. A mechanism that can create a sizeable effect (perceptible by ordinary human sense organs) from a microscpic attribute or signal is required. This amplification mechanism discards any quantumness as it grows in size and can be treated as a classical signal produced from the microscopic values. It is very similar to the amplification mechanism discussed in the eye that a photon hitting the rhodopsin molecule causes. Modern developments in the theory of single photon detection retains this fundamental structure. The single photon detection process is subdivided

16

into a transduction+amplification part. As reasons that would be discussed later, transduction for the case of optical photons is explained in terms of a quantum mechanical transmission probability. Amplification drives the process of measurement. The DARPA DETECT ([19]) consortium (this dissertation is result of the collaboration) in the 2010s have summarized this fundamental structure.
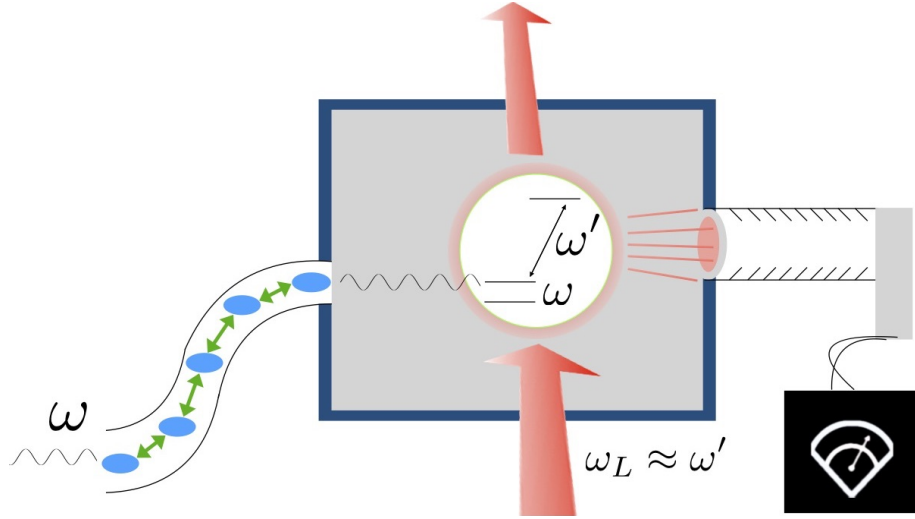
FIGURE 1.4. The three parts of the single photon detection process: transmission, amplification, and measurement.
The input photons with frequency components ωs are transmitted irreversibly via network of discrete states and absorbed into the atom or molecule that changes in shape and irreversibly initiates an amplification mechanism at its higher state. In the figure, a laser with frequency ω_L drives a single mode cavity which populates massively at a optical frequency, $\omega' \approx \omega_L$. This method of creating fluorescence excitations when a molecule is at a higher state is also called "electron shelving". The amplified signal can be considered a classical macroscopic signal and human eyes can perform a measurement of it trivially (Not unlike Bohr's idea mentioned before or the process in the rod cells of human eyes). (Reproduced with permission from [20])

Historically, writing down a quantum mechanical description for a measurement problem had been ripe with challenges and pitfalls and caveats and unsolved enigmas. At initial stages, Copenhagen interpretation have guided us in the interpretation of the physical world and their perception in our minds. Over
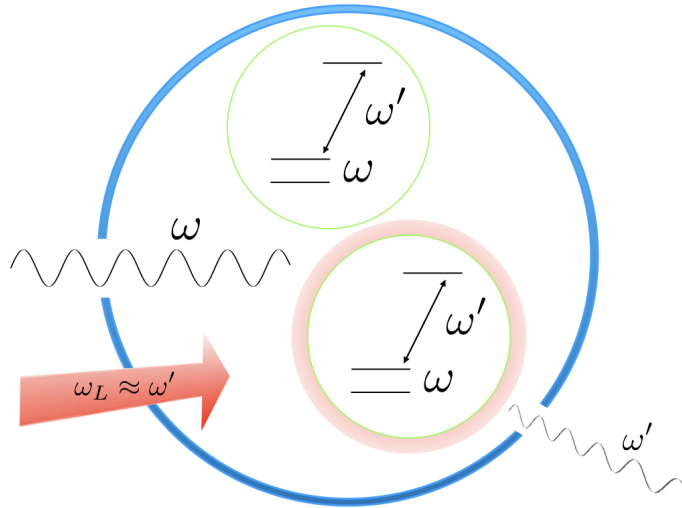
FIGURE 1.5. Photon with frequency ω initiates amplification into a macroscopic signal via electron-shelving [21, 22, 23]:
A resonant photon lifts an atom (modelled here as a three-level system) enters the first excited state. A laser beam tuned to the second transition frequency $\omega_L \approx \omega'$, induces fluorescence. (Reprinted with permission from [1])

time, from the shorthand narrative of Copenhagen interpretation for describing measurements, we have evolved to the more austere von Neumann measurement which ultimately has fallen short of eliminating the need for an interpretative process for outcomes. Von Neumann school of thought makes a methodical attempt to construct an evolution that supersedes the collapse of wavefunction of the Copenhagen interpretation. The missing link of emergence of classicality from the quantum domain is nailed down more narrowly.

The work of Wojciech Zurek has been a revelation in Quantum Information Science (QIS) and quantum measurement problem. The theory of decoherence, a strictly quantum effect with no classical analogue has become the language of choice in quantum information experiments. Although we cannot yet discard the need for an interpretive process in the emergence of classical outcomes in a measurement process, we can certainly capitalize on the redundant information

accrued in the environment over the course of measurement evolution through decoherence. Zeh and then Zurek have demonstrated that to resolve a problem called "preferred basis" in quantum measurement theory it is necessary to treat system and meter to be open systems (coupled to their environment) [2]. Performing a measurement on a closed system energy eigenstate would definitely perturb it. A closed system maybe preferable for precluding the undesired coupling effects (decoherence) from environment. But is it not a little too optimistic hoping to have closed systems absorbing the information from the photon wavepacket? Since realistically, we would expect optical photons, stray background radioactivity, air molecules, cosmic muons, solar neutrinos, and even the ubiquitous 3 K cosmic background radiation to couple to the quantum system of interest. Therefore, a faithful or realistic model would include an environment that model the decoherence that any and all quantum systems are subject to.

Our best understanding of the emergence of the classical objective reality from quantum mechanical observables is the structure of system-environment interaction– as pointed out by Zurek. Niels Bohr's intuition in the early days was correct– an irreversible amplification process will render a quantum system "classical". However, the quantum to classical transitions were better understood only post 2000 with the theories of Quantum Darwinism and decoherence. All single photon detectors have the physical mechanism where a classical macroscopic signal is produced in response to the quantum mechanical photon transduction. Fundamentally there exists no reason for microscopic and macroscopic objects to be governed by different rules of nature. Physicists have referred to this appearance of classical behaviour from large objects with the umbrella term "quantum to classical transition". In our everyday experience, we observe certain

(few in number) features of classical objects like position and speed to be measurable, underlying quantum mechanical models have a long list of quantum numbers and observables that could possibly be observed. Yet "position eigenstate" or "momentum eigenstate" is the quantum observable (of a bouncing basketball, for example) is what we typically observe. Also, quite puzzlingly, we never observe classical objects to be in superposition. How do we make sense of it without incurring the Copenhagen interpretation? The idea of decoherence can resolve these two puzzles [2].

A fundamental quantum mechanical model of a single photon detector can utilize an "environment simulator" or "meter" that would become correlated with the system observables and reveal the system observable through a measurement of itself. This system-meter(environment) interaction would lead to decoherence of the system and certain pointer states emerge as the "preferred basis" for the system, resolving the first puzzle. In the spirit of von Neumann theory, the system state $|\psi\rangle$ and meter ("environment simulator") is initialized as a product state (the environment's initial state is called "ready" state).

The desired evolution will produce the following,

$$
|\psi_1\rangle|\text{"ready"}\rangle \rightarrow |\psi_1\rangle|1\rangle
$$
$$
|\psi_2\rangle|\text{"ready"}\rangle \rightarrow |\psi_2\rangle|2\rangle \tag{1.2}
$$

The $|1\rangle$ and $|2\rangle$ states of the environment would indicate the system states at the end of the evolution. So if we are able to measure the meter ("environment simulator") projectively, we are able to measure the system, indirectly. $|\psi_1\rangle$ and $|\psi_2\rangle$ are the states in the double slit experiment when the photon passes through

the first or second slit respectively. If unobserved, the superposition of the two states will evolve accordingly,

$$\frac{1}{\sqrt{2}}\left(|\psi_1\rangle + |\psi_2\rangle\right)|\text{``ready''}\rangle \rightarrow \frac{1}{\sqrt{2}}\left(|\psi_1\rangle|1\rangle + |\psi_2\rangle|2\rangle\right) \tag{1.3}$$

There are two things to note from eq. B.18. Firstly, an entanglement has been created between the system and meter dynamically. Secondly, the superposition originally in the photon states have delocalized into a larger system of system+meter.

The density matrix can now be written out as well as the particle density, $\varrho(x)$ at the detector screen,

$$\hat{\rho}_{particle} = \frac{1}{2}\left[|\psi_1\rangle\langle\psi_1| + |\psi_2\rangle\langle\psi_2| + |\psi_1\rangle\langle\psi_2|\langle 2|1\rangle + |\psi_1\rangle\langle\psi_1|\langle 1|2\rangle\right]$$

$$\varrho(x) \equiv \hat{\rho}_{particle}(x,x) \equiv \langle x|\hat{\rho}_{particle}|x\rangle$$

$$= \frac{1}{2}|\psi_1(x)|^2 + \frac{1}{2}|\psi_2(x)|^2 + Re\left\{\psi_1(x)\psi_2^*(x)\langle 2|1\rangle\right\} \tag{1.4}$$

The two extremes (Einstein and Bohr's original stances) of perfect distinguishability (complete knowledge of "which-path" information) and null "which-path" information are due to the detector states $\langle 2|1\rangle = 0$,

$$\varrho(x) = \frac{1}{2}|\psi_1(x)|^2 + \frac{1}{2}|\psi_2(x)|^2 \tag{1.5}$$

and $\langle 2|1\rangle = 1$ respectively,

$$\varrho(x) = \frac{1}{2}|\psi_1(x)|^2 + \frac{1}{2}|\psi_2(x)|^2 + Re\left\{\psi_1(x)\psi_2^*(x)\right\} \tag{1.6}$$

The extraction of the "which-path" information destroys the interference pattern (in eq. 1.5). This is the process called decoherence, where a quantum system loses its "quantumness" through interaction with an environment. The second puzzle of non-observability of interference is understood in this way. Environmental monitoring causes superposition properties to disappear. Also the intermediate values of $\langle 2|1 \rangle$ between 0 and 1 is when we have partial "which-path" information and the interference pattern has a lesser contrast (but not completely washed out).

Eq. 1.2's evolution would be achieved with an explicit Hamiltonian in a von-Neumann formulation.

$$\hat{H} = \hat{H}_S + \hat{H}_{\mathbb{E}} + \hat{H}_{int} \tag{1.7}$$

where $\hat{H}_S$ and $\hat{H}_{\mathbb{E}}$ are the self-Hamiltonians of the system and environment respectively. $\hat{H}_{int}$ is the system-environment interaction Hamiltonian.

The choice of $\hat{H}_{int}$ tries to make different relative environmental states to be distinguishable or orthogonal (τ_d being a characeristic time).

$$\langle E_i(t)|E_j(t) \rangle \propto e^{-t/\tau_d} \text{ for } i \neq j \tag{1.8}$$

If the relative environmental states are correlated with the center-of-mass of the system at x, we would want to design $\hat{H}_{int}$ to produce

$$\langle E_x(t)|E_{x'}(t) \rangle \propto e^{-\Gamma_{tot}t} \tag{1.9}$$

, where τ_d is a characeristic rate.

Clearly, the proper design and selection of $\hat{H}_{int}$ enables the measurement of the system observable to be possible. $\hat{H}_{int}$ is also responsible for the decoherence of the system states. For a particular choice of $\hat{H}_{int}$, certain basis states of the system will be more prone to decoherence (their phase relations will decay fast) and some other basis states will be more robust against phase information losses. System states can be written in multiple bases of course,

$$|\psi\rangle = \sum_i c_i |s_i\rangle = \sum_{i'} c_{i'} |s_{i'}\rangle \tag{1.10}$$

The system states more robust against environmental decoherence are the so-called pointer states or preferred states or quantities. Therefore classically certain eigenstates are more accessible, like the position or speed of a basketball. Alternatively, the preferred pointer states can be thought of as the states that get least entangled with the environment.

In a typical von-Neumann measurement interaction, A microscopic system, S, with a Hilbert space $\mathscr{H}_S$ having basis vecors $\{|s_i\rangle\}$, and a measuring apparatus $\mathscr{A}$, with a Hilbert space $\mathscr{H}_A$ having basis vectors $\{|a_i\rangle\}$ ($|a_i\rangle$ are the pointer states),

$$|\psi\rangle|a_r\rangle = \left(\sum_i c_i |s_i\rangle\right)|a_r\rangle \rightarrow |\psi\rangle = \sum_i c_i |s_i\rangle|a_i\rangle \tag{1.11}$$

Now we assume an environment (for both system and measuring apparatus) which is initialized in the state $|E_0\rangle$.

$$|s_i\rangle|a_i\rangle|E_0\rangle \rightarrow |s_i\rangle|a_i\rangle|E_i\rangle, \quad \text{for all } i \tag{1.12}$$

23

In most cases it is assumed that mostly the apparatus interacts with the environment and therefore $|a_i\rangle$ are the environment superselected robust preferred states. For the socalled *quantum measurement limit*, $\hat{H} = \hat{H}_S + \hat{H}_\mathbb{E} + \hat{H}_{int} \approx \hat{H}_{int}$, and the eigenstates of $\hat{H}_{int}$ becomes stationary under the evolution. Hence, measurement superselected pointer states are none other than the eigenstates of $\hat{H}_{int}$. For example, for the following $\hat{H}_{int}$,

$$\hat{H}_{int} = \hat{x} \otimes \hat{E} \tag{1.13}$$

environment continuously monitors the position of the system.

$$e^{-i\hat{H}_{int}t}|s\rangle|E_0\rangle = |x\rangle e^{-ix\hat{E}t}|E_0\rangle \equiv |x\rangle|E_x(t)\rangle \tag{1.14}$$

The more general form of the interaction Hamiltonian,

$$\hat{H}_{int} = \sum_\alpha \hat{S}_\alpha \otimes \hat{E}_\alpha, \tag{1.15}$$

$$\hat{S}_\alpha|s_i\rangle = \lambda_i^{(\alpha)}|s_i\rangle, \quad \text{for all } \alpha \text{ and } i. \tag{1.16}$$

Eq. 1.18 can produce,

$$e^{-i\hat{H}_{int}t}|s_i\rangle|E_0\rangle = |s_i\rangle|E_i(t)\rangle, \quad \text{a product state} \tag{1.17}$$

Because $|s_i\rangle$ does not get entangled with the environment, $|s_i\rangle$ is an environment-superselected preferred state, since it is immune to decoherence and does not get entangled with the environment. For reasons to be mentioned soon, there can be subspaces of pointer states that are immune to decoherence. If $\{|s_i\rangle\}$ is an

orthonormal basis and all $|s_i\rangle$ are simultaneous degenerate eigenstate of each $\hat{S}_\alpha$,

$$\hat{S}_\alpha|s_i\rangle = \lambda^{(\alpha)}|s_i\rangle, \quad \text{for all } \alpha \text{ and } i. \tag{1.18}$$

we get

$$e^{-i\hat{H}_{int}t}|\psi\rangle|E_0\rangle = |\psi\rangle|E_\psi(t)\rangle, \quad \text{a product state} \tag{1.19}$$

Existence of a Decoherence Free Subspace (DFS) is a consequence of a symmetry in $\hat{H}_{int}$. Such dynamical symmetries can be exploited in preserving quantum information more robustly. System-environment interaction is all we need to look at for the availability of a DFS. It derives from a symmetry in the structure of the system-environment interaction, a dynamical symmetry.

The theory development at Los Alamos National Lab led by Zurek has been a tour de force. The procession of ideas can be time ordered into some interesting descriptions or names: environment as a witness.

In essence, we should capitalize on Zurek's seminal ideas of decoherence, the larger family of problems of quantum-to-classical transitions and quantum Darwinism. Coupling to the environment would involve decoherence, be it for measurement purposes or unwarranted coupling to stray baths of particles. Judicious choices of pointer states (states more robust against decoherence) and strategies of battling decoherence with Decherence Free Subspaces (DFS) can help us design photodetectors with superior performance.

1.4.1. Positive Operator Valued Measure (POVM)

POVM are the most general description for quantum measurement. This elucidates the observables that we can define that we would be interested in for

learning about the photon signal. Measurement of an observable in the linear vector space of the operators acting on $\mathcal{H}_A$ can be done indirectly through a projective measurement on another system, B once it is correlated/entangled with the former. This is formulated as a generalized measurement on A. A generalized measurement $\mathcal{M}$ on A is defined to be a set of operators (Hermitian or otherwise), M_i of $\mathcal{M}$ in $(L(\mathcal{H}_A)$, the linear space of operators acting on $\mathcal{H}_A)$ which yields the result m_i with the probability π_i, given by

$$\pi_i = Tr\left[M_i \rho_A M_i^\dagger\right] \tag{1.20}$$

which projects A conditionally into the final mixed state,

$$\rho_{A|i} = \frac{M_i \rho_A M_i^\dagger}{\pi_i} \tag{1.21}$$

They have the normalization condition:

$$\sum_i M_i^\dagger M_i = \mathbf{1} \tag{1.22}$$

If M_i are orthogonal projectors, P_i with the conditions, $P_i^\dagger = P_i$, $P_i^\dagger P_i = P_i^2 = P_i$, we have our projective measurement postulates back.

Without the orthogonality postulate, the generalized procedure, $\mathcal{M}$ performed on A can be viewed as resulting from a projective measurement on an environment simulator B, after it has been entangled to A by a proper unitary operation, $U_\mathcal{M}$. We need the dimension of $\mathcal{H}_B$ to be equal or larger than the number of M_i operators. We then define an orthonormal basis set of $|u_i^{(B)}\rangle$ for B and associate one to each M_i.

The operation of $U_\mathcal{M}$ on a A in a statistical mixture is,

$$U_\mathcal{M} \left(\rho^{(A)} \otimes |0^{(B)}\rangle\langle 0^{(B)}| \right) U_\mathcal{M}^\dagger$$

$$= U_\mathcal{M} \left(\sum_i p_i |\phi_i^{(A)}\rangle\langle\phi_i^{(A)}| \otimes |0^{(B)}\rangle\langle 0^{(B)}| \right) U_\mathcal{M}^\dagger$$

$$= \sum_{i,j} M_i \rho^{(A)} M_j^\dagger \otimes |u_i^{(B)}\rangle\langle u_j^{(B)}| \tag{1.23}$$

For, an eigenbasis $|u_j^{(B)}\rangle$ of B with result m_j, a projective measurement of observable O_B of B projects A into $\rho_{A|i}$ with probabilities, π_i.

POVM is the most general method for the interpretation of measurent results in Quantum Mechanics. It is a set of positive operators $(\hat{\Pi}_k)$ that add up to the identity operator and each operator represents a measurement outcome and projects onto orthonormal quantum states with a calculated weight, $w_i^{(k)}$. $w_i^{(k)}$ is the conditional probability of obtaining outcome k given the input i, i.e. $w_i^{(k)} = Pr(k|i)$.

$$\hat{\Pi}_k = \sum_i w_i^{(k)} |\phi_i^{(k)}\rangle\langle\phi_i^{(k)}|. \tag{1.24}$$

The experimentalist can at best have a probability distribution for possible inputs calculated from the measurement outcomes at hand. Knowing $w_i^{(k)} = Pr(k|i)$ values, an experimentalist can calculate $P(i|k)$ through Bayes' theorem and update their idea for the inputs i.e. the probability distribution over the inputs. Knowledge of $\hat{\Pi}_k$ is therefore useful and is calculated theoretically.

1.5. Single Photon Detection (SPD) in a device

Many ingenious ideas have been implemented to detect (as well as create) single photons with high efficiency in a device. The major ideas include PhotoMultiplier Tube (PMT), Single Photon Avalanche Photodiode, quantum dot field-effect transistor based detector, Superconducting Nanowire Single Photon Detector (SNSPD), and up-conversion single photon detector. Few photon detection have been developed in a Photon Number Resolving (PNR) fashion. Examples include superconducting tunnel junction (STJ) based detector, superconducting nanowire-based single photon detector, quantum dot field-effect transistor-based detector. superconducting transition edge sensor, frequency up conversion and visible light photon counter [24, 25, 26, 27, 28]. For a short and concise introduction to the figures of merit (spectral range, dead time, dark count rate, detection efficiency, timing jitter, photon number resolution, Noise Equivalent Power (NEP)) characterizing single photon detectors, see [25, 26]. The state of the art capabilities in terms of the figures of merit are also presented in [25]. Modern capabilities record The timing jitters in the tens of picoseconds in superconducting nanowire SPDs [29, 30], dark count rates on the order of a single dark count per day [31, 32]. Quantum dot field transistor detectors and superconducting transition-edge sensors have a longer dead time ($\sim 10\mu s$) [25]. SNSPDs [31, 32, 33, 34] with low dark count rates ($\sim 10Hz$) and dead times ($\sim 1ns$) are becoming a popular choice these days. The prospects of robust performance for SPDs in room temperature have also improved [35, 36].

Classic works dating as far back as 1939 [37] deserve a mention. The first PMT was invented on 4 August 1930 in Soviet Union by L.A. Kubetsky [38], and avalanche photodiode was invented by Jun-ichi Nishizawa in 1952 [39].

These two platforms function based on the photoelectric effect. The myriad of investigations done on PMT ([40, 41]), superconducting tunnel junction ([42, 43]), superconducting transition edge sensors ([44, 45]), superconducting nanowire SPD ([31, 32]), single Photon Avalanche photodiodes (SPAD) ([46, 47]), quantum dot field effect transistor photon detector ([48, 49, 50]) can be found.

Photoelectric effect is at the heart of the longest serving (since 1949) single photon detector, PMT. Electrons from a photocathode with low work function (in a vacuum tube) is liberated by incident photon due to photoelectric effect. A cascade of secondary electrodes biased progressively higher multiplies the initial single electron current. The Single Photon Avalanche Diode (SAPD) has a p-n or p-i-n junction reverse biased above its breakdown voltage, the carriers generated by photon absorption trigger a macroscopic breakdown of the junction and create an avalanche. In a superconducting Transition Edge Sensor (TES), a superconducting material is biased at the tipping point of a superconducting transition; the incident photon heats up the material and it undergoes a phase transition to lose its superconductivity. Both the energy of the incident photon and number can be measured through the response in the current. Ultrathin NbN films of superconducting is biased just below its critical current for Superconducting Nanowire Single Photon Detectors (SNSPD). An impinging photon creates a resistive hotspot and blocks the entire channel and a fast voltage pulse is observed in response to the change in current. Quantum Dot Field Effect Transistors use the conventional field effect to modulate the channel conductivity in response to an absorbed photon. More details about individual platforms can bee found in [25, 27, 51]. Some of the platforms mentioned can have PNR functionality [45, 52].

Photon number resolution has become a sought-after functionality in order to reduce errors in QIS applications.[53, 54] There exists two classes of methods for PNR detection process. Certain platforms of single photon detectors produce output electrical pulses that are commensurate with the number of absorbed photons [55]. The second class uses spatial or temporal multiplexing [56]. Spatial multiplexing combines the outputs from an array of detectors [57, 58], temporal multiplexing uses the same detector but a cascade of beam splitters separates and delays the input pulse so as to feed them to the detector sequentially [59]. The coherent dynamics of an array of SPDs performing PNR with multiplexing was investigated theoretically recently [60]. Inspired by biological abilities of phootodetection, some experiments have been done investigating the abilities of toad rods with fixed number of photons [61].

DARPA DETECT program has been instrumental in developing a unified and general natural theory that can provide fundamental description of a single photon detector valid across all platforms and which facilitates determination of fundamental constraints between figures of merit. [1, 20, 35, 60, 62, 63, 64, 65, 66, 67, 68, 69, 70] The general model separates the whole process into three subprocesses transmission, amplification and measurement (fig 1.4). A review of biological photodetectors and device photodetectors all have this general underlying structure. Participants of DARPA detect have also formulated new ideas for weak signal amplification [71, 72, 73]. New device architecture and concepts were realized by the Sandia Livermore group [74, 75, 76, 77]. Another particular avenue explored by the group is bio-inspired photodetectors ([36]). They would be more vulnerable to elevated thermal noise at room temperature and larger dark count rates, but with a high enough signal to noise ratio interesting

new devices may be found. A host of work in the traditional single photon detectors' phenomenological models were also conducted [30, 35, 64, 78, 79].

1.6. Genealogy of theories of photodetection and single photon detectors

Although DARPA detect program developed the general theory for a single photon detection "device", it is built on years of progress of our knowledge of the fundamental natural laws. For the physics of single photon, classical Maxwellian theory proves inadequate and the need for quantization has driven the advancement of our understanding of quantum light. The theories of photodetection can be separated into few genres. Classic works by Glauber, Kelley and Scully helped reveal fundamental features of the theory of quantum light [80, 81, 82]. Einstein's work on the photoelectric effect ([83]) and A-B coefficients also belong to this fundamental physics genre. Dirac's formulation of Quantum Electrodynamics finally enabled the complete quantum treatment of field and matter and subsequent contributions from others (Wigner, Oppenheimer, Fermi, Bloch, Weisskopf, Tomonoga, Schwinger, and Feynman) gave us the full understanding of light-matter interactions [84, 85, 86, 87, 88, 89, 90, 91, 92].

The basic results in the theory of photodetection is reviewd here. For a single polarization μ of the quantized electromagnetic field, [93]

$$\hat{E}_\mu(\vec{r}, t) = \hat{E}_\mu^+(\vec{r}, t) + \hat{E}_\mu^-(\vec{r}, t) = \hat{E}_\mu^+(\vec{r}, t) + H.c. \tag{1.25}$$

$$\hat{E}_\mu^+(\vec{r}, t) = -\sum_j \sqrt{\frac{\hbar\omega_j}{2\epsilon_0}} e^{i(\vec{k}_j \cdot \vec{r} - \omega_j t)} \hat{\epsilon}_\mu \hat{a}_j \tag{1.26}$$

where $\hat{E}_\mu^+(\vec{r}, t)$ and $\hat{E}_\mu^-(\vec{r}, t)$ are positive and negative frequency components respectively. $\hat{\epsilon}_\mu$ is the polarization vector, $\vec{k}_j = \vec{p}/\hbar$ the wave number, $\vec{p}$, ϵ_0 the permittivity of free space, $\hbar$ Planck's reduced constant, $i = \sqrt{-1}$, and $\hat{a}_j$ the annihilation operator corresponding to the mode j.

Glauber's work in connecting quantized electromagnetic field correlations to experimentally measurable physical quantities may be the most useful contribution to quantum mechanical photodetection theory ever [80]. The theory facilitates the calculation of transition probabilities (that experimental detection is correlated with) as well as quantum coherence between field components in the framework of QED. Glauber defines first and second order correlation function of the field (due to pointlike interaction),

$$G^{(1)}(\vec{r}_1, \vec{r}_2; t_1, t_2) = \langle \hat{E}_\mu^-(\vec{r}_1, t_1)\hat{E}_\mu^+(\vec{r}_2, t_2) \rangle = Tr[\rho \hat{E}_\mu^-(\vec{r}_1, t_1)\hat{E}_\mu^+(\vec{r}_2, t_2)]$$

$$G^{(2)}(\vec{r}_1, \vec{r}_2, \vec{r}_2, \vec{r}_2; t_1, t_2, t_3, t_4) = \langle \hat{E}_\mu^-(\vec{r}_1, t_1)\hat{E}_\mu^-(\vec{r}_2, t_2)\hat{E}_\mu^+(\vec{r}_3, t_3)\hat{E}_\mu^+(\vec{r}_4, t_4) \rangle$$

$$= Tr[\rho \hat{E}_\mu^-(\vec{r}_1, t_1)\hat{E}_\mu^-(\vec{r}_2, t_2)\hat{E}_\mu^+(\vec{r}_3, t_3)\hat{E}_\mu^+(\vec{r}_4, t_4)] \qquad (1.27)$$

where $\rho = \sum_i P_i |i\rangle\langle i|$ is the classical mixture of the (initial) field. Photoelectric effect can enable an absorber atom to make local field measurements. The electrons produced in a photoionization process are observed. A detector atom placed at position $\vec{r}$ in the radiation field has a transition probability (by absorbing a photon between time t and t+dt) proportional to, [51, 94, 95]

$$w_1(\vec{r}, t) = \sum_f |\langle f|\hat{E}_\mu^+(\vec{r}, t)|i\rangle|^2 = \sum_f \langle i|\hat{E}_\mu^-(\vec{r}, t)|f\rangle\langle f|\hat{E}_\mu^+(\vec{r}, t)|i\rangle$$

$$= \langle i|\hat{E}_\mu^-(\vec{r}, t)\hat{E}_\mu^+(\vec{r}, t)|i\rangle \qquad (1.28)$$

Eq. 1.28 dictate the probability of a photodetection event with a transition in the (pure) state of the field $|i\rangle \rightarrow |f\rangle$. For a classical mixture of the initial field, we resort to the density operator for the field,

$$w_1(\vec{r}, t) = \sum_i P_i \langle i | \hat{E}_\mu^-(\vec{r}, t) \hat{E}_\mu^+(\vec{r}, t) | i \rangle = Tr[\rho \hat{E}_\mu^-(\vec{r}, t) \hat{E}_\mu^+(\vec{r}, t)] = G^{(1)}(\vec{r}, \vec{r}; t, t) \quad (1.29)$$

so we can appreciate the physical significance of Glauber's first correlation function.

Likewise, the joint probability of observing one photoionization at point $\vec{r}_2$ between t_2 and $t_2 + dt_2$ and another one at point $\vec{r}_1$ between t_1 and $t_1 + dt_1$ with $t_1 < t_2$ is proportional to $w_2(\vec{r}_i, \vec{r}_2; t_1, t_2) dt_1 dt_2$, [94]

$$w_2(\vec{r}_i, \vec{r}_2; t_1, t_2) = G^{(2)}(\vec{r}_1, \vec{r}_2, \vec{r}_2, \vec{r}_1; t_1, t_2, t_2, t_1) \quad (1.30)$$

The other enduring contribution by Glauber is the theory of coherent states of electromagnetic field [96]. Coherent states were originally formulated by Schrödinger as he was trying to find solutions to his namesake equation that follows Neils Bohr's correspondence principle. Simply put, the principle states that in the limit of large quantum numbers quantum mechanics follows classical mechanics. Coherent states are the most classical a quantum mechanical state can be. The Heisenberg's uncertainty principle saturates for them. They are the eigenstates of the annihilation operator of a quantum harmonic oscillator. In terms of the Bosonic Fock (number) basis, a coherent state is written as

$$|\alpha\rangle = exp\{-|\alpha|^2/2\} \sum_{n=0}^{\infty} \left(\alpha^n / \sqrt{n!} \right) |n\rangle \quad (1.31)$$

Laser states are coherent states and they are characterized by a single complex number (or magnitude). They play a crucial role in quantum-to-classical transition theories, since a "classical" state can be written out in a quantum mechanical basis.

The time-correlation measurements of Hanbury Brown and Twiss ([97]) and Glauber's thories inspired a trail of photoelectron counting theories produced by photoionization by electromagnetic fields (especially Glauber states/coherent states). The most notable ones are due to Mandel and Kelly-Kleiner and Scully-Lamb[81, 82, 98]. A particular theme of interest would be the measurement induced back-action on the field and back-action evading measurement schemes [99, 100, 101]. The ideas of back-action evading measurement and quantum non demolition measurements will be popular in modern quantum computing platforms [102].

The underlying physics of photoionization is quantum mechanical photoelectric effect. However, the photodetection events recorded in a photoionization experiment is a classical quantity. On the receiving end, statistical rules can be used to produce counting formulas such as Mandell's counting formula [98],

$$P(n, t, T) = \int_0^\infty \frac{1}{n!} W^n e^{-W} \mathcal{P}(W) dW \tag{1.32}$$

with

$$W = \eta \int_t^{t+T} I(t') dt' \tag{1.33}$$

34

where η is the photodetection efficiency, $I(t)$ is the intensity of the electromagnetic field, and $\mathcal{P}(W)$ is the quasi-probability distribution of the integrated intensity. Mandell's formula has had success due to its simplicity and elegance. One particular example is that, for a thermal distribution of light eq. 1.32 yields a Bose-Einstein distribution for photodetection events [103]. Photoionization is the nexus between quantum mechanical interaction of light-matter and classical measurement results of photodetector click counts. The Carmichael school and chain of thought from [104] in using the Kelley-Kleiner (KK) ([81]) formula to derive the photocurrent statistics from quantum-mechanical operator expressions is a way of defining a Heisenberg cut at the detector. The photocurrent (units of counts/time), a time series of numbers, can be treated as a classical random variable. The signal has been demoted into a classical standing, but amplification of a current carried by bosons/fermions have to abide by quantum laws all the same ([105]).

The KK formula degenerates into the semiclassical Mandel photon counting formula if the incident field is a coherent state, a result from the *Optical Equivalence Theorem*.

$$P(k, \mathcal{T}) = \langle : \frac{\hat{\Omega}(\mathcal{T})^k}{k!} e^{-\hat{\Omega}(\mathcal{T})} : \rangle = \langle : \frac{(\epsilon_Q \bar{n} \Delta T)^k}{k!} e^{-\epsilon_Q \bar{n} \Delta T} : \rangle$$

where, $\hat{\Omega}(\mathcal{T})$ is the integrated photon flux and enclosure with ':'s denote normal and time ordering. It quantifies the probability of k detection events in a time window $\mathcal{T}$. This enables us to find, $\langle i(t) \rangle = e\epsilon_Q \bar{n}$, indicating the quantum efficiency, ϵ_Q to be the number of electrons produced in the photocurrent for each electron on average. Classical $i(t)/e/\epsilon_Q$ and quantum mechanical, $\hat{n}(t)$ can be shown to have same statistical features (mean, variance, correlation functions etc.).

35

Another commonly used quantum model for light-matter interaction is the Jaynes-Cummings model. A two-level atom interacting with a quantized mode of an optical cavity (or a bosonic field), with or without the presence of light (in the form of a bath of electromagnetic radiation that can cause spontaneous emission and absorption)[106].

$$H_{JC} = \sum_{j=1}^{d} \omega_j A_{jj} - \frac{i}{2} \sum_{j \neq k=1}^{d} \mu_{jk} \left(\sigma^+ a - \sigma^- a^\dagger \right) \qquad (1.34)$$

This Hamiltonian commutes with the total excitation number, $a^\dagger a + \sigma^+ \sigma^-$. From ref. [106], if the two possible energy level of the molecule is, $\psi_m, m = 1, 2$ and the number of quanta in the field oscillator is n, $\Phi_n, n = 0, 1, 2, 3, \ldots$.

Another avenue of theory for relating classical measurement results from an underlying quantum theory is quantum stochastic processes [107]. They are the natural language for the description of continuous quantum measurements [108]. Multi-photon Fock space driven absorber atom models have been formulated as a quantum noise driven process [109]. One interesting contribution to motivating the photoelectron counting formulae is [110]. Quantum trajectory theory or unravelling of the quantum master equation is the theoretical method for simulation of measurement records [111]. Ref. [64] used the following abstract amplification model, formulated as a continuous measurement.

$$\mathcal{A}\hat{o}(t) = \mathcal{D}[\chi |X\rangle\langle X|]\hat{o}(t) \qquad (1.35)$$

χ is the amplification strength, and the designated final internal state being monitored is X. X is also called the "shelving state", or the state that drives the amplification. D is the Liouvillian superoperator representing the measurement.

(for example in [64], the stochastic photocurrent, $I_t = \int_{t-t_m}^{t} \chi^2 \rho_{XX}(t')dt' + \chi dW(t')$ was used) and a conditioned (upon I_t) density matrix can be simulated from it.

The quantum optics laboratory methods offer ways of extracting information from a quantum system under study through continuous measurements. The quantum observables are mathematically connected to the number or rate of photoelectron sweeping. For example, The x-quadrature of the system dipole can be measured from the rate of photoelectrons, (γ a real number) ([112]).

$$\hat{x} = \hat{c} + \hat{c}^\dagger, \quad \hat{y} = -i(\hat{c} - \hat{c}^\dagger)$$

$$E\left[\frac{d}{dt}N(t)\right] = Tr\left[(\gamma^2 + \gamma\hat{x} + \hat{c}^\dagger\hat{c})\rho_I(t)\right] \tag{1.36}$$

For $\gamma \gg \langle c^\dagger c \rangle$, eq. 2.81 has the inside the trace a large constant altered by a small term and a term proportional to $\hat{x}$. This gives an idea about how information is extracted in a continuous measurement. It is related to the number of particles swept per unit time in the output.

1.7. Can we write a general and useful model?

We have learnt that single photon detector models should have the functionality embodying photon transducton, amplification and measurement. Biological photon detectors or eyes have photoreceptive molecules that make a structural change to itself when a photon is absorbed. The changed molecule is in a "shelving state" and can drive an amplification mechanism. The environmental states should be discernible to a classical observer. The photon wavepacket should be stored in preferred basis state of the meter or states robust against environmental decoherence. We can envisage a system+meter+environment

structure for the photodetector. Though the system will be exposed to environmental decoherence, the dynamics should mostly be dominated by meter-environment interaction. The meter-environment interaction Hamiltonian, $\hat{H}_{meter-environment}$ dictates the nature of the decoherence that meter states are subject to. Naturally, the meter states should be chosen so as to enable be robust against environmental decoherence. The symmetries of $\hat{H}_{meter-environment}$ can facilitate Decoherece Free Subspaces (DFS) and Noise Subsystems (NS). The "quantum information" of temporal rise in the occupation levels of the absorber atom is better preserved in the meter states that are robust against as much decoherence as possible. States that are immune to environmental effects are also called "dark" states as their evolution as completely decoupled from the evolution of the environment.

- UNITARITY Glauber's fundamental theory of photoionization calculates transition probabilities between field states. The transition amplitude for $i \to f$ is [51, 93],

$$\langle f | \hat{U}(i \to f) | i \rangle \quad \propto \quad \langle f | \hat{E}_{\mu}^{+}(\vec{r}, t) | i \rangle \tag{1.37}$$

The transduction of photon is fundamentally a unitary process. However, a photodetecto atoms have a special property. The structural change that happens in a photodetector absorber innitiates a chain of events going forward and the probability of the photon leaking back out into the continuum of electromagnetic modes is statistically small (this spontaneous emission does happen in typically a small fraction of times). Naturally, practical photodetector physics is modelled with quantum stochastic

38

calculus often that models irreversible quantum processes. Liouville master equations that model the dynamics of a discrete system's evolution coupled to a continuum of modes depict an irreversible dynamics for the discrete system for the timescale concerned. Excellent works have been done on modelling irreversible photon transduction into absorber molecules with a cascaded driven process for modelling photodetection [113, 114, 115]. Since the complete Hamiltonian (system+environment) in these models are understood, the unitarity of evolution (preservation of commutation rules) is explicitly verifiable. A photodetector model can capitalize on these theories [116, 117].

- AMPLIFICATION OF WEAK SIGNALS Bohr's initial intuition still holds. Our measurement of quatum observables are only confirmable through an amplified classical readout. The problem of amplifying weak signals, therefore, is not new in quantum physics research. Famous examples of techniques in use are SU(1,1) interferometry [118, 119] and Ramsey interferometry [120]. A host of new proposals and theories exist on new techniques for amplifying quantum observables [1, 121, 122]. The theories offer quantum mechanically allowed evolution of operators that carry the signal. So these input-output relationships of the operators need to be commutator relationship preserving. The most precise description of such unitarity preserving evolution is through a Hamiltonian that describes all the interactions in play.

  Our ability to project onto input photon wavepackets is contingent upon experimentally obtaining the temporal shape of the rising occupation level of the "dark state" of the absorber molecule [70]. This is the quantum

information we need to protect and amplify and read out. By modern standards, we do not rely upon Copenhagen interpretation, rather formulate suitable system+meter+environment who have entwined dynamics in the spirit of the von Neuman measurement theory. Effectively we measure meter through the environment. The quantum information in the system and meter should be protected against measurement backaction as much as possible. "Which-path" information leaks into the environment from the meter through decoherence. This redundantly encoded classical information in the environment is available to all classical observers. Relative environmental states are preferably clearly distinguishable [2]. A judicious design of $\hat{H}_{meter-environment}$ would be required. Naturally, it would be easier to measure 100spins or atoms in a collective state than an absorber single molecule state. So 100spins could be the meter that serves the purpose of amplifying the weak signal from the absorber molecule [71, 72]. Modern quantum optics techniques allow classical readout of temporal evolution of quantum observables [123].

- PRESERVING QUANTUM INFORMATION The dynamical symmetry of the evolution, the symmetry of $\hat{H}_{meter-environment}$ can help protect against certain errors in the quantum information. A model for a single photon detector should consider errors attacking the quantum information. Beyond a mathematical equivalence, physical formulations should be augmented with error models that they can possibly protect against.

The occupation in shelving state, X's occupation can be coupled to a bound optical cavity mode with a Hamiltonian term, $i|X\rangle\langle X|(c - c^{\dagger})$. The cavity mode becomes our "meter", it needs to interact with the environment or we

do not find out any information about its dynamics. If the cavity is coupled to a bath of electromagnetic (continuum) modes, it would leak out and that reveals information about it. The bath or "environment" monitors the state of the oscillator performing continuous weak measurement. If unobserved by an environment, the driven oscillator (initiated in the ground state, $|0\rangle$, a coherent state with amplitude 0) continues to stay a coherent state with amplitude being the integral of the coherent drive amplitude [124] (it's the time integration of the occupation we need to measure experimentally).

$$\dot{\rho} = -(i/\hbar)[H_{sys}, \rho]$$

$$\gamma(t) = |X\rangle\langle X|(t)$$

$$\hat{H}_{drive} = i\hbar\left(\gamma(t)a^\dagger - \gamma^*(t)a\right)$$

$$a_{out} = a_{in} + \alpha(t) \qquad \alpha(t) = \int_0^t dt'\gamma(t') \tag{1.38}$$

With the cavity leaking out at a rate κ to the environment, a cavity oscillator of resonance frequency ω_c (no driving present), initiated in coherent state $|\alpha\rangle$, evolves as a coherent state of decaying magnitude $\alpha e^{-i\omega_c t}e^{-\kappa t/2}$ [125]. With driving proportional to the waveshape ($\gamma(t) = |X\rangle\langle X|(t)$) we wish to measure, the quadratures of the oscillator bears information about the waveshape we are interested in, and they can be measured with a homodyne setup [123]. But it is quite obvious the measurement damping is going to affect the amplitude of the cavity mode.

Another clarifying comment is in order here. The measurement result of an atom undergoing spontaneous decay would be a discontinuous one [125]. Such trajectories can be simulated with quantum trajectory methods. So if

our desired function $\gamma(t)$ was driving an atom, and the fluorescence signal leaking from it would be broken up ones as well. However if it was driving an ensemble of atoms and their output was monitored the observed signal would be almost continuous similar to the solutions of the master equation, that calculates ensemble average dynamics.

The ideas of quantum non demolition observables and deoceherence free subspaces are useful here. Whether we are monitoring the oscillator amplitude or the collective atomic operators, they can be made immune to certain errors that preserve the symmetry of the $\hat{H}_{meter-environment}$ interactions. These ideas are borrowed from quantum information theory and they can preserve quantum information better. Quantum non demolition measurements, on the other hand can carry out measurements without backaction and such methods can help purer information about the photon wavepackets initiating the detection event.

In summary, the interactions in the model that define the dynamics from a weak signal to the amplified classical signal need to abide by natural or quantum mechanical rules. The unitarity requirement is most precisely enforced by a Hamiltonian formulation. A complete Hamiltonian can elucidate the interrelations between all constituents of the theory, i.e. particles and modes and shed light onto fundamental constraints of photodetector figures of merit. With a host of cavity-QED system apparatus and Hamiltonians representing them at our disposal, we can design very precise and fundamental descriptions of single photon detectors in terms of the Hamiltonians.

CHAPTER II

SUMMARY OF RELEVANT THEORY

> You know only insofar as you can measure.
>
> ———————————————
>
> Lord Kelvin

2.1. A Photon Wavepacket

Fundamentally, photon is the excitation of the electromagnetic fields. However, from a practical point of view of an experimentalist working on an apparatus of photo-electric effect or an atom's spontaneous decay that definition is of no particular practical use. Rather definitions of photon tailored to the purpose at hand may be more useful. Rather more useful definitions can be procured from a wavepacket point of view. For a photon generating experiment like a spontaneous emission of an excitation from an atom into a bath of electromagnetic field or for a photon detection experiment where an excitation is absorbed into an atom from the bath we can define coherent superpositions of frequency (or time) components normalized with a particle number of 1.

Classical electrodynamics has a simple form in the reciprocal space and the electromagnetic field is decomposed into longitudinal and transverse components. [51, 126]

$$i\mathbf{k} \cdot \mathcal{E} = \frac{1}{\epsilon_0}\rho$$

$$i\mathbf{k} \cdot \mathcal{B} = 0$$

$$i\mathbf{k} \times \mathcal{E} = -\dot{\mathcal{B}}$$

$$i\mathbf{k} \times \mathcal{B} = \frac{1}{c^2}\dot{\mathcal{E}} + \frac{1}{\epsilon_0 c^2}j \tag{2.1}$$

A classical electric field can be represented by the complex representation, or analytical signal $E^{(+)}(\mathbf{r}, \mathbf{t})$. [127] All solutions of the Maxwell's equations, $E^{(+)}(\mathbf{r}, \mathbf{t})$ can be considered a vector in the Hilbert space of modes, the modal space. See ref. [127] for a review of the definitions and structures of the space. The mode is defined to be a vector field that is a normalized solution of the Maxwell equations in vacuum.

For a field propagating in the +z direction,

$$E^{(+)}(\mathbf{r}, t) = \sum_{i,p,r} \mathcal{F}_{i,p,r}\mathbf{f}_{i,p,r}(\mathbf{r}, t) = \sum_{m} \mathcal{F}_m\mathbf{f}_m(\mathbf{r}, t) \tag{2.2}$$

$$\mathbf{f}_{i,p,r}(\mathbf{r}, t) = \epsilon_{\mathbf{i}}\mathbf{f}_p^{(T)}(x, y, z)\mathbf{f}_r^{(L)}(t, z) \tag{2.3}$$

where $\epsilon_{\mathbf{i}}$ are the two orthogonal polarization vectors in the x-y plane, $\mathbf{f}_{\mathbf{p}}^{(\mathbf{T})}(\mathbf{x}, \mathbf{y}, \mathbf{z})$ is the transverse or spatial part, $\mathbf{f}_{\mathbf{r}}^{(\mathbf{L})}(\mathbf{t}, \mathbf{z})$ the longitudinal or temporal. This separation of mode functions help identify the possible excitations (photons) in the quantized version of the electromagnetic fields. In a beamlike geometry or a one dimensional waveguide (oriented along the z-axis), the translationaly symmetric direction is the z-axis alone and the reciprocal vector representations in eq. has

only k_z points. The transverse component of the mode function, $\mathbf{f_p^{(T)}}(\mathbf{x}, \mathbf{y}, \mathbf{z})$ is determined by the transverse boundary conditions.

Under the paraxial approximation (wave-vectors close to a particular $\vec{k}_0$) and narrow-band approximation (frequencies close to a central frequency, $\omega_0 = c|\mathbf{k_0}|$); the $E^{(+)}(\mathbf{r}, \mathbf{t})$ can be resolved into a product of envelope functions and the plane wave, $e^{i(k_0 z - \omega t)}$.

$$E^{(+)}(\mathbf{r}, \mathbf{t}) = \mathbf{e^{i(k_0 z - \omega t)}} \sum_{\mathbf{i}, \mathbf{p}, \mathbf{r}} \epsilon_{\mathbf{i}} \mathbf{f_p^{(T)}}(\mathbf{x}, \mathbf{y}, \mathbf{z}) \mathbf{f_r^{(L)}}(\mathbf{t}, \mathbf{z}) \tag{2.4}$$

The quantum extension of the classical complex field $E^{(+)}(\mathbf{r}, \mathbf{t})$, is written in the Heisenberg picture so as to get the time dependence for the operators. [127]

$$\hat{E}(\mathbf{r}, \mathbf{t}) = \hat{\mathbf{E}}^{(+)}(\mathbf{r}, \mathbf{t}) + \hat{\mathbf{E}}^{(-)}(\mathbf{r}, \mathbf{t})$$

$$\hat{E}^{(+)}(\mathbf{r}, \mathbf{t}) = \sum_{\mathbf{l}} \mathscr{E}_{\mathbf{l}}^{(\mathbf{1})} \hat{\mathbf{a}}_{\mathbf{l}} \mathbf{u}_{\mathbf{l}}(\mathbf{r}, \mathbf{t}) \tag{2.5}$$

$$\mathbf{u}_{\mathbf{l}}(\mathbf{r}, \mathbf{t}) = \epsilon_{\mathbf{l}} \mathbf{e^{k_i \cdot r - \omega_l t}}$$

$$\mathscr{E}_l^{(1)} = \sqrt{\frac{\hbar \omega_l}{2 \epsilon_0 V}}$$

The expansion is in the basis of monochromatic plane wave modes $u_l(\mathbf{r}, \mathbf{t})$. The expansion eq. (2.5) is not unique, $\hat{E}^{(+)}(\mathbf{r}, \mathbf{t})$ can be expanded into other modal bases (solutions of the wave equations). [128] Unitary transformations can be found between modal bases and also between the the corresponding creation and annihilation operators. [127, 128]

In a waveguide oriented along the z-axis, we once again have k_z the only continuous mode (plane wave mode) index. The transverse functions have mode

labels determined by the boundary conditions.

$$\mathbf{u_l(r,t)} = \epsilon_l \mathbf{f_p^{(T)}(x,y,z)} e^{\mathbf{k_i \cdot z} - \omega_l t} \tag{2.6}$$

We can identify the degrees of freedoms (DOF) that a photon can have from the translational symmetry of the problem and polarization. In free space, light has four DOFs e.g. helicity and the three components of the momentum vector. [129] In a beamlike geometry or an one dimensional waveguide we have polarization, two transverse mode profile and the longitudinal (or time) profile ([129]). A photon can reside in any of the DOFs that light has and quantized electromagnetic field theories have been developed for all possible photon wavepackets. The excitations can be separated into two components. The Transverse Electric (TE) and transverse Magnetic (TM) modes. TMs are defined with the condition $H_z = 0$ and only electric field has a component parallel to the z-axis (E_z). Knowledge of E_z is sufficient for complete determination of the relevant modes,

$$E_x = -i\frac{k_z}{k_\rho^2}\frac{\partial E_z}{\partial x}, \quad E_y = -i\frac{k_z}{k_\rho^2}\frac{\partial E_z}{\partial y}, \quad H_x = i\frac{\omega\mu}{k_\rho^2}\frac{\partial E_z}{\partial y}, \quad H_y = -i\frac{\omega\mu}{k_\rho^2}\frac{\partial E_z}{\partial x} \tag{2.7}$$

The field-orthogonal temporal modes (connected to the longitudinal DOF or temporal DOF only) enable us to define a photon wavepacket as a coherent superposition of monochromatic wave modes [129, 130].

$$|A_j\rangle = \int d\omega f_j(\omega)\hat{a}^\dagger(\omega)|0\rangle \equiv \hat{A}_j^\dagger|0\rangle \tag{2.8}$$

In the time domain we have corresponding creation operators,

$$|A_j\rangle = \int dt \tilde{f}_j(t) \hat{A}^\dagger(t)|0\rangle \equiv \hat{A}_j^\dagger|0\rangle \tag{2.9}$$

The definitions of the Fourier transform are

$$\hat{a}^\dagger(\omega) = \frac{1}{\sqrt{2\pi}} \int dt e^{i\omega t} \hat{A}^\dagger(t), \qquad \hat{A}^\dagger(t) = \frac{1}{\sqrt{2\pi}} \int d\omega e^{-i\omega t} \hat{A}^\dagger(\omega) \tag{2.10}$$

$$\tilde{f}_j(t) = \frac{1}{\sqrt{2\pi}} \int d\omega e^{i\omega t} f_j(\omega), \qquad f_j(\omega) = \frac{1}{\sqrt{2\pi}} \int dt e^{-i\omega t} \tilde{f}_j(t) \tag{2.11}$$

The broadband mode operator $\hat{A}_j$ follows the Bosonic commutation relations [129],

$$\hat{A}_j^\dagger = \int d\omega f_j(\omega) \hat{a}^\dagger(\omega) = \int dt \tilde{f}_j(t) \hat{A}^\dagger(t) \tag{2.12}$$

$$\left[\hat{A}_i, \hat{A}_j^\dagger\right] = \delta_{ij} \tag{2.13}$$

Temporal modes are orthogonal in both time and frequency domain and are important for Quantum Information Science (QIS) applications.

$$\int d\omega f_j^*(\omega) f_k(\omega) = \int dt \tilde{f}_j^*(t) \tilde{f}_k(t) = \delta_{jk} \tag{2.14}$$

Similar single photon wave-packet creation operator can be defined for twisted photon pulse, [131], (where the photon resides in the helicity degree of freedom)

$$\hat{a}_{\xi\lambda}^\dagger = \int d^3k \xi_\lambda(\mathbf{k}) \hat{\mathbf{a}}_{\mathbf{k}\lambda}^\dagger \tag{2.15}$$

47

The Spectral Amplitude Function (SAF), $\xi_\lambda(\mathbf{k})$ of a twisted pulse with deterministic Orbital Angular Momentum (OAM) can be written

$$\xi_\lambda(\mathbf{k}) = \frac{1}{\sqrt{2\pi}}\eta_\lambda(\mathbf{k_z}, \rho_{\mathbf{k}})\mathbf{e^{im\phi_k}} \tag{2.16}$$

In this dissertation, we are interested in the photon wavepackets in the temporal or longitudinal DOF. The photon absorber is placed at the end of a one dimensional waveguide and interacts with any photon or photons travelling through the waveguide. Two (frequency) un-entangled single-photon wavepackets in two polarizations (or spatial) modes

$$|\psi_2\rangle = |\psi_\alpha\rangle|\psi_\beta\rangle \tag{2.17}$$

$$= \int d\omega_1 g_\alpha(\omega_1)b_1^\dagger(\omega_1) \int d\omega_2 g_\beta(\omega_2)b_2^\dagger(\omega_2)|vac\rangle \tag{2.18}$$

We do not consider entangled photons. Parametric Down Conversion (PDC) can generate spectrally (time) entangled photon pairs. [129, 130]

$$|\Psi\rangle = \int d\omega_s d\omega_i f(\omega_s, \omega_i)\hat{a}^\dagger(\omega_s)\hat{b}^\dagger(\omega_i)|0, 0\rangle \tag{2.19}$$

where the Joint Spectral Amplitude ($f(\omega_s, \omega_i)$) cannot be factorised as in eq. (4.22). But the important point is the transverse spatial mode profile is decoupled which is determined solely by the waveguide's features.

Note that the two photons in eq. (4.22) need not have the same polarization. In fact it is extremely unlikely for the two to have the same polarization (as well as transverse profile) i.e. reside in the same continuum.

2.2. Atoms in a single mode Electromagnetic Field

Optical transition and resonance fluorescence problems exploit the dipole coupling of the field and atom. For a d-level atom, we consider the single mode field nearly resonant with two of the levels of the atom. So, $|e\rangle$ and $|g\rangle$ are two of the d-levels, H_I mentioned would fit inside the d-dimensional Hamiltonian for the d-level [132].

$$H_I = (|g\rangle\langle e| + |e\rangle\langle g|)\,\langle g|H_I|e\rangle \tag{2.20}$$

Eq. 2.20 only clarifies the structure of the Hamiltonian matrix elements in the linear space of operators acting on the atomic part of the Hilbert space. The explicit H_I act on the product space of the atom and field Hilbert space and will be presented shortly (in eq. 2.23).

The single mode electromagnetic field is a classical plane-wave field of the form,

$$\mathbf{E}(\mathbf{x}, \mathbf{t}) = \mathbf{E_0}\left[\mathbf{e^{i(kx-\omega t)}} + \mathbf{c.c.}\right] \tag{2.21}$$

where, the field amplitude, $\mathbf{E_0}$ is taken to be real. Quantization of the electromagnetic field is not always necessary [132]. We take, $\hbar\omega \approx E_e - E_g$, hence all electronic states except $|g\rangle$ and $|e\rangle$ will be less important in the rotating frame of the field..

2.2.1. The Dipole Approximation

The d-level atomic Hamiltonian (a d dimensional operator) can be written as,

$$H_a = \sum_{k,j=1}^{d} (H_a)_{kj} |k\rangle\langle j| = \sum_{j=1}^{d} E_j |j\rangle\langle j| \tag{2.22}$$

The single mode electromagnetic field with frequency, ω would have the energy of a single harmonic oscillator with $H_f = \hbar\omega a^\dagger a$ and interact with the atom with the Hamiltonian part, $H_{af} = -\vec{d}.\vec{E}$. Here $\vec{d} = e\vec{r}$ denotes the dipole moment operator and $\vec{E}$ the external quantum electric field at the position of the atom. In the rotating wave defined by, $H_0 = e^{i\omega t/\hbar a^\dagger a + i/\hbar \sum_{j=1}^{d} \omega_j A_{jj} t}$, and in the long wavelength approximation ($e^{i\vec{k}.\vec{x}} \approx 1$), the interaction is, (ref. [133, 134])

$$H_I = H_{af} = -\frac{i}{2} \sum_{j\neq k=1}^{d} \mu_{jk} (|j\rangle\langle k| + |k\rangle\langle j|) (a - a^\dagger) \tag{2.23}$$

with $\mu_{jk} = \sqrt{\frac{2\pi\hbar\omega}{V}} \sum_\beta \left(\vec{E}_0.\vec{e}_\beta(x_\beta)_{jk}\right)$, $E_0 = \sqrt{\frac{\hbar\omega}{2\epsilon_0 V}}$. $\Omega = d_{ge}E_0/\hbar$, where d_{ge} is the matrix element of the electric dipole operator. The complete Hamiltonian would be,

$$H = \sum_{j=1}^{d} \omega_j A_{jj} - \frac{i}{2} \sum_{j\neq k=1}^{d} \mu_{jk} (|j\rangle\langle k| + |k\rangle\langle j|) (a - a^\dagger) \tag{2.24}$$

2.2.2. The Jaynes Cummings Interaction

The interaction Hamiltonian, (ref. [132, 134])

$$H = \sum_{j=1}^{d} \omega_j A_{jj} - \frac{i}{2} \sum_{j \neq k=1}^{d} \mu_{jk} \left(\sigma^+ + \sigma^- \right) \left(a - a^\dagger \right)$$

$$= \sum_{j=1}^{d} \omega_j A_{jj} - \frac{i}{2} \sum_{j \neq k=1}^{d} \mu_{jk} \left(\sigma^+ a - \sigma^- a^\dagger - \sigma^+ a^\dagger + \sigma^- a \right) \tag{2.25}$$

In the original frame of the laboratory or "lab-frame", $\sigma^+ a - \sigma^- a^\dagger$ is accompanied by no time dependence and $-\sigma^+ a^\dagger + \sigma^- a$ is accompanied by the time dependence of $e^{\pm i2\omega t}$. The Jaynes Cummings Hamiltonian ignores the high frequency components. Also, $\sigma^+ = |j\rangle\langle k|$ if $E_j - E_k = E_e - E_g > 0$.

$$H_{JC} = \sum_{j=1}^{d} \omega_j A_{jj} - \frac{i}{2} \sum_{j \neq k=1}^{d} \mu_{jk} \left(\sigma^+ a - \sigma^- a^\dagger \right) \tag{2.26}$$

This Hamiltonian commutes with the total excitation number, $a^\dagger a + \frac{1}{2}\sigma_z$. We can call the two possible energy level of the atom or molecule $\psi_m, m = 1, 2$ and the number of quanta in the field oscillator n, $\Phi_n, n = 0, 1, 2, 3, ...$ [106]. Then, the state vectors, $\Phi_n \otimes \psi_m$ form a basis of the Hamiltonian. We can write out the matrix elements of the Hamiltonian in the said basis,

$$\langle mn|H|m'n' \rangle = (E_m + n\hbar\omega)\delta_{mm'}\delta_{nn'} + \langle mn|H_{int}|m'n' \rangle$$

$$H_{int} = -\vec{\mu}.\vec{E}$$

$$\langle mn|\mu_z|m'n' \rangle = \mu(1 - \delta_{mm'})\delta_{nn'}$$

$$\langle mn|H_{int}|m'n' \rangle = \hbar\alpha(1 - \delta_{m,m'})[\sqrt{n}\delta_{n,n'+1} + \sqrt{n+1}\delta_{n+1,n'}]. \tag{2.27}$$

2.3. Open System dynamics

The Liouville representation of quantum map, S can be done with the aid of S expressed in a particular basis. In a d-dimensional quantum system with the Hilbert space, $\mathcal{H}_d$, operator A is a map, $A : \mathcal{H}_d \to \mathcal{H}_d$, and S is a mapping for the operator A, $S : L(\mathcal{H}_d) \to L(\mathcal{H}_d)$. L is the vector space of linear operators acting on $\mathcal{H}_d$ [135]. We define a Liouvillian dissipator map for density matrix, $\mathcal{D} : \rho \to X\rho X^\dagger - \frac{1}{2}X^\dagger X\rho - \frac{1}{2}\rho X^\dagger X$ and a Liouvillian-type dissipator map for operator A, $\mathcal{D}' : A \to X^\dagger AX - \frac{1}{2}X^\dagger XA - \frac{1}{2}AX^\dagger X$, commonly known as superoperators. X is called a quantum jump operator. The Schrödinger picture evolution of the density matrix and the Heisenberg picture evolution of the system operator are determined by the Liouvillian and the Liouvillian type equation respectively.

$$\dot{\rho} = \mathcal{L}\rho = -\frac{i}{\hbar}\left[H_{sys}, \rho\right] + \mathcal{D}_X\rho \tag{2.28}$$

$$\mathcal{D}_X\rho = X\rho X^\dagger - \frac{1}{2}X^\dagger X\rho - \frac{1}{2}\rho X^\dagger X$$

$$\dot{\hat{A}} = \mathcal{L}'\hat{A} = \frac{i}{\hbar}\left[H_{sys}, \hat{A}\right] + \mathcal{D}'_X\hat{A} \tag{2.29}$$

$$\mathcal{D}'_X\hat{A} = X^\dagger \hat{A}X - \frac{1}{2}X^\dagger X\hat{A} - \frac{1}{2}\hat{A}X^\dagger X$$

Choosing $\{P_n\}_{n=1}^{d^2}$ for a Hermitian operator orthonormal basis (w.r.t. Hilbert-Schmidt inner product), we can represent any operator at any time with its components in the basis. The inner product of A and B is defined as

$(A|B) := Tr[A^\dagger B].$

$$A = \frac{1}{d} \sum_k Tr[P_k A] P_k$$

$$S(A) = \frac{1}{d} \sum_{n,m} S_{nm} Tr[P_m A] P_n$$

$$S_{nm} = \frac{1}{d} Tr[P_n S(P_m)]$$

$$(P_n|P_m) := Tr[P_n^\dagger P_m]$$

The operator A and map S both can be specified with the orthonormal basis $\{P_n\}$. This is the most crucial tool for the calculations. The basis $\{P_n\}$ can be taken to be time stationary. There exists an under-appreciated method for solving equations like (2.28) and (2.29) from [136]. For a total system that is a cascade of three or more constituent quantum mechanical Hilbert spaces, the density matrix can be expanded in one, two or all three constituent Hilbert space bases to solve eq. (2.28). The coefficients of expansion are complex numbers if expanded in all three constituent Hilbert space bases. And they are operators if expended in less than three constituent Hilbert spaces. The same structure applies in expanding into vector spaces of operators in solving eq. (2.29) for the evolution of an operator.

For a cascaded system of a discrete bosonic cavity a (with a maximum photon of N_a), a N level atom F and another discrete bosonic cavity mode, c (with a maximum photon of N_c) under the action of a system Hamiltonian and some

collapse operators, an arbitrary operator, $\hat{K}$ can be expanded as

$$\hat{K} = \sum_{i,j=1}^{N_a} \sum_{k,l=1}^{N} \hat{K}_{ij\otimes kl}(t)|a^\dagger a = i, F_k\rangle\langle a^\dagger a = j, F_l| \qquad (2.30)$$

$$= \sum_{i,j=1}^{N_a} \sum_{k,l=1}^{N} \sum_{m,n=1}^{N_c} K_{ij\otimes kl\otimes ab}(t)|a^\dagger a = i, F_k, c^\dagger c = m\rangle\langle a^\dagger a = j, F_l, c^\dagger c = n| \qquad (2.31)$$

The expansion coefficients in eq. (2.30) are operators and in eq. (2.31) are complex numbers. The basis in either case is time stationary and the time dependence is entirely in the expansion coefficients. If the Schrödinger picture is opted for, eq. (2.31) is solved with the density matrix, ρ expanded (gradually) in complete bases. The two picture solutions are to be consistent with the condition,

$$Tr[\rho(t)K(t_0)] = Tr[\rho(t_0)K(t)] \qquad (2.32)$$

An example of such expansion in operator coefficients to solve a Liouvillian equation (2.28) can be found in [136]. In a problem that is solved in chapter 3, a cascaded system of a discrete bosonic cavity ($N_a = 1$), a N=3 level atom F, and a discrete cavity c, with the atom F driving mode c in the state $|F_2\rangle$ with the Hamiltonian term $H_{F-c} = i|F_2\rangle\langle F_2|(c - c^\dagger)$, we get the following equation set

(decoupled from all the other) of equations. This set has an interesting feature.

$$\dot{\hat{K}}_{00\otimes00} = \mathcal{D}'_{\sqrt{\Gamma}c}\hat{K}_{00\otimes00}$$

$$\dot{\hat{K}}_{00\otimes22} = i[iF(c - c^\dagger), \hat{K}_{00\otimes22}] + \mathcal{D}'_{\sqrt{\Gamma}c}\hat{K}_{00\otimes22}$$

$$\dot{\hat{K}}_{00\otimes11} = -(\gamma_1 + \gamma_2)\hat{K}_{00\otimes11}$$

$$+\mathcal{D}'_{\sqrt{\Gamma}c}\hat{K}_{00\otimes11} + \gamma_1\hat{K}_{00\otimes00} + \gamma_2\hat{K}_{00\otimes22}$$

$$\dot{\hat{K}}_{10\otimes01} = \dot{\hat{K}}_{01\otimes10} = -\frac{(\gamma_1 + \gamma_2 + \kappa)}{2}\hat{K}_{10\otimes01}$$

$$+\sqrt{\kappa\gamma_1}(\hat{K}_{00\otimes00} - \hat{K}_{00\otimes11}) + \mathcal{D}'_{\sqrt{\Gamma}c}\hat{K}_{10\otimes01}$$

In the composite operator, $\hat{1} \otimes \hat{1} \otimes \hat{c}(t)$ operator, all the diagonal operators, $\hat{K}_{ii\otimes jj}$ are $\hat{c}$ itself. So the first two equations look like the following,

$$\dot{\hat{c}} = \mathcal{D}'_{\sqrt{\Gamma}c}\hat{c}$$

$$\dot{\hat{c}} = i[iF(c - c^\dagger), \hat{c}] + \mathcal{D}'_{\sqrt{\Gamma}c}\hat{c} \tag{2.33}$$

The two equations are for a cavity mode under dissipative dynamics and a driven cavity mode under dissipative dynamics.

In essence, every single equation in the set above behaves as a stand-alone (except for the coupling to other ones) system initialized in a certain density matrix (in the sense of eq. (2.32)). The have the appearance of copies of the same system running in parallel initialized in all the different possibilities. The off-diagonal elements contribute to the noise in the output signal. Schrödinger equation evolution and quantum mechanics is determinsitic. Our Heisenberg evolution is a counting problem of how many initial state matrices can end up in the observable eigenvalue observed. The probability of an observable expectation

value is proportional to the number of initial states that evolved deterministically would end up in states consistent with it. As our model shows initial unphysical density matrices contribute to the measurement fluctuations the same way the physical density matrices do. Mathematically invalid solutions are supported by nature sometimes. ρ_{01} is a physically invalid state, but it has a bearing on physical observable statistics!

We can emulate the multi-photon Fock state equations of ref. [113] with expanding the density matrix, $\rho(t)$ in a complete basis. In chapter 4, we have an explicit example of this. The operator evolution calculation is also facilitated by expanding them in the complete orthonormal basis, where the sparsity of the couplings between the equations make analytical computation possible.

The variance of a quantum mechanical observable (represented by a Hermitian matrix M) is

$$var(M) = \langle M^2 \rangle - (\langle M \rangle)^2$$

$$var(M) = (Tr[M \times M \times \rho(t_0)])^2 - (Tr[M \times \rho(t_0)])^2 \tag{2.34}$$

For the case of initial density matrix being a pure state, $\rho(t_0) = \sum_{i,j} \delta_{i,i_0}\delta_{j,i_0}$, we get an elegant expression for $var(M(t))$,

$$var(M(t)) = \sum_{k \neq i_0} |M_{i_0 k}(t)|^2 \tag{2.35}$$

So off-diagonal couplings in the equation (2.29) for any diagonal element, add to the variance and hence noise. If the initial density matrix is a mixed state, the expression for noise would account for the added classical uncertainty as well.

2.4. Systems and meters

A brief review from [112]. The initial system state vector is $|\psi(t)\rangle$ and the meter system has initial state vector $|\theta(t)\rangle$. Hence, the initial combined state

$$|\Psi(t)\rangle = |\theta(t)\rangle|\psi(t)\rangle \qquad (2.36)$$

The product state can be written for only at time t. The two systems evolve together for a time T_1 by a unitary evolution operator $\hat{U}(t + T_1, t) \equiv \hat{U}(T_1)$. The combined system-meter at time T_1 is

$$|\Psi(t + T_1)\rangle = \hat{U}(T_1)|\theta(t)\rangle|\psi(t)\rangle \qquad (2.37)$$

Let the meter be measured projectively over a time interval T_2, and $T = T_1 + T_2$. We can assume the system+meter does not evolve in this interval (T_2 may be negligible or the coupling time-dependent)

The projection operator for the meter is $\hat{\Pi}_r = \hat{\pi}_r \otimes \hat{1}$, where $|r\rangle$ forms an orthonormal basis for the meter Hilbert space. The final combined state is

$$|\Psi_r(t + T)\rangle = \frac{|r\rangle\langle r|\hat{U}(T_1)|\theta(t)\rangle|\psi(t)\rangle}{\sqrt{\rho_r}} \qquad (2.38)$$

$$\rho_r = Pr[R = r] = \langle\psi(t)|\langle\theta(t)|\hat{U}^\dagger(T_1)[|r\rangle\langle r| \otimes \hat{1}]\hat{U}(T_1)|\theta(t)\rangle|\psi(t)\rangle \qquad (2.39)$$

ρ_r is the probability of obtaining the value r for the result R.

Post measurement system and meter are disentangled once again.

$$|\Psi_r(t + T)\rangle = |r\rangle\frac{\hat{M}_r|\psi(t)\rangle}{\sqrt{\rho_r}} \qquad (2.40)$$

$$\hat{M}_r = \langle r|\hat{U}(T_1)|\theta(t)\rangle, \qquad a\ measurement\ operator \qquad (2.41)$$

57

where $\hat{M}_r$ is an operator that acts only in the system Hilbert space. The probability distribution for R can be written as

$$\Phi_r = \langle \psi(t)|\hat{M}_r^\dagger \hat{M}_r|\psi(t)\rangle \tag{2.42}$$

2.4.1. Measurement operators and effects

Measurement can be completely specified in terms of the measurement operators, $\hat{M}_r$. Given that after the measurement of duration T, the result R has the value r, the conditional state of the system is

$$|\psi_r(t+T)\rangle = \frac{\hat{M}_r|\psi(t)\rangle}{\sqrt{\Phi_r}} \tag{2.43}$$

The probability operators, or effects are defined to be

$$\hat{E}_r = \hat{M}_r^\dagger \hat{M}_r \tag{2.44}$$

Their expectation values give the probabilities. Probabilities need to add up to unity and a completeness condition on the measurement operators is imposed:

$$\sum_r \hat{E}_r = \hat{1}_S \tag{2.45}$$

There are two restrictions on the set of measurement operators: 1) they have to be positive, 2) $\hat{E}_r : r$ is a resolution of the identity for the system Hilbert space.

Generalized measurement does not require physical observables. Measurement results r are simply labels, they can be integers, fractions, real or complex (unlike physical observables that are real and eigenvalues of a Hermitian

operator). The set of $\hat{E}_r$ constitute a Positive Operator Valued Measure (POVM) on the space of results r. We do not need a probability distribution over space of r, but rather only the POVM. For the general case of mixed states, the conditioned state for the measurement result r is,

$$\rho_r(t+T) = \frac{\mathcal{J}[\hat{M}_r]\rho(t)}{\rho_r}$$

$$\rho_r = Tr[\rho(t)\hat{E}_r]$$

$$\mathcal{J}[\hat{A}]\hat{B} \equiv \hat{A}\hat{B}\hat{A}^\dagger$$

$\mathcal{O}_r = \mathcal{J}[\hat{M}_r]$ the $operation$ for $r:$ a $superoperator$

Superoperators map operators to operators, $\mathcal{J}$ is a superoperator. The class of superoperators (called the completely positive maps) can map physical states to states.

In summary:

1. It is good enough to assume that we projectively measure the 'meter' i.e. the electromagnetic continua, although subsequent measurements are also done. They involve electronic signal, number plate, retina, brain signal etc. But macroscopic objects decohere fast. So, a projective measurement on the meter is a good enough description, we have a classical signal.

2. Measurement disentangles the system and meter.

3. $\hat{M}_r$ are the measurement operators, act only on the system and in general, are not unitary.

4. What state we prepare the meter state at time, t=0, (called the fiducial state) can give rise to quantum noise. If the measurement basis states of the meter (that we can take projective measurements on) are different from the fiducial state

(even if it is a pure state), we shall have a distribution of outputs, a quantum noise. If the fiducial state is a mixed state, we get a noise of classical nature on top of it.

5. There is a way of representing the evolution during $T_1 + T_2$ using the unitary operator,G.

6. The most general formulation of quantum measurement theory: The operator $\mathcal{O}_r$ for the result r is a Completely Positive (CP) superoperator. An operation can always be written as,

$$\mathcal{O}_r = \sum_j \mathcal{J}[\hat{\Omega}_{r,j}] \tag{2.46}$$

for some set of operators, $\hat{\Omega}_{r,j} : j$ which is not unique. $\hat{\Omega}_{r,j} : j$ is the basic element of the theory, which takes the a-priori system state to the conditioned a-posteriori state:

$$\tilde{\rho}_r(t+T) = \mathcal{O}_r \rho(t) \tag{2.47}$$

And now we have completely replaced the measurement operators, $\hat{M}_r$.

It is worth mentioning here that Quantum Darwinism theory takes a different approach and we discuss that later.

A Back-Action Evading (BAE) measurement is one where the statistics of an observable does not change. A projective measurement before or after the BAE would give the same statistics. A Quantum Non Demolition measurement is a stronger condition, demanding that the observable, $\hat{X}$ does not evolve in the Heisenberg picture (all but ensures preserving the statistics).

BAE: The total operation for the measurement in question being $\mathcal{O} = \sum_r \mathcal{O}_r$,

$$Tr[\hat{\Pi}_x \rho] = Tr[\hat{\Pi}_x \mathcal{O}\rho] \tag{2.48}$$

QND: X is a QND observable (effects/probabilities are functions of $\hat{X}$) if $\hat{X}$ $(= \hat{X}_S \otimes \hat{1}_A)$ is a constant of motion in the Heisenberg picture.

$$\hat{X} = \hat{U}^\dagger(T_1)\hat{X}\hat{U}(T_1) \tag{2.49}$$

$\hat{U}(T_1)$ is the system-meter coupling.

2.4.2. Classical and Quantum uncertainties

For two quantum operators, $\hat{x}$ and $\hat{y}$, we take up the definition

$$\delta\hat{x} = \hat{x} - \langle\hat{x}\rangle, \qquad \delta\hat{y} = \hat{y} - \langle\hat{y}\rangle$$

where, $\langle..\rangle$ refers to complete expectation values arrived at from a combination of quantum mechanical and classical uncertainties. We have the constraint [137],

$$\langle\delta x^2\rangle\langle\delta y^2\rangle \geq \frac{1}{4}|\langle[\delta x, \delta y]\rangle|^2 + \frac{1}{4}|\langle\{\delta x, \delta y\}\rangle|^2 \tag{2.50}$$

In classical noise theory, $\hat{x}$ and $\hat{y}$ commutes and, we have,

$$\langle\delta x^2\rangle\langle\delta y^2\rangle \geq \sigma_{xy}^2 \tag{2.51}$$

But in quantum mechanical open systems (once we integrate out the bath modes), we have a mixed state with classical and quantum statistical properties.

$$\Delta x \Delta p \geq \sqrt{\frac{1}{4}\hbar^2 + \sigma_{xp}^2} \tag{2.52}$$

Therefore, in our open system model of photodetection, the uncertainty relationships of canonically conjugate varibles have the extra contribution from the classical statistics as well. I refer to a discussion in chapter 1 of ref. [137], to point out that certain operator (or observable) may be measured with more certainty than others. One quadrature of a harmonic oscillator mode (say $\hat{p}$) may be a more attractive choice for measurement observable than the other quadrature ($\hat{x}$). For the motion of a free particle without any thermal noise, the classical Hamilton equations and the quantum Heisenberg equations of motion are of the same form,

$$m\dot{x} = p \qquad \dot{p} = 0$$

We now consider the repeated measurement of the position of the free particle at intervals of τ.

$$x(t+\tau) = p(t)\tau/m + x(t)$$

$$\langle \delta x(t+\tau)^2 \rangle = \langle \delta x(t)^2 \rangle + (\tau/m)^2 \langle \delta p(t)^2 \rangle + \tau/m \langle \delta x, \delta p \rangle$$

A precise measurement of x(t) would cause $\langle \delta p(t)^2 \rangle \to \infty$ and $\langle \delta x(t+\tau)^2 \rangle \to \infty$. It becomes impossible to measure x precisely at any subsequent moment. However, p can be measured repeatedly without introduction of such measurement back action. $p(t+\tau) = p(t)$.

For a specific choice of the Hamiltonian, $\tilde{H}_c(F) = 2iF\cos(\omega_F t)(c - c^\dagger)$, $\hat{p} \propto i(c - c^\dagger)$ (commutes with the Hamiltonian for zero detuning) would be preferred as a Quantum Non Demolition Observable over the other quadrature variable, $\hat{x} \propto (c + c^\dagger)$ for repeated measurements.

2.5. Linear and nonlinear quantum amplification

In principle, the "input-output relationship" for some operator are always obtainable with a brute-force calculation.

$$\hat{b}(t) = e^{i\hat{H}_{tot}t/\hbar}\hat{b}(0)e^{-i\hat{H}_{tot}t/\hbar}$$

$$\text{for, } \hat{H}_{tot} = \hat{H}_0 + \hat{V} \tag{2.53}$$

$$\hat{b}(t) = e^{i\hat{H}_0 t/\hbar}\hat{b}(0)e^{-i\hat{H}_0 t/\hbar} \tag{2.54}$$

A lot of the times, the important part of the transformation can be achieved by splitting the Hamiltonian, $\hat{H}_{tot}$ into a tractable part, $\hat{H}_0$ and a complex part, $\hat{V}$ (in eq. (2.53)) as is done in the famous Caves' model. The primary mode, $\hat{a}$ interacts with the ancillary mode, $\hat{b}$ (can be called amplifier's internal mode)

$$\hat{H}_I = \hat{\tilde{H}}_{LPA} = i\hbar\kappa(\hat{a}\hat{b} - \hat{a}^\dagger\hat{b}^\dagger)$$

$$\hat{U}_I(t) = e^{-i\hat{H}_I t/\hbar} = e^{r(\hat{a}\hat{b} - \hat{a}^\dagger\hat{b}^\dagger)} \equiv \hat{S}(r), \quad r = \kappa t$$

$\hat{S}(r)$ is the two mode squeezing operator. The a mode evolves in the Heisenberg picture,

$$\hat{a}_{out} = \hat{S}^\dagger\hat{a}\hat{S} = \hat{a}\cosh(r) - \hat{b}^\dagger\sinh(r) = g\hat{a} - \hat{b}^\dagger\sqrt{g^2 - 1} \tag{2.55}$$

The transformation belongs to SU(1,1) algebra. Quantum Mechanics demands unitarity of evolution (for the system+environment or the universe) and hence requires commutation relationships to be preserved.

$$\hat{a}_{out} = \sqrt{G}\hat{a}_{in} + \sqrt{G-1}\hat{b}_{in}^{\dagger} = \sqrt{G}\hat{a}_{in} + \hat{L}^{\dagger} \qquad (2.56)$$

$$\left[\hat{L}, \hat{L}^{\dagger}\right] = G - 1 \qquad (2.57)$$

$$\Delta\hat{L}\Delta\hat{L}^{\dagger} \geq \hbar[\hat{L}, \hat{L}^{\dagger}] = \frac{\hbar}{2}(G^2 - 1) \qquad (2.58)$$

The $\hat{b}_{in}$ operator is the amplifier's internal noise mode which must be added to preserve canonical commutation relationships. The relationship was generalized to show that amplifying currents carried by either Fermions or Bosons require addition of noise currents holding a relationship similar to eq. (2.57) [105]. It was also noted that, a phase sensitive amplifier can amplify one of the $\hat{x}$ or $\hat{p}$ quadratures noiselessly while attenuating the other.

$$\hat{x}_{out} = \sqrt{G}\hat{x}_{in}, \qquad \hat{p}_{out} = \hat{p}_{in}/\sqrt{G} \qquad (2.59)$$

Eq.s (2.56) and (2.59) are both linear in the annihilation operators. The problem with linear amplification is that the noise mode is necessarily amplified Eq. (2.56). More generally, for linear amplifiers,

$$\hat{a}_{out} = e^{i\hat{H}_{tot}/\hbar}\hat{a}_{in}e^{-i\hat{H}_{tot}/\hbar} = \sqrt{G}\hat{a}_{in} + \sqrt{G-1}\hat{b}_{in}^{\dagger}$$

$$\hat{a}_{out}^{\dagger}\hat{a}_{out} = e^{i\hat{H}_{tot}/\hbar}\hat{a}_{in}^{\dagger}\hat{a}_{in}e^{-i\hat{H}_{tot}/\hbar}$$

$$= G\hat{a}_{in}^{\dagger}\hat{a}_{in} + (G-1)\hat{b}_{in}^{\dagger}\hat{b}_{in} + \sqrt{G(G-1)}(\hat{b}_{in}\hat{a}_{in} + \hat{a}_{in}^{\dagger}\hat{b}_{in}^{\dagger})$$

Diagonalizing equations like Eq. (2.60) are the reason the transformation in eq. (2.55) is given the name Bogoliubov transformation after the famous example of BCS superconductivity. $\hat{a}_{out}^{\dagger}\hat{a}_{out}$ is the diagonalized form. The output excitation expectation value, $\langle\hat{n}_{out}\rangle$ is calculated from either evolved states (Schrödinger picture) or evolved operators (Heisenberg picture) in accordance with eq. (2.62).

$$\langle\hat{n}_{out}\rangle = \langle\psi_{in}|e^{i\hat{H}_{tot}/\hbar}\hat{a}_{in}^{\dagger}\hat{a}_{in}e^{-i\hat{H}_{tot}/\hbar}|\psi_{in}\rangle \tag{2.60}$$

$$= \langle\psi_{out}|\hat{a}_{in}^{\dagger}\hat{a}_{in}|\psi_{out}\rangle \;\; The \; Schrdinger \; Picture \tag{2.61}$$

$$= \langle\psi_{in}|\hat{a}_{out}^{\dagger}\hat{a}_{out}|\psi_{in}\rangle \;\; The \; Heisenberg \; Picture \tag{2.62}$$

Eq. (2.60) enables calculation of the quantity in eq. (2.62) through initial state relationships alone. If we assume that G excitations are to be considered a classical macroscopic signal, we can see what initial state can cause such a click simply from the number of excitations in the initial state. For an initial state, $|\psi_{in}\rangle = |\hat{n}_a = 1, \hat{n}_b = 0\rangle$, the quantity $\hat{n}_{out}$ comes out to be G. So a single photon signal would be amplified to a "click". However, the initial state, $|\psi_{in}\rangle = |\hat{n}_a = 0, \hat{n}_b = 1\rangle$ would cause a click just as well (with G-1 excitations), with no input photons. This would count as a dark count, where a thermal excitation causes a click in the detector. The linear transformation in eq. (2.60) amplifies noise almost as much as it does the signal. Linear amplification transformations are plagued with this noise amplification property that render them non-ideal for the purpose of single photon detection ([1]).

The particular form of the transformation is mandated by the requirement of the commutation preservation. It was noted in [1] that, nonlinear amplification

transformations can be conceived of, that offer ways of amplifying an input signal without amplifying the noise excitations.

$$\hat{b}_{out}^{\dagger}\hat{b}_{out} = G\hat{a}_{in}^{\dagger}\hat{a}_{in} + \hat{b}_{in}^{\dagger}\hat{b}_{in} \qquad (2.63)$$

With such a nonlinear amplification scheme, $|\psi_{in}\rangle = |\hat{n}_a = 1, \hat{n}_b = 0\rangle$ would cause a click, $|\psi_{in}\rangle = |\hat{n}_a = 0, \hat{n}_b = 1\rangle$ would not. So nonlinear amplification (eq. (2.65)) mechanism would far outperform linear amplification schemes in terms of the Signal to Noise (SNR) ratios. Nonlinear amplification can be achieved with the addition of a single noise mode operator which is not amplified. That one mode of noise operator is, however, essential. Amplification with minimum noise addition is called "minimum noise amplification".

$$\hat{a}_{out} = \sqrt{G}\hat{a}_{in} + \sqrt{G-1}\hat{b}_{in}^{\dagger} \qquad \text{The Caves' relation}(linear)$$
$$\hat{b}_{out}^{\dagger}\hat{b}_{out} = \hat{b}_{in}^{\dagger}\hat{b}_{in} + G\hat{a}_{in}^{\dagger}\hat{a}_{in} \quad \text{Number amplification (nonlinear)} \qquad (2.64)$$
$$\hat{b}_{out} = \hat{S}\sqrt{(b^{\dagger}b)_{in} + G((b^{\dagger}b)_{in}}, \qquad (2.65)$$

$\hat{S}$ is a unitary operator which is designed so as to preserve the commutation relationship of the operator, $\hat{b}_{out}$ in eq. (2.65). Number amplification like in eq. (2.65) has improved SNR performance.

The Heisenberg evolution of an operator yields an input-output relationship for the operator, which enables easy calculation of the time evolved expectation values (such as $\langle\hat{n}_{out}\rangle$), only eigenvalue equations of the initial state suffice for the computation. This is always a good way for interpreting results in the Heisenberg picture. The matrix elements of the operators in some basis help calculate the time evolution of the expectation values of an operator (for a initial condition) which

66

coincide with the Schrödinger picture since matrix elements are the same across all pictures.

For the more general case of mixed/entangled states,

$$Tr[\rho(t_0)^\dagger g(t)] = Tr[\rho^\dagger(t)g(t_0)] \tag{2.66}$$

$$Tr[\rho(t_0)g(t)] = Tr[\rho(t)g(t_0)] \tag{2.67}$$

Each individual element of g(t), e.g. $\langle i|g(t)|j\rangle$ in a chosen basis can be interpreted as the expectation value of g(t) for a system initialized in $\rho(t_0) = \delta_{r,i}\delta_{c,j}$

2.6. Access to some example observables: Techniques of quantum optics

The number operator holds a special place in quantum mechanics, since the methods of measurement are reliant on photocurrent clicks that are proportional to intensity of a mode which is proportional to the number operator. Also, we have talked about why a quadrature of the field may be better suited for low noise detection in repeated weak measurements over the other. Therefore, we can do better by finding more suitable observables for low noise detection and better readout of the steadystate population of the atom. I now talk about a few schemes of finding more observables inside our absorber atom.

The Balanced Homodyne Detection (BHD) gives us photocurrent proportional to the difference between two intensities, $I_c - I_d = \langle \hat{n}_{cd} \rangle = \langle \hat{c}^\dagger\hat{c} - \hat{d}^\dagger\hat{d} \rangle$. $\hat{c}$ and $\hat{d}$ are mixed combinations of signal, $\hat{a}$ and reference $\hat{b}$, $\hat{c} = \frac{1}{\sqrt{2}}(\hat{a} + i\hat{b}), \quad \hat{d} = \frac{1}{\sqrt{2}}(\hat{b} + i\hat{a})$. In a homodyne detection scheme, a strong coherent field local oscillator (lo) is added to the field to be measured (the source field) and continuous

photoelectric detection is performed on the sum. For the continuous photoelectric detection of the field, $\hat{\mathcal{E}}(t)$

$$\hat{\mathcal{E}}(t) = e^{-i\omega_C t}\left[\hat{\mathcal{E}}_{lo} + \sqrt{\xi}\sqrt{2\kappa}\Delta\hat{\tilde{a}}(t')\right]$$

$\hat{\mathcal{E}}(t), \hat{\mathcal{E}}_{lo}$ are in units of photon flux. $\langle\hat{\mathcal{E}}_{lo} = \mathcal{E}_{lo}$, a c-number, is the local oscillator coherent amplitude, t' is a retarded time, ξ is the collection efficiency, $\sqrt{2\kappa}$ scales the source field for $2\kappa\Delta\hat{\tilde{a}}^\dagger\hat{\tilde{a}}(t)$ to have units of photon flux.

2.6.1. Quantum Stochastic Calculus

By coupling a microscopic system to a macroscopic system, the quantum features should be transferrable to the classical objects– a measurement readout. Decoherence is a consequence of environmental monitoring of a system via system-entanglement. Environmental monitoring has three main consequences, a) the suppression of interference effects at the level of the system, b) the selection of quasi-classical preferred states, and c) the robust and redundant encoding of information about the preferred states in the environment.

2.6.1.1. Stochastic Difference Equations

At each time, the solution to a stochastic difference equation is a random variable, which changes variable at each time step (not different random variables at each time points). $y_0, y_1, y_2, ...$ (noise increments) are random variables (x(0) may or may not be a random variable), and so $x(\Delta t), x(2\Delta t), x(3\Delta t), x(4\Delta t)$ are random variables.

Solution of a stochastic Difference equation: calculating the probability density functions of $x(t_n)$ (from the probability densities for all noise increments (y_ns) and x(0)).

2.6.1.2. Stochastic Differential Equation (SDE)

Stochastic Differential Equations are obtained by taking the $\Delta t \to 0$ limit of stochastic difference equations. The solution of a stochastic differential equation is a probability density for the value of x at all future ts. A process that fluctuates randomly in time is called a stochastic process. SDEs are thus driven by stochastic processes. The random increments that drive an SDE are referred to as noise ("the noise driven"). A set of values of the random increments (values sampled from the probability density) is called a "realization of the noise". A particular evolution for x, given a specific noise realization is called "a sample path for x".

The full solution to SDE: complete set of all possible sample paths and their probabilities. Simpler solution: Probability density for x at each time, correlation of x at one time with another.

Stochastic integral are defined as,

$$W(T) = \int_0^T dW, \qquad dW \text{ are called "Wiener process"} \tag{2.68}$$

The continuum limit of the Gaussian increments, dW, are referred to as being infinitesimal. A general SDE for a single variable x(t), is,

$$dx = f(x,t)dt + g(x,t)dW \tag{2.69}$$

2.6.2. Quantum Trajectories

We take the ideology of ref. [112], in defining a quantum trajectory as the path taken by the conditional state of a quantum system for which the unconditioned system evolves continuously. The unconditioned state is the one obtained by averaging over the random measurement results which condition the system. Quantum jumps are discontinuous conditioned evolution. Quantum jumps can be related to photon-counting measurements on the bath.

The evolution of an isolated quantum system in the absence of measurement is

$$|\psi(t+T)\rangle = U(T)|\psi(t)\rangle = exp(-iHT)|\psi(t)\rangle \tag{2.70}$$

We find the finite differential,

$$\lim_{\tau \to 0} \frac{|\psi(t+\tau)\rangle - |\psi(t)\rangle}{\tau} = -iH(t)|\psi(t)\rangle = finite \tag{2.71}$$

which governs the continuous evolution. The unconditioned state is obtained by averaging over all the possible measurement results. For a system we are monitoring, the differential of the density matrix,

$$\lim_{\tau \to 0} \frac{\rho(t+\tau) - \rho(t)}{\tau} = \dot{\rho}(t) \tag{2.72}$$

With T taken to be infinitesimal, the state matrix at time t+dt, averaging over all possible results,

$$\rho(t+dt) = \sum_r \mathcal{J}[\hat{M}_r(dt)]\rho(t)$$

70

where, $\rho(t + \tau) = \mathcal{L}_\tau[\rho(t)] = \rho(t) + O(\tau)$. $O(\tau)$ is a first-order contribution in τ. One of the operators, M_μ should be of order of unity. We can write it,

$$M_0 = \mathbf{1} - \mathbf{i K}\tau + \mathbf{O}(\tau^{\mathbf{2}})$$

K can also be put in terms of its Hermitian and antiHermitian parts, H and J respectively.

$$H = \hbar\frac{K + K^\dagger}{2}, \quad J = i\frac{K - K^\dagger}{2}$$
$$K = \frac{H}{\hbar} - iJ$$

Clearly, if $M_0 = 1 - Jdt - iH/\hbar dt$ was the only measurement operator, enforcing $\sum_r M_r^\dagger(dt)M_r(dt) = \mathbf{1}$ would require, $M_0^\dagger(dt)M_0(dt) = \mathbf{1} - 2Jdt \neq \mathbf{1}$ or $J = 0$ and the measurement operator would only be an unitary operator (the irreversibility would not be facilitated). The minimum number of measurement operators are 2 and we must define,

$$M_1(dt) = \sqrt{dt}c$$
$$c_1^\dagger c_1 = 2J$$
$$M_0^\dagger M_0 + M_1^\dagger M_1 = \mathbf{1}$$

In fact, we can add $N_K - 1$ measurement operators, M_μ to the set instead of just 1 defined as,

$$M_\mu(dt) = \sqrt{dt}c_\mu$$

$$\sum_{\mu=0}^{N_K-1} M_\mu^\dagger M_\mu = \mathbf{1} - 2Jdt + \sum_{\mu \neq 0} c_\mu^\dagger c_\mu = \mathbf{1}$$

$$\implies J = \frac{1}{2}\sum_{\mu \neq 0} c_\mu^\dagger c_\mu$$

To the first order in dt,

$$M_0(dt)\rho_A M_0^\dagger(dt) = \rho_A - \frac{i}{\hbar}[H, \rho_A]dt - (J\rho_A + \rho_A J)dt$$

$$= \rho_A - \frac{i}{\hbar}[H - i\hbar J, \rho_A]dt$$

$$\text{for } \mu > 0, \ M_\mu(dt)\rho_A M_\mu^\dagger(dt) = \left(c_\mu \rho_A c_\mu^\dagger\right)dt$$

$$\sum_{\mu=0}^{N_K} M_\mu \rho_A M_\mu^\dagger = -\frac{i}{\hbar}[H_A, \rho_A]dt + \sum_{\mu=1}^{N_K} \left(c_\mu \rho_A c_\mu^\dagger - \frac{1}{2}c_\mu^\dagger c_\mu \rho_A - \frac{1}{2}\rho_A c_\mu^\dagger c_\mu\right)dt \quad (2.73)$$

2.6.3. Stochastic evolution

We now confine the number of our measurement operators to 2. The probability for the result r=1 is,

$$\mathcal{P}_1(dt) = Tr\left[\mathcal{J}[M_1(dt)]\rho\right] = dtTr\left[c^\dagger c\rho\right] \quad (2.74)$$

Provided that $c^\dagger c$ is bounded, $\mathcal{P}_0(dt) = 1 - \mathcal{P}_1(dt) = 1 - O(dt)$ is much larger than $\mathcal{P}_0(dt)$. Clearly, r=0 is the most likely measurement result each infinitesimal time, dt. In these majority of dt segments with outcome r=0, the system state changes infinitesimally (and not unitarily) with the operator, $M_0(dt)$ (not a unitary operator); we call these segments null results. And at random times,

72

happening at a rate of $\mathcal{P}_0(dt)/dt$, we get the r=1 result, that we call a detection. The evolution for these dt segments happen with $M_1(dt)$. We call these changes "a quantum jump". These discontinuous changes take place in the knowledge of the observer and not in the physical state of the system.

In a simulation of an experiment where emitted photons from a cavity are registered with photodetectors, the conditioned state can be thought of as the state the system was in at the time of emission, since there may be delays from the emission to detection.

Let us assume, the system state at time t is a pure state, $|\psi(t)\rangle$, and the number of photodetections up to time t is N(t). Then,

$$dN(t)^2 = dN(t) \quad \text{It is either 0 or 1}$$

$$E[dN(t)] = \langle M_1^\dagger(dt)M_1(dt)\rangle = dt\langle\psi(t)|c^\dagger c|\psi(t)\rangle$$

For the dt segment, dN(t)=1, the state ket changes to,

$$|\psi_1(t+dt)\rangle = \frac{M_1(dt)|\psi(t)\rangle}{\sqrt{\langle M_1^\dagger(dt)M_1(dt)\rangle(t)}} = \frac{c|\psi(t)\rangle}{\sqrt{\langle c^\dagger c\rangle(dt)}} \tag{2.75}$$

For the dt segment, dN(t)=0, the state ket changes to,

$$|\psi_0(t+dt)\rangle = \frac{M_0(dt)|\psi(t)\rangle}{\sqrt{\langle M_0^\dagger(dt)M_0(dt)\rangle(t)}} = \left\{\hat{1} - dt\left[iH + \frac{1}{2}c^\dagger c - \frac{1}{2}\langle c^\dagger c\rangle(t)\right]\right\}|\psi(t)\rangle \tag{2.76}$$

Combining them, we get the Stochastic Nonlinear Schrödinger Equation (SSE),

$$d|\psi(t)\rangle = \left[dN(t) \left\{ \frac{c}{\sqrt{\langle c^\dagger c \rangle (dt)}} - 1 \right\} \right.$$
$$\left. +(1 - dN(t))dt \left(\frac{\langle c^\dagger c \rangle (dt)}{2} - \frac{c^\dagger c}{2} - iH \right) \right] |\psi(t)\rangle \qquad (2.77)$$

For the general case of mixed/entangled state matrix,

$$\hat{\pi}(t) = |\psi(t)\rangle\langle\psi(t)|$$

$$d\hat{\pi}(t) = |d\psi(t)\rangle\langle\psi(t)| + |\psi(t)\rangle\langle d\psi(t)| + |d\psi(t)\rangle\langle d\psi(t)|$$

$$d\hat{\pi}(t) = \left\{ dN(t)\mathcal{G}[\hat{c}] - dt\mathcal{H}\left[i\hat{H} + \frac{1}{2}c^\dagger c \right] \right\} \hat{\pi}(t) \mathcal{G}[\hat{r}]\rho = \frac{\hat{r}\rho\hat{r}^\dagger}{Tr[\hat{r}\rho\hat{r}^\dagger]} - \rho$$

$$\mathcal{H}[\hat{r}]\rho = \hat{r}\rho + \rho\hat{r}^\dagger - Tr[\hat{r}\rho + \rho\hat{r}^\dagger]\rho \qquad (2.78)$$

Then, we define,

$$\rho(t) = E[\hat{\pi}(t)]$$

$$E\left[dN(t)g(\hat{\pi}(t)) \right] = dtE\left[Tr[\pi(t)c^\dagger c]g(\hat{\pi}(t)) \right] \qquad (2.79)$$

The identity eq. (2.79) can be used to find,

$$d\rho = -idt\left[\hat{H}, \rho \right] + dt\mathcal{D}[\hat{c}]\rho \qquad (2.80)$$

2.7. Measurement Methods

2.7.1. Direct Photodetection

The unitary operator representing the interaction between the system and the bath in the infinitesimal interval $[t, t + dt)$ is

$$\hat{U}(t + dt, t) = exp[\hat{c}d\hat{B}^\dagger - \hat{c}^\dagger d\hat{B} - i\hat{H}dt]$$

$$d\hat{B} = d\hat{B}_{z:=-t}$$

The noise operators are all defined in the interaction frame, as is the Hamiltonian. The entangled system-bath state after the dt segment $[t, t_d t)$ is $\hat{U}(t + dt, t)|0\rangle|\psi(t)\rangle$. Since, $d\hat{B}|0\rangle = 0$. we need only keep the non-normally ordered second-order terms, $d\hat{B}d\hat{B}^\dagger = dt$,

$$\hat{U}(t + dt, t)|0\rangle|\psi(t)\rangle = \left[\hat{1} - dtc^\dagger c/2 - i\hat{H}\right]|0\rangle|\psi(t)\rangle + d\hat{B}^\dagger|0\rangle c|\psi(t)\rangle$$

$d\hat{B}^\dagger|0\rangle$ is a bath state containing one photon. However, it is non-normalized one-photon state with a norm of $\langle 0|d\hat{B}d\hat{B}^\dagger|0\rangle = dt$. The probability of finding one photon in the bath is

$$\langle 0|d\hat{B}d\hat{B}^\dagger|0\rangle\langle\psi(t)|c^\dagger c|\psi(t)\rangle = \mathcal{P}_1(dt)$$

$\mathcal{P}_1$ was defined in (2.74). Eq. (2.75) gives the system state conditioned on the bath containing a photon. The probability of finding no photons in the bath is $\mathcal{P}_0(dt) = 1 - \mathcal{P}_1(dt)$, and the conditioned system state is given in eq. (2.76).

The field state at the beginning of the following interval $[t + dt, t + 2dt)$ is a vacuum state; it is a vacuum state for a new field operator, which comes from the part of the field which has been initiated to interact with the system while the previous part has moved on to be detected.

2.7.2. Homodyne Detection

Eq. (2.80) is invariant under the transformations,

$$c \to c + \gamma$$

$$\hat{H} \to \hat{H} - \frac{i}{2}\left(\gamma^* c - \gamma c^\dagger\right)$$

Under the transformation, the measurement operators transform to,

$$M_1(dt) = \sqrt{dt}(\hat{c} + \gamma)$$

$$M_0(dt) = \hat{1} - dt\left[i\hat{H} + \frac{1}{2}(\hat{c}\gamma^* - c^\dagger\gamma) + \frac{1}{2}(c^\dagger + \gamma^*)(\hat{c} + \gamma)\right]$$

Therefore, a deterministic master-equation can be unravelled into multiple stochastic quantum trajectories. Physically, the above transformation can be realized by homodyne detection. A Beam-Splitter (BS) of transmittance η performs the transformations below.

$$\hat{b} \to \sqrt{\eta}\hat{b} + \sqrt{1 - \eta}\hat{o}$$

$$\hat{o} \to \sqrt{\eta}\hat{b} - \sqrt{1 - \eta}\hat{o}$$

The strong local oscillator of a coherent field (with the same frequency as the system dipole), $\hat{o}$ is reflected into the path of the transmitted beam itself. The

mode $\hat{o}$ can be modelled as, $\hat{o} = \gamma/\sqrt{1-\eta} + \hat{\nu}$, $\gamma/\sqrt{1-\eta}$; the coherent amplitude, $\gamma/\sqrt{1-\eta}$ ($|\gamma|^2/(1-\eta)$ being its photon flux) comes in accompanied with vacuum fluctuations, $\hat{\nu}$.

$$[\hat{\nu}(t), \hat{\nu}^\dagger(t')] = \delta(t - t')$$

The transformation and measurement operators talked about before can be achieved with $\eta \to 1$ with the transforation,

$$\hat{b} \to \hat{b} + \gamma$$

The x-quadrature of the system dipole can be measured from the rate of photodetections if we take γ to be real.

$$\hat{x} = \hat{c} + \hat{c}^\dagger, \quad \hat{y} = -i(\hat{c} - \hat{c}^\dagger)$$

$$E\left[\frac{d}{dt}N(t)\right] = Tr\left[(\gamma^2 + \gamma\hat{x} + \hat{c}^\dagger\hat{c})\rho_I(t)\right] \tag{2.81}$$

For $\gamma \gg \langle c^\dagger c \rangle$, eq. (2.81) has the inside the trace a large constant altered by a small term and a term proportional to $\hat{x}$.

The differential in conditioned state and state matrix equations are found as (with the new measurement operators):

$$d\rho_I(t) = \left\{dN(t)\mathcal{G}[\hat{c} + \gamma] + dt\mathcal{H}\left[-\hat{H} - \gamma\hat{c} - \frac{1}{2}c^\dagger c\right]\right\}\rho_I(t) \tag{2.82}$$

$$d|\psi_I(t)\rangle = \left[dN(t)\left\{\frac{\hat{c} + \gamma}{\sqrt{\langle(c^\dagger + \gamma)(c + \gamma)\rangle_I(dt)}} - 1\right\}\right.$$
$$\left. + dt\left(\frac{\langle\hat{c}^\dagger\hat{c}\rangle_I(dt) - \hat{c}^\dagger\hat{c}}{2} - \frac{\langle\hat{c}^\dagger\gamma + \gamma\hat{c}\rangle_I(t)}{2} - \gamma\hat{c} - i\hat{H}\right)\right]|\psi(t)\rangle \tag{2.83}$$

77

2.8. Excitation of a Two-level System

If we only considered the evolution of a pure state, we could expand it

$$|\psi(t)\rangle = a_b(t)|\psi_R, 0\rangle + a_1(t)||vac\rangle_R, 1\rangle \qquad (2.84)$$

and evolve it with the Hamiltonian, $H = i\sqrt{\gamma_1}\left[\hat{c}\hat{b}_{in}^\dagger(t) - \hat{c}^\dagger\hat{b}_{in}(t)\right]$ (which conserves the number of excitations and the expansion (eq. (2.84)) is sufficient) if $|\psi(0)\rangle = |\psi_R, 0\rangle$. If we restrict the problem to a single excitation, the Bosonic annihilation operator of a quantum harmonic oscillator, $\hat{c}$ can be used in place of $|F_0\rangle\langle F_1|$. One of the basis vector has the excitation in the b-field (amplitude $a_b(t)$) and the other has it in the absorber atom (amplitude $a_1(t)$). Remembering $[\hat{c}, \hat{b}_{in}] = 0$, but $[\hat{c}, \hat{b}_{in}^\dagger] \neq 0$, and $|\psi_R\rangle = \int d\omega u_\alpha(\omega) b^\dagger(\omega)|vac\rangle$; we can calculate the Heisenberg Langevin equation of motion for $\hat{c}$. If we opted for the Schrödinger picture, we would find a differential equation for the quantum amplitude, $a_1(t)$.

$$\frac{d}{dt}\hat{c}(t) = -\frac{\gamma_1}{2}\hat{c}(t) - \sqrt{\gamma_1}\hat{b}_{in}(t) \qquad (2.85)$$

$$\frac{d}{dt}a_1(t) = -\frac{\gamma_1}{2}a_1(t) - \sqrt{\gamma_1}u_\alpha(t) \qquad (2.86)$$

So, the quantity $T(t) = \sqrt{\gamma_1}e^{-\frac{\gamma_1}{2}t}\Theta(t)$ for the two level system are Green's functions for the first order differential equation (2.88), (2.85) or (2.86). Another interpretation is that they are the decaying wavepacket shape leaked into a bath mode if the atom is initiated in the final state and is allowed to spontaneously relax [1] (the process of absorption in reverse). These Green's functions, T(t) play an important role in the mathematical structure of the problem and also help identify the physical criteria for efficient excitations. For example, ref. [138]

concludes with a Wigner-Weisskopf theory that the input photon needs the time reversed properties of a spontaneously emitted photon for efficient excitation of a two level atom. It is quite easy to see from the solution of eq. (2.86)

$$a_1(t) = -\left\{\sqrt{\gamma_1}e^{-\frac{\gamma_1}{2}t}\Theta(t)\right\} * u_\alpha(t). \tag{2.87}$$

$\rho_{11,11}(t)$ (same as $|a_1(t)|^2$ calculated from eq. (2.87)) and $a_1(t)$ in eq. (2.87) are both maximized if $u_\alpha(t)$ has the time reversed shape of the Green's function $T(t)$ (spontaneous emission waveshape) because of the convolution between them. The reciprocity of optimal storage and retrieval holds for a three level Λ atom like ours as well according to [139]. In the two level absorber the development of the excited state population is hindered by amplification backaction and for optimal photon absorber the three level Λ atom is required [64].

For the absortption in the quantum harmonic oscillator's lowest two states with one excitation, we have from the scattering theory,

$$\hat{\tilde{b}}_{in/out}(\omega) = \frac{1}{\sqrt{2\pi}}\int dt \hat{b}_{in/out}(t)e^{i\omega t}$$
$$\hat{\tilde{b}}_{out}(\omega) = R(\omega)\hat{\tilde{b}}_{in}(\omega)$$
$$\hat{c}(\omega) = -T(\omega)\hat{\tilde{b}}_{in}(\omega).$$
$$T(\omega) = \frac{\sqrt{\gamma_1}}{-i\omega + \frac{\gamma_1}{2}}$$
$$R(\omega) = \frac{-i\omega - \frac{\gamma_1}{2}}{-i\omega + \frac{\gamma_1}{2}}$$

And we deduce that in frequency domain, the functions, $T(\omega)$ would serve as a transmission coefficient. In the absence of cubic and higher order terms of the annihilation operator in the Hamiltonian, the Heisenberg-Langevin operator

equation of motion is that of a damped harmonic oscillator. Therefore, it is the Green's function for a damped quantum Harmonic oscillator amplitude. It is an equation of motion shared by the excited state quantum amplitude, the annihilation operator and the coherence of the generalized density matrix, $\rho_{\alpha,0}$.

We are also able to relate the quantum amplitude of the excited state with the transmission coefficient and input wavepacket.

$$a_1(t) = -u_\alpha(t) * T(t)$$

$$a_1(\omega) = -\frac{1}{\sqrt{2\pi}} u_\alpha(\omega) T(\omega)$$

The damped quantum harmonic oscillator equation also arises if the density matrix formalism was used [64],

$$\frac{d}{dt}\rho_{01}(t) = -\frac{\gamma_1}{2}\rho_{01}(t) - \sqrt{\gamma_1} u_\alpha(t) \tag{2.88}$$

CHAPTER III

THE HEISENBERG PICTURE OF PHOTODETECTION

> I have no satisfaction in formulas
> unless I feel their numerical
> magnitude.
>
> ———————————————
> Lord Kelvin

We construct a class of Hamiltonians that describe the photodetection process from beginning to end. Our Hamiltonians describe the creation of a photon, how the photon travels to an absorber (such as a molecule), how the molecule absorbs the photon, and how the molecule after irreversibly changing its configuration triggers an amplification process—at a wavelength that may be very different from the photon's wavelength—thus producing a macroscopic signal. We use a simple prototype Hamiltonian to describe the single-photon detection process analytically in the Heisenberg picture, which neatly separates desirable from undesirable effects. Extensions to more complicated Hamiltonians are pointed out.

3.1. Introduction

We may distinguish two traditional types of photodetection theory. The first tries to determine what quantum field observable is measured when photoelectrons are produced by photoabsorption and the photoelectrons are subsequently detected and/or counted. This sort of theory is exemplified by the classic papers Refs. [80, 81], which take as starting point the Hamiltonian describing the interaction between photons and an electric dipole, but which do not describe

the remainder of the detection process quantum mechanically. The second type of theory models actual photodetectors phenomenologically, taking great care to model the many mechanisms involved in converting the initial photon energy to the final macroscopic current. This type of theory is exemplified by recent work on the superconducting nanowire detector [140, 141, 142].

Neither of the above types of photodetection theory establishes *fundamental* limits of photodetection, that is, platform-independent limitations arising from the laws of physics on, e.g., single-photon detection efficiency, dark count rates, time and wavelength resolution and tradeoffs between these figures-of-merit.

For just this purpose—finding fundamental limits on photodetectors—a third type of theory has been developed in recent years. Here the aim is to develop fully quantum-mechanical and sufficiently realistic models that include all stages of the photodetection process, including the crucial amplification process [1, 62, 64, 65, 66, 68, 71, 72]. The point of this paper is to continue this recent work and present a quantum description of the processes involved in the detection of a single photon, especially the connection between the photoabsorption and amplification processes. Moreover, we perform our calculations *in the Heisenberg picture.* That picture may not be the most intuitive—it may be easier to follow the trajectory of an excitation through the system in the Schrödinger picture—but it does have its merits. We mention two reasons here to use this picture.

First, lower limits on noise accompanying quantum amplification are most easily derived in the Heisenberg picture. Caves [143] studied linear amplification of electricmagnetic (EM) field amplitudes and formulated the problem in terms of the Heisenberg evolution of the annihilation operator of a single discrete EM field

mode of the schematic form

$$a_{\text{out}} = \sqrt{G}a_{\text{in}} + N_{\text{in}}, \tag{3.1}$$

with $G > 1$ the gain factor and N_{in} a noise term. The left-hand side here represents the annihilation operator for the mode to be amplified at the end of the amplification process, the operators on the right-hand side represent input operators, i.e., initial values just before the amplification process starts. Ideally, the number of excitations in the output equals the number of input excitations multiplied by G, and this would be the case if it were not for the noise term N_{in}.

The commutator $[a, a^\dagger] = \mathbf{1}$ has to be preserved, i.e., at any time t we must have $[a(t), a^\dagger(t)] = \mathbf{1}$ for the Heisenberg-picture operators $a(t)$ and $a^\dagger(t)$. This puts a restriction on the noise operator N_{in}. In particular, it cannot be zero. For example, phase-insensitive amplification is obtained by setting

$$N_{\text{in}} = \sqrt{G - 1}b_{\text{in}}^\dagger, \tag{3.2}$$

in terms of the creation operator of an additional discrete bosonic mode b. As is easily verified, the addition of that noise term preserves the commutator. Thermal excitations in the additional mode b are amplified, too, by a factor of $G - 1$; and even if mode b starts in the vacuum state (at zero temperature) the fact that it is the mode's *creation* operator appearing here still causes noise. We refer to the lower limit on noise reached here as the Caves limit on linear amplification.

Second, in a recent paper [66] we showed that the first part of the photo detection process (the part preceding amplification, including absorption of the incident photon) can be described compactly in the Heisenberg picture as

well. The input-output relations for the annihilation operators (which now are continuous-mode operators indexed by frequencies ω) consist of two clearly distinct terms, one desired, the other undesired but inevitable so as to satisfy the commutator $[a_{\text{out}}(\omega), a_{\text{out}}^\dagger(\omega')] = \delta(\omega - \omega')$. We can write

$$a_{\text{out}}(\omega) = T(\omega)a_{\text{in}}(\omega) + \tilde{N}_{\text{in}}(\omega), \qquad (3.3)$$

where $T(\omega)$ is a complex transmission amplitude, with the physical meaning that a photon with frequency ω will survive the pre-amplification stage with probability $|T(\omega)|^2$ (we will encounter this interpretation in Eqs. (4.28–3.38)). Here the noise term is of the form

$$\tilde{N}_{\text{in}}(\omega) = R(\omega)c_{\text{in}}(\omega), \qquad (3.4)$$

with $c_{\text{in}}(\omega)$ the annihilation operators for external bosonic modes at frequency ω, and

$$|R(\omega)|^2 + |T(\omega)|^2 = 1 \qquad (3.5)$$

so as to preserve the commutator $[a_{\text{out}}(\omega), a_{\text{out}}^\dagger(\omega')]$. Once again, thermal excitations at arbitrary frequencies ω in the mode $c_{\text{in}}(\omega)$ contribute noise as soon as $R(\omega) \neq 0$.

There are several reasons for wishing to describe the whole photo-detection process with one Hamiltonian. First, although in a recent paper [1] it was shown that one can write down commutator-preserving (nonlinear) amplification relations that beat the above-mentioned Caves limit, no explicit Hamiltonians

were considered there that may reach that improved limit. Here, we reach the same improved limit, but in a new way and with a (fairly simple) Hamiltonian. Second, that same paper also noticed how one can formally express the idea that one can amplify at a frequency that differs substantially from the incoming photon frequency. We show here explicitly how that idea can be implemented, quite straightforwardly, by a Hamiltonian.

3.2. A class of model Hamiltonians

3.2.1. Description

We wish to represent the whole photo-detection process (including absorption of the photon and amplification) plus the generation of the photon to be detected, by a Hamiltonian. We start with what seems to be a minimal model (various possible extensions of the model are discussed in the concluding Section). There are 6 quantum systems in total; we have 3 *discrete* quantum systems a, F, and c (with small Hilbert-space dimensions, which generate the photon, absorb the photon, and amplify the signal, respectively) and 3 *continuous-mode* quantum systems that connect the discrete systems and that are used to model irreversible processes (see Fig. 1).

The continuous modes are modeled by bosonic mode operators $b(\omega_b), d(\omega_d), g(\omega_g)$ with $\omega_i = ck_i$ proportional to the wave number k_i (using just 1 spatial dimension, the x-axis) of the bosonic excitations of type $i = b, d, g$. When there is no confusion possible, e.g., when we integrate over all frequencies ω_i, we will use the symbol ω without subscript to denote those. Positive frequencies $\omega > 0$ describe waves traveling from left to right (towards positive x), $\omega < 0$ waves traveling from right to left.
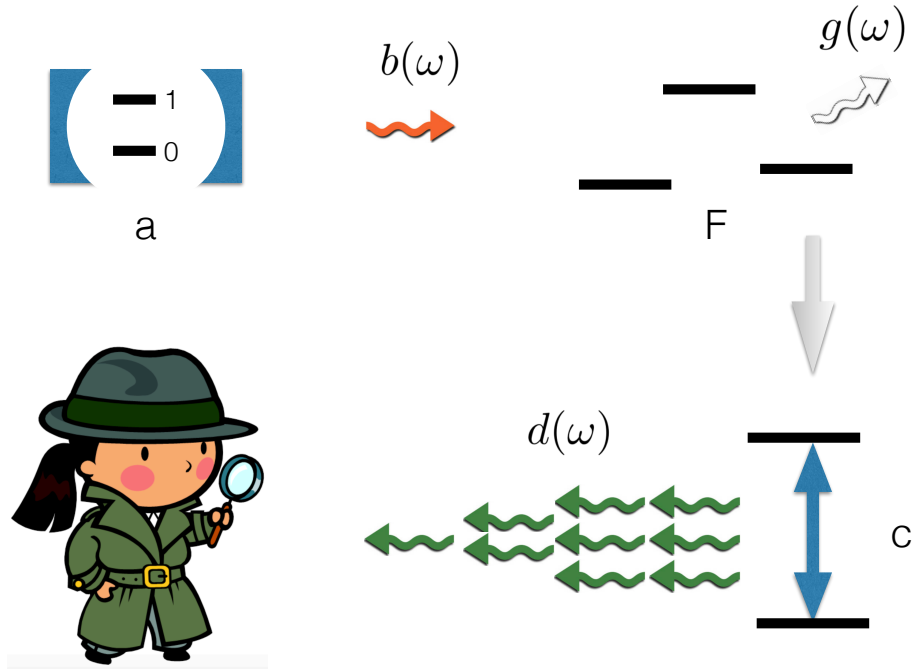
FIGURE 3.1. From a single photon to a macroscopic signal: a cavity a which contains one excitation generates one single-photon wavepacket (in a continuum $b(\omega)$). That photon is (resonantly) absorbed by a molecule F. The molecule may decay back to its initial state $|F_0\rangle$ or it may decay to a different state $|F_2\rangle$ by emitting a different photon (in a continuum $g(\omega)$) that escapes. In the state $|F_2\rangle$ the molecule's shape and/or dipole moment have changed. That physical change triggers an amplification process in another system c, which eventually reaches a steady state in which spontaneous decay is balanced by a "classical" drive, thus producing a stream of fluorescence photons (in a continuum $d(\omega)$) that a classical (human) observer can observe. The final macroscopic signal may be at a (very) different wavelength than that of the single photon.

System a is a cavity that contains a single excitation that leaks out into the continuum described by $b(\omega)$, and this is the single photon wave packet that we intend to detect. That single excitation couples to to first leg of a three-level Λ system—a "molecule" which we denote by F because it is the driving force behind

amplification. The photon may excite the molecule from its initial state, the lower level $|F_0\rangle$, to an excited state $|F_1\rangle$. That level could decay back to $|F_0\rangle$ or it could decay to the state $|F_2\rangle$ through coupling to the continuum $g(\omega)$ [the excitation in g thus produced is assumed to escape; this is an irreversible transition]. When the molecule F is in the state $|F_2\rangle$ the accompanying physical change in the molecule triggers an amplification process in system c.

This aspect of the model mimics the mechanism used in the human eye: a retinal molecule changes its configuration from cis to trans, and that change of shape in turn induces a conformational change in the protein the retinal binds to. Further changes in shapes of proteins then finally lead to a change in the charge distribution, that then can generate an electric signal (see [144]). This idea can be exploited in a bioinspired photodetector [36, 145] where a chromophore molecule changes its shape upon absorbing a single photon and thereby changes its dipole moment, which then affects a (macroscopic) current.

Finally, the many excitations generated by c leak out to the continuum mode $d(\omega)$. The macroscopic signal present in continuum $d(\omega)$ is what we then (classically) observe (see Fig. 1).

3.2.2. Hamiltonian

We follow here the ideas of Gardiner [116, 117] (see also [114]) for describing how the output of one quantum system may serve as the input for the next quantum system, without the latter acting back on the first system. This is done simply by setting the coupling to the right-to-left traveling waves equal to zero. That is, we only need the positive frequencies here. The (electric) field operators describing fields that travel from left to right corresponding to the modes b, d,

and g are denoted by corresponding capital letters $B(x)$, $D(x)$ and $G(x)$, and are expanded as

$$
\begin{aligned}
B(x,t) &= \frac{1}{\sqrt{2\pi}} \int_0^\infty d\omega\, b(\omega,t) \exp(i\omega x/c), \\
D(x,t) &= \frac{1}{\sqrt{2\pi}} \int_0^\infty d\omega\, d(\omega,t) \exp(i\omega x/c), \\
G(x,t) &= \frac{1}{\sqrt{2\pi}} \int_0^\infty d\omega\, g(\omega,t) \exp(i\omega x/c).
\end{aligned}
\tag{3.6}
$$

It is through these field operators together with their hermitian conjugates $B^\dagger(x)$, $D^\dagger(x)$ and $G^\dagger(x)$ that the discrete systems interact (at their respective locations on the x axis) with the continuous modes, where we will make both Markov and rotating-wave approximations (RWA), as detailed below.

The Hamiltonian is of the following form

$$
H = H_a + H_{a-b} + H_b
$$

$$
+ H_{b-F} + H_F + H_{F-g} + H_g
$$

$$
+ H_{F-c} + H_c
$$

$$
+ H_{c-d} + H_d.
\tag{3.7}
$$

System a is a single cavity mode with resonance frequency ω_a (which, in all generality, would be time-dependent), whose Hamiltonian we write as (setting $\hbar = 1$ everywhere)

$$
H_a = \omega_a a^\dagger a.
\tag{3.8}
$$

The cavity mode is located at $x = -c\tau$ with τ the time delay between a signal (a photon) leaving system a and interacting with system F (which we take to be

located at $x = 0$). The cavity mode is coupled to the field $B(x = -c\tau, t)$ like so:

$$H_{a-b} = i\sqrt{\kappa}[aB^\dagger(-c\tau, t) - B(-c\tau, t)a^\dagger], \tag{3.9}$$

with the field B described by the Hamiltonian (recall we leave out negative frequencies since they do not couple to the systems of interest)

$$H_b = \int_0^\infty d\omega\, \omega b^\dagger(\omega)b(\omega). \tag{3.10}$$

We can anticipate that the main terms contributing to the interaction are those at $\omega \approx \omega_a$. That is, in the Heisenberg picture $a(t) \sim \exp(-i\omega_a t)$ and $b^\dagger(\omega, t) \sim \exp(+i\omega t)$ so that the main terms not averaging to zero over time come from $\omega \approx \omega_a$. In numerical simulations, we always transform to a rotating frame, i.e., we solve equations for the slowly-varying operators $\exp(i\omega_a t)a(t)$ rather than $a(t)$, etcetera.

The next line of (4.37) contains four Hamiltonians that describe how the Λ system F interacts with two different continua (namely, b and g) at position $x = 0$.

The four terms are written as

$$
\begin{aligned}
H_{b-F} &= i\sqrt{\gamma_1}[|F_0\rangle\langle F_1| B^\dagger(x = 0, t) - B(x = 0, t)|F_1\rangle\langle F_0|] \\
H_F &= \sum_{k=0,1,2} \omega_k |F_k\rangle\langle F_k| \\
H_{F-g} &= i\sqrt{\gamma_2}[|F_1\rangle\langle F_2| G^\dagger(x = 0, t) - G(x = 0, t)|F_2\rangle\langle F_1|] \\
H_g &= \int_0^\infty d\omega\, \omega g^\dagger(\omega)g(\omega)
\end{aligned}
\tag{3.11}
$$

and we again can anticipate that the most important terms are those with $\omega \approx \omega_1 - \omega_0 := \omega_{10}$ for the interaction between F and $b(\omega)$ and for $\omega \approx (\omega_1 - \omega_2)$ for the

89

interaction between $g(\omega)$ and F. An important parameter is the detuning of the photon from resonance with the molecular transition from $|F_0\rangle$ to $|F_1\rangle$,

$$\delta = \omega_a - \omega_{10}. \tag{3.12}$$

The third line of (4.37) is going to be crucial as it models the amplification process and how the F system triggers it. We construct the two Hamiltonians H_{F-c} and H_c in several steps. First, assume we have a system c that is driven by an external "force" F. That is, we assume the Hamiltonian for system c contains a driving term proportional to a parameter F. For example, we may use a Hamiltonian that describes *electron shelving* [23, 146], which is used as a method to perform quantum state measurements on ions: in one state the ion, driven by a laser, produces large amounts of fluorescence whereas in another state (from which there is no transition resonant with the laser) it remains dark. The simple Hamiltonian is [in Section 4.6 below we suggest several more involved examples of suitable Hamiltonians]:

$$\tilde{H}_c(F) = 2iF\cos(\omega_F t)(c - c^\dagger), \tag{3.13}$$

which in the RWA becomes

$$\tilde{H}_c(F) \approx iF(\exp(i\omega_F t)c - \exp(-i\omega_F t)c^\dagger). \tag{3.14}$$

Alternatively, we could introduce yet another pair of bosonic mode operators α and $\alpha^\dagger$ to replace $F\exp(-i\omega_F t)$ and $F\exp(i\omega_F t)$, respectively, and add another Hamiltonian $H_\alpha = \omega_F \alpha^\dagger \alpha$; the initial state of that mode would then be a coherent

state with amplitude F, i.e., an eigenstate of α with eigenvalue F (which indeed can model a strong laser field). This would have the formal advantage of making our Hamiltonian completely independent of time.

Now in order to couple system c to our quantum system F we replace the parameter F by the quantum operator

$$\tilde{F} = \sum_{k=0,1,2} F_k |F_k\rangle\langle F_k|, \tag{3.15}$$

so that we replace

$$\tilde{H}_c(F) \mapsto \tilde{H}_c(\tilde{F}). \tag{3.16}$$

Note we may apply this substitution trick to *any* Hamiltonian $\tilde{H}_c(F)$ that models amplification. For the simple example (3.14) we have

$$\tilde{H}_{F-c} = i\tilde{F}(\exp(i\omega_F t)c - \exp(i\omega_F t)c^\dagger). \tag{3.17}$$

For $\tilde{H}_c$ we assume the simple form

$$\tilde{H}_c = \omega_c c^\dagger c, \tag{3.18}$$

appropriate for a bosonic mode c (but we could also use a two-level atom). An interaction proportional to a projector $|F_2\rangle\langle F_2|$, implements the idea (mentioned above) that it is a physical property of the state $|F_2\rangle$ that triggers amplification. For the RWA to apply all we need is that the driving frequency ω_F be close to the frequency ω_c, *independent* of the frequencies ω_k for the three states of system F and *independent* of ω_a, the frequency of the photon to be detected. And so amplification happens at the frequency ω_F, not at ω_a. It may be important

to be able to amplify at a different frequency so as to suppress thermal noise (which could lead to dark counts) by amplifying at a frequency ω_F such that (reinserting $\hbar$) $\hbar\omega_F \gg kT$. Pre-amplification thermal excitations at a frequency ω_a [either thermal photons in the input mode a or thermal fluctuations exciting the transition to level $|F_1\rangle$] are amplified, and so, too, should be suppressed by operating at a temperature T such that $\hbar\omega_a \gg kT$. (For example, this is how our eyes can detect optical photons at room temperature.)

We may move to a frame rotating at frequency ω_F and replace our first guesses for Hamiltonians $\tilde{H}_{F-c}$ and $\tilde{H}_c$ by the final results

$$
\begin{aligned}
H_{F-c} &= i\tilde{F}(c - c^\dagger), \\
H_c &= \Delta c^\dagger c,
\end{aligned}
\tag{3.19}
$$

with $\Delta = \omega_c - \omega_F$ the detuning from resonance.

Finally, for the fourth line in (4.37) we stay in the same rotating frame and write

$$
\begin{aligned}
H_{c-d} &= i\sqrt{\Gamma}[cD^\dagger(x = 0, t) - D(x = 0, t)c^\dagger], \\
H_d &= \int_0^\infty d\omega\,(\omega - \omega_F)d^\dagger(\omega)d(\omega)
\end{aligned}
\tag{3.20}
$$

3.3. Heisenberg equations of motion

3.3.1. Eliminating the continua

For any operator O that does not explicitly depend on time, we have the equation of motion

$$
\frac{d}{dt}O = i[H, O]
\tag{3.21}
$$

with H the total Hamiltonian (4.37). We choose a time t_0 in the past at which we start the calculation (i.e., we solve the equations for $t > t_0$), and at which time the Heisenberg and Schrödinger picture operators are taken as equal. Those operators at that special time are our input operators and thus are also indicated by the subscript "in."

We first formally solve the equations for the continuum operators $b(\omega), g(\omega)$, and $d(\omega)$ and substitute those results into the equations of motion for arbitrary operators acting on the discrete quantum systems a, F and/or c, thus eliminating the continua from the description. For example, starting at the end, with modes $d(\omega)$ and the field operator $D(x)$, we obtain [117]

$$D(x = 0, t) = d_{\text{in}}(t) + \sqrt{\Gamma} c(t) \tag{3.22}$$

with the "free field" given by

$$d_{\text{in}}(t) = \frac{1}{\sqrt{2\pi}} \int_0^\infty d\omega \, d_0(\omega) \exp(-i(\omega - \omega_F)(t - t_0)). \tag{3.23}$$

The operator $d_0(\omega) := d(\omega, t_0)$ is an initial value for $d(\omega, t)$ at time $t = t_0$.

For the field operator $G(x)$ we similarly obtain

$$G(x = 0, t) = g_{\text{in}}(t) + \sqrt{\gamma_2} \, |F_1\rangle \langle F_2| \, (t) \tag{3.24}$$

with the free field

$$g_{\text{in}}(t) = \frac{1}{\sqrt{2\pi}} \int_0^\infty d\omega \, g_0(\omega) \exp(-i\omega(t - t_0)). \tag{3.25}$$

93

For the field $B(x)$ which couples both to a and to F we find that at $x = 0$ it contains two driving terms

$$B(x = 0, t) = b_{\text{in}}(t) + \sqrt{\kappa}a(t - \tau) + \sqrt{\gamma_1}\,|F_0\rangle\,\langle F_1|\,(t) \qquad (3.26)$$

with the free field

$$b_{\text{in}}(t) = \frac{1}{\sqrt{2\pi}}\int_0^\infty d\omega\, b_0(\omega)\exp(-i\omega(t - t_0)). \qquad (3.27)$$

At the location $x = -c\tau$ of the cavity we get just one driving term

$$B(x = -c\tau, t) = b_{\text{in}}(t) + \sqrt{\kappa}a(t). \qquad (3.28)$$

We can now write down the equations of motion for the operators corresponding to the three discrete quantum systems. For example, for the cavity mode annihilation operator $a(t)$ we get

$$\frac{d}{dt}a = -i\omega_a a - \sqrt{\kappa}[b_{\text{in}} + \frac{1}{2}\sqrt{\kappa}a]. \qquad (3.29)$$

(The "extra" factor of $1/2$ on the r.h.s. comes from the use of $\int_{t_0}^t dt'\,\delta(t - t')a(t') = \frac{1}{2}a(t)$, where the delta function inside the integral comes from the approximation $\int d\omega\,\exp(-i\omega(t - t')) = 2\pi\delta(t - t')$ [117]. Instances of the same factor of $1/2$ appear in several equations below.)

We can solve Eq. (3.29) to obtain

$$\begin{aligned} a(t) &= a(t_0)\exp[(-i\omega_a - \kappa/2)(t - t_0)] \\ &\quad -\sqrt{\kappa}\int_{t_0}^t dt'\,\exp[(i\omega_a + \kappa/2)(t' - t)]b_{\text{in}}(t'). \end{aligned} \qquad (3.30)$$

94

For the evolution of c we find

$$\frac{d}{dt}c = -i\Delta c - \sqrt{\Gamma}(d_{\text{in}} + \frac{1}{2}\sqrt{\Gamma}c) - \tilde{F}. \qquad (3.31)$$

The equation for system F and hence for $\tilde{F}$ is more complicated and in general has to be solved numerically. We can formally solve (3.31)

$$
\begin{aligned}
c(t) &= c(t_0)\exp[(-i\Delta - \Gamma/2)(t - t_0)] \\
&\quad - \int_{t_0}^{t} dt'\exp[(i\Delta + \Gamma/2)(t' - t)][\sqrt{\Gamma}d_{\text{in}}(t') + \tilde{F}(t')].
\end{aligned}
$$
$$(3.32)$$

and this is an explicit solution provided we can ignore the backaction of system c on system F, i.e., when the operator $\tilde{F}(t)$ does not depend on "downstream" system c operators, but only on "upstream" system a operators.

3.3.2. Steady-state solutions

Our Hamiltonian is such that the F system will reach a steady state, The reason is that the force driving system F is the single photon emitted by the cavity, and that photon will have disappeared after a few cavity life times κ^{-1}. The F system then decays to either the $|F_0\rangle$ state or to the $|F_2\rangle$ state, and stays there. The operator $\tilde{F}$ will eventually become constant, apart from fluctuating noise (Langevin) terms. Eq. (3.32) then shows that the operator c will reach a steady state, too (all transient effects decay away at a rate Γ), up to noise terms.

We now focus on terms in $\tilde{F}$ proportional to $|F_0\rangle\langle F_0|$ only. (These terms describe the response of molecule F when it starts from state $|F_0\rangle$, where it is supposed to start. Other nonzero terms are discussed in Section 4.5.) We also

assume $\delta = 0$ for the moment (this is the optimum case, of course, for detecting the photon). Moreover, we set $F_0 = F_1 = 0$ and $F_2 =: \mu > 0$, so that the molecule triggers amplification only in the state $|F_2\rangle$. In that case we simply have $\tilde{F} = \mu|F_2\rangle\langle F_2|$, and we find its steady-state value to be

$$\tilde{F}_{\text{ss}} = \mu P_{\text{abs}} a^\dagger a \otimes |F_0\rangle\langle F_0|, \tag{3.33}$$

where

$$P_{\text{abs}} = \frac{4\gamma_1\gamma_2}{(\gamma_1 + \gamma_2)(\gamma_1 + \gamma_2 + \kappa)} \tag{3.34}$$

is the probability that the photon transfers the population from the initial state $|F_0\rangle$ to $|F_2\rangle$. This probability is maximized for $\gamma_1^2 = \gamma_2^2 + \kappa\gamma_2$, and for $\kappa \ll \gamma_{1,2}$ this maximum approaches unity arbitrarily closely. This result confirms the "ideal detection" result of Ref. [64].

We can in fact generalize this result to arbitrary detuning δ. Apart from obtaining the answer by replacing κ by $\kappa - 2i\delta$ and taking the real part,

$$P_{\text{abs}} = \text{Re}\left[\frac{4\gamma_1\gamma_2}{(\gamma_1 + \gamma_2)(\gamma_1 + \gamma_2 + \kappa - 2i\delta)}\right] \tag{3.35}$$

we can write the result more insightfully in the form

$$P_{\text{abs}} = \int d\omega \, |\phi(\omega)|^2 |T(\omega)|^2 \tag{3.36}$$

where

$$T(\omega) = \frac{\sqrt{\gamma_1\gamma_2}}{(\gamma_1 + \gamma_2)/2 - i(\omega - \omega_{10})} \tag{3.37}$$

is the transmission coefficient describing the transmission of a single excitation through the Λ system (which for a single excitation is equivalent to a Fabry-Perot filter cavity) [63, 66] and where

$$\phi(\omega) = \frac{1}{\sqrt{2\pi}} \frac{\sqrt{\kappa}}{\kappa/2 - i(\omega - \omega_a)} \tag{3.38}$$

is the (properly normalized) spectral shape of the photon produced by the cavity. This way of writing the probability can be generalized to other systems than a three-level molecule by substituting other transmission functions $T(\omega)$ that describe the initial (absorption) stage of the photodetection process, as discussed in great detail in Ref. [66].

When the system reaches its steady state, the expression for $c(t)$ becomes

$$c_{\mathrm{ss}}(t) = \tilde{d}(t) - \frac{\tilde{F}_{\mathrm{ss}}}{\Gamma/2 + i\Delta}, \tag{3.39}$$

where $\tilde{d}(t)$ is a single-mode "noise" annihilation operator given by (for large t, i.e., $t - t_0 \gg 1/\Gamma$)

$$\tilde{d}(t) = -\int_{t_0}^{t} dt' \exp[(i\Delta + \Gamma/2)(t' - t)]\sqrt{\Gamma}d_{\mathrm{in}}(t') \tag{3.40}$$

One can verify that

$$[c_{\mathrm{ss}}(t), c_{\mathrm{ss}}^{\dagger}(t)] = 1 \tag{3.41}$$

thanks purely to the noise term.

What we observe in the end is a macroscopic amount of excitations in the continuum mode $d(\omega)$, or, equivalently, the field $D(x = 0)$. The excitations are

97

collected over some finite time interval of duration T from T_0 to $T_0 + T$ [much later than t_0] with some low efficiency η. We could assume that our signal is determined by

$$S_D(T) = \eta \int_{T_0}^{T_0+T} dt \ \left\langle D^\dagger(x=0,t)D(x=0,t) \right\rangle =: \eta N_D(T), \qquad (3.42)$$

which corresponds to collecting a fixed fraction η of all excitations in the field D. We could also assume we collect data continuously as a function of T, by continuously monitoring the field D. Leaving out the noise terms we can write

$$\begin{aligned} N_D(T) &= \Gamma \int_{T_0}^{T_0+T} dt \int_{t_0}^{t} d\tau \int_{t_0}^{t} d\tau' \ \left\langle \tilde{F}(\tau)\tilde{F}(\tau') \right\rangle \times \\ &\quad \exp\left((-i\Delta + \Gamma/2)(\tau - t) + (i\Delta + \Gamma/2)(\tau' - t')\right). \end{aligned}$$

$$(3.43)$$

Here the expectation value $\left\langle \tilde{F}(\tau)\tilde{F}(\tau') \right\rangle$ must be calculated using the Quantum Regression Formula (or Theorem) [147].

Alternatively we could assume we collect a fraction of excitations in a particular single discrete time-integrated mode

$$N'_D(T) = \eta \left\langle d_T^\dagger d_T \right\rangle \qquad (3.44)$$

where, for example, when $\Delta = 0$, we choose

$$d_T = \frac{1}{\sqrt{T}} \int_{T_0}^{T_0+T} dt \ D(x=0,t), \qquad (3.45)$$

which similarly would contain $\left\langle \tilde{F}(\tau)\tilde{F}(\tau') \right\rangle$. For either choice, the signal grows linearly with T once c reaches a steady state. We will focus on the former choice

in the numerical calculations, i.e., we assume that $N_D(T)$ contains our macroscopic signal.

Consider now the noise in our amplification process. We can write our discrete mode operator d_T (in the steady state) as

$$d_{T,\text{out}} = P_{\text{abs}}\sqrt{G}(a^\dagger a)_{\text{in}} \otimes (|F_0\rangle\langle F_0|)_{\text{in}} + \tilde{e}_{\text{in}}, \tag{3.46}$$

where we explicitly added back in the subscripts "out" and "in" to indicate the operators on the right-hand side are all input operators and the left-hand side is an output operator. (Recall that we did leave out here other terms to be discussed in 4.5, given that the initial state of our molecule is $|F_0\rangle$.) The gain factor G here—which is the gain one gets if the molecule ends up in the desired state $|F_2\rangle$—is linear in T

$$G = \frac{4\mu^2}{\Gamma}T, \tag{3.47}$$

and $\tilde{e}_{\text{in}}$ is a single-mode discrete annihilation noise operator fully determined by d_{in}:

$$\tilde{e}_{\text{in}} = \frac{1}{\sqrt{T}} \int_{T_0}^{T_0+T} dt \ (\sqrt{\Gamma}\tilde{d}(t) + d_{\text{in}}(t)), \tag{3.48}$$

since the operator $\tilde{d}$ is determined by d_{in} according to Eq. (3.40).

Note that (i) the noise is not amplified, (ii) the first (gain) term is hermitian and, therefore, commutes with its hermitian conjugate, so that the presence of $\tilde{e}_{\text{in}}$ is sufficient to preserve the commutator. Of course, our operator $a^\dagger a$ is restricted here to the very narrow range of 0 or 1 excitations [so that we can use

that $(a^\dagger a)^2 = a^\dagger a$ when we calculate either $N_D(T)$ or $d_T^\dagger d_T$]. The main point is, Eq. (3.46) is not of the Caves form for linear amplification, but is, rather, a nonlinear minimum-noise form that is akin to but different from the input-output relation found in Ref. [1].

3.3.3. Numerical integration

Without noise terms, we can find the gain term and the steady-state values numerically as well. If the Schrödinger-picture evolution equation for the density operator can be formally solved as $\rho(t) = \exp(\mathcal{L}(t - t_0))\rho(t_0)$ with $\mathcal{L}$ the time-independent Liouvillian superoperator, then in the Heisenberg picture observable O evolves as $O(t) = \exp(\mathcal{L}^\dagger(t - t_0))O(t_0)$.

For the Heisenberg operator $|F_2\rangle\langle F_2|(t)$ we plot all nonzero terms (there are five for $\delta = 0$) as functions of time in Fig. 2. Here are the five types of terms with their interpretations (where we ignore operators acting on the Hilbert space for the "downstream" system c)

1. $K_1 = |1\rangle\langle 1| \otimes |F_0\rangle\langle F_0|$: This term describes how an initial state with 1 cavity excitation and the molecule starting in $|F_0\rangle$ transfers the molecule to state $|F_2\rangle$ (blue curve).

2. $K_2 = |0\rangle\langle 0| \otimes |F_1\rangle\langle F_1|$: This term describes how the molecule reaches state $|F_2\rangle$ even without a photon present provided it starts in the upper state $|F_1\rangle$. It decays to $|F_2\rangle$ with probability $1/2$, given that $\gamma_1 = \gamma_2$ here (green curve).

3. $K_3 = |1\rangle\langle 1| \otimes |F_1\rangle\langle F_1|$: This term again corresponds to the molecule starting in the upper state $|F_1\rangle$, from which it decays to $|F_2\rangle$ with probability $1/2$. Initially it behaves like the previous case. However, because of the presence

of the photon, the molecule can also be transferred to the desired final state $|F_2\rangle$ by first decaying to $|F_0\rangle$ and then absorbing the photon (orange curve).

4. $K_4 = \mathbf{1} \otimes |F_2\rangle\langle F_2|$: This term describes the trivial case where the molecule starts in $|F_2\rangle$ and just stays there, independent of the presence or absence of a photon (dashed purple curve).

5. $K_5 = a \otimes |F_1\rangle \langle F_0| + a^\dagger \otimes |F_0\rangle \langle F_1|$: This term describes the influence of coherence: if we start with a coherent superposition of no photon and 1 photon, *and* the molecule is in a superposition of $|F_0\rangle$ and $|F_1\rangle$, then the contributions from $|0\rangle \otimes |F_1\rangle$ and $|1\rangle \otimes |F_0\rangle$ to the probabillity of ending up in $|F_2\rangle$ interfere destructively (dashed black/red curve). Moreover, this term does contribute to the signal though the combination $K_5^\dagger K_5$, see main text.

   (There is the similar sixth term, $K_6 = ia \otimes |F_1\rangle \langle F_0| - ia^\dagger \otimes |F_0\rangle \langle F_1|$ which is nonzero only for nonzero detuning δ.)

We also plot the amplitude of system c and the total number of excitations in the field $D(x = 0)$ in Figs. 3 and 4. More precisely, we plot the time evolutions of the terms in $c(t)$ and $N_D(T) = D^\dagger(x = 0)D(x = 0)$ proportional to $|1\rangle\langle 1| \otimes |F_0\rangle\langle F_0| \otimes |0\rangle\langle 0|$, which correspond to the system starting in the initial state with 1 excitation in the cavity, the molecule in state $|F_0\rangle$ and no excitations in mode c. We choose $T_0 = t_0$ in the definition of $N_D(T)$. Note that it is not just the first term of the five terms we just discussed that contributes to $N_D(T)$: the fifth term contributes as well and so do the noise terms; together they ensure that $N_D(T)$ scales linearly with P_{abs} (as it should), rather than quadratically. (Numerically, we used the Quantum Regression Theorem to calculate $N_D(T)$.)
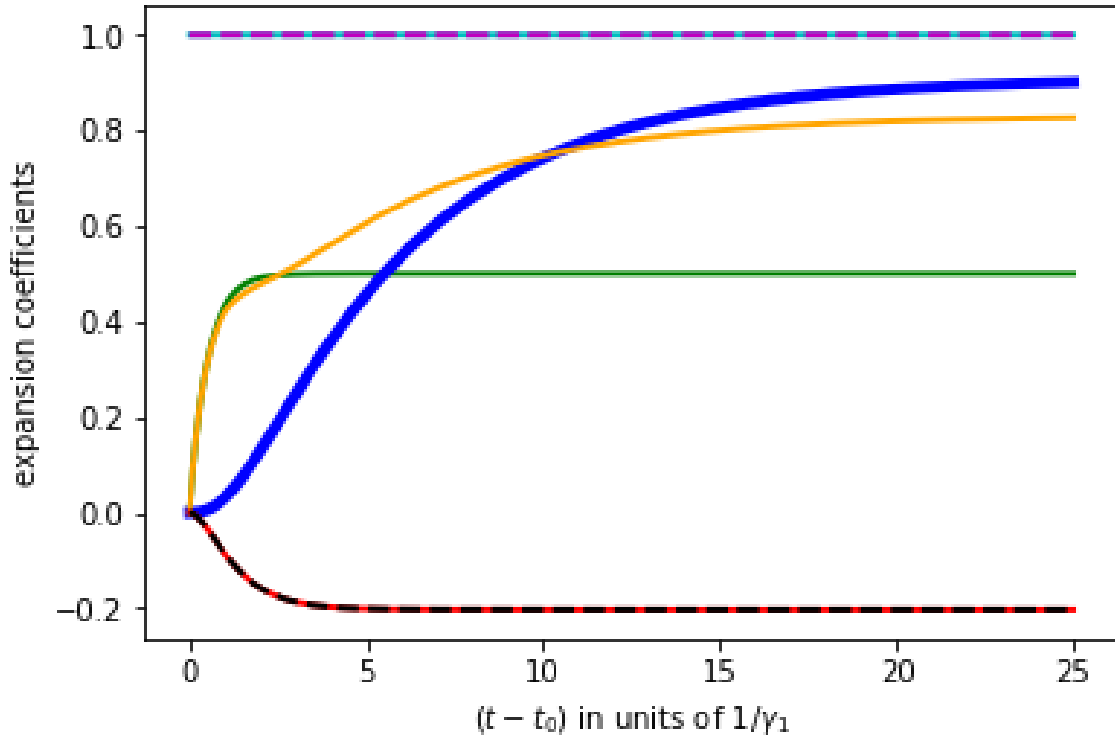
FIGURE 3.2. The five types of nonzero terms in $|F_2\rangle\langle F_2|(t)$ as functions of time in units of γ_1^{-1},
where $\delta = 0$, $\gamma_2 = \gamma_1$ and $\kappa = \gamma_1/5$. The probability P_{abs} for the photon to trigger amplification is $P_{\text{abs}} = 10/11$ in this case. For details, see main text.
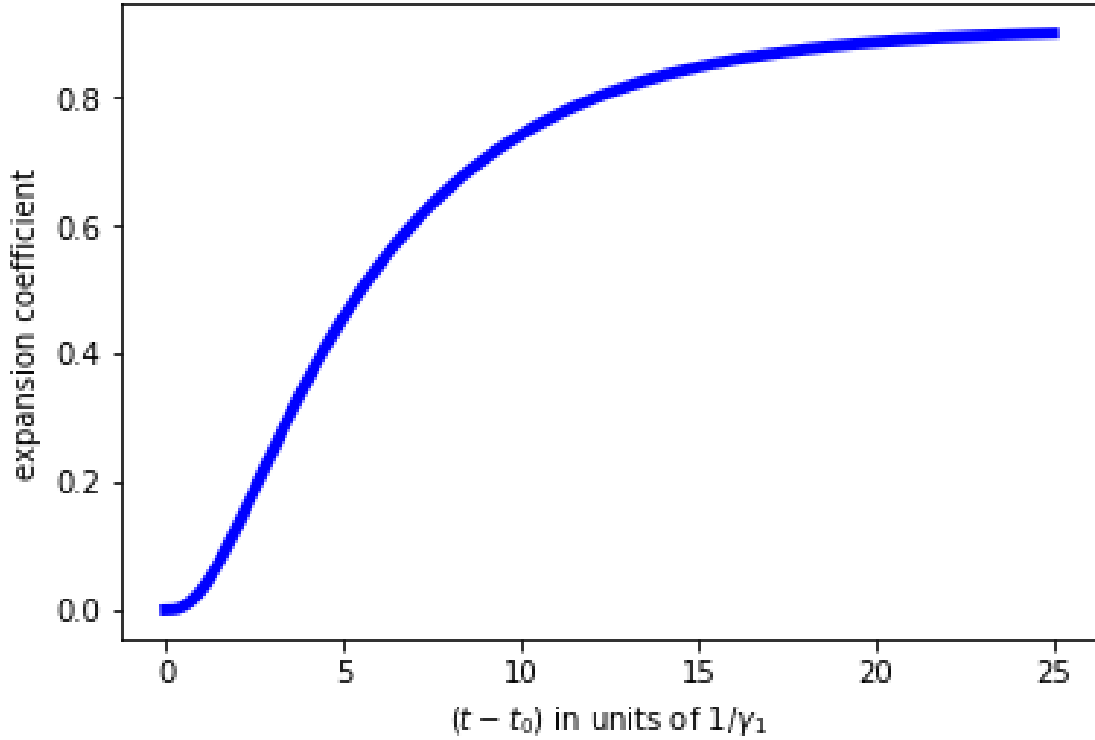
FIGURE 3.3. The term in $c(t)$(in units of μ/Γ) prop. to $|1\rangle\langle 1| \otimes |F_2\rangle\langle F_2| \otimes |0\rangle\langle 0|$ which describes how the expectation value of the amplitude of our final quantum system c grows with time (in units of γ_1^{-1}), if the cavity starts with 1 excitation, the molecule starts in $|F_0\rangle$ and the mode c itself starts in the vacuum. Parameter values are $\mu = \Gamma = \gamma_2 = \gamma_1$, $\Delta = \delta = 0$, and $\kappa = \gamma_1/5$. The steady-state value of c for these values is $c_{\text{ss}} = -20\mu/11\Gamma$.
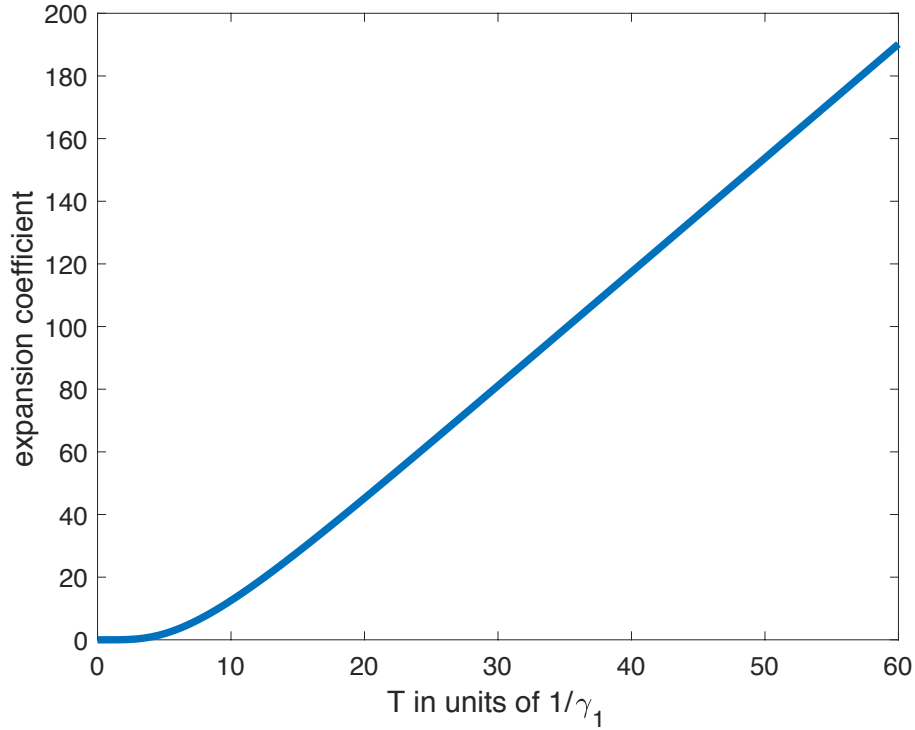
FIGURE 3.4. The term in $N_D(T)$, given by Eq. (3.43), proportional to $|1\rangle\langle 1| \otimes |F_0\rangle\langle F_0| \otimes |0\rangle\langle 0|$ as a function of the integration time T (in units of γ_1^{-1}). Parameter values are as in the previous Fig. This represents the macroscopic signal produced by detection of a single photon, i.e., the expectation value of the number of excitations in the field $D(x = 0)$. This expectation value increases linearly with T once the system has reached a steady state, after a few κ^{-1}, with a slope given by $P_{\text{abs}}4\mu^2/\Gamma$.

The behavior of our signal plotted here and the efficiency η with which that macroscopic signal is measured determine when the photodetector can be reset. Namely, as soon as a few excitations (in principle, even a single one, if we can ignore dark counts) have been detected (which requires the number of excitations to have been of order $1/\eta$), a photon has been detected, and our detector may be reset in order to be able to detect a next photon. Resetting involves emptying the system c (which takes several Γ^{-1}) and resetting the molecule to the state $|F_0\rangle$ (which takes several γ_1^{-1}).

If we include the Langevin terms we could solve the stochastic differential equations by standard methods (using Ito calculus, for example [117]). Much more simply, we could determine what the generic form of the noise terms must be, by making use of the fact that commutators for our output operators like d_T should be preserved. For example, if the steady-state value of d_T is $d_{T,\text{ss}}$ (which is expressed in terms of the input operators of our discrete systems) and the noise term in d_T is e_{in} (which is expressed in terms of continuum input operators and which, therefore, commutes with $d_{T,\text{ss}}$ and $d_{T,\text{ss}}^\dagger$), then we must have

$$[e_{\text{in}}, e_{\text{in}}^\dagger] = \mathbf{1} - [d_{T,\text{ss}}, d_{T,\text{ss}}^\dagger],\tag{3.49}$$

which limits the operator form for e_{in} severely.

3.4. Conclusions and outlook

We used a fairly simple Hamiltonian model to describe quantum mechanically the photodetection process from beginning (generation and absorption of a single photon) to end (amplification). We solved the equations

105

in the Heisenberg picture, because the end result compactly describes the essence of the whole process including the noise therein (see Eq. (3.46), where we consider the optimum case $P_{\text{abs}} = 1$):

$$d_{\text{out}} = \sqrt{G}(a^\dagger a)_{\text{in}} \otimes |F_0\rangle\langle F_0| + e_{\text{in}}. \tag{3.50}$$

Here d_{out} is the annihilation mode operator for a time-integrated mode that contains the macroscopic output signal (a large number of excitations) that we ultimately observe classically. We have to place the Heisenberg cut somewhere, and we place it as far along the whole photodetection process as we can, *after amplification.* Unlike for linear amplification [143] where the gain term would be $\sqrt{G}a_{\text{in}}$, here the gain term indicates the amplification process is nonlinear [1].

The noise term (needed to preserve the commutator $[d, d^\dagger] = \mathbf{1}$) is just an input mode operator, rather than $\sqrt{G-1}e^\dagger$, which is the noise term accompanying phase-insensitive linear amplification. That is, the noise in our case is not amplified, and a vacuum input gives zero noise, unlike for linear amplification.

The projector $|F_0\rangle\langle F_0|$ projects onto the initial state of a molecule that triggers the amplification process once it has changed its configuration by absorbing the photon. Confirming results of Refs. [64, 65] the probability of absorption (and detection) can indeed be nearly 100%.

Several aspects of our minimal prototype Hamiltonian can be generalized and/or extended:

(i) In order to detect more than a single excitation we could include more levels in the F molecule (and more excitations either in the same cavity or in multiple cavities, all coupled to the same system F). For example, to be able to detect a second photon we could introduce two more F levels, such that a

transition from $|F_2\rangle$ to another upper level could occur (triggered by the second photon), which then could decay to a level $|F_4\rangle$ where the value of the parameter F_4 would be substantially larger than $F_2 = \mu$. This then would allow us to distinguish the signal produced by the second photon from that produced (triggered) by just a single photon.

(ii) In [71] a quantum phase transition was proposed and analyzed as a means of amplifying a weak signal (such as a single photon). Here we could use a *dissipative* phase transition [148, 149, 150, 151] to achieve minimum-noise amplification. The Hamiltonian $H_c(F)$ we used is for either a driven atom or a driven cavity. A dissipative phase transition arises even for the simple system of an atom inside (and coupled to) a cavity, with either the atom or the cavity driven. The presence of a phase transition may make the amplification process more robust against deviations from the ideal Hamiltonian.

(iii) The single-photon wavepacket to be detected is fixed here by the resonance frequency and the decay rate of the cavity that generates the photon. We could make these two parameters arbitrary functions of time so that an arbitrary single-photon wavepacket can be created [113, 114, 115]. That should allow us to formulate the POVM (projecting onto a specific temporal state of the photon) that describes our detector, as in Ref. [68].

(iv) We assumed a *bosonic* mode to contain the amplified signal. Alternatively we may use many spin-1/2 particles, as in the model discussed in Refs. [71, 72]. This extension would increase the scope of our description to include fermionic systems.

In conclusion, the main point here was to present a class of Hamiltonians that describe the photodetection process fully quantum-mechanically from

beginning to end, including nonlinear, minimum-noise amplification [1] and near-perfect photoabsorption [64].

CHAPTER IV

DETECTING TWO PHOTONS WITH ONE MOLECULE

We apply input-output theory with quantum pulses [AH Kiilerich, K Mølmer, Phys. Rev. Lett. **123**, 123604 (2019)] to a model of a new type of two-photon detector consisting of one molecule that can detect two photons arriving sequentially in time. The underlying process is distinct from the usual two-photon absorption process where two photons arriving simultaneously and with frequencies adding up to the resonance frequency are absorbed by a single molecule in one quantum jump. Our detector model includes a Hamiltonian description of the amplification process necessary to convert the microscopic change in the single molecule to a macroscopic signal.

4.1. Introduction

There are two standard ways of detecting two photons in a photon-number resolved (PNR) manner: (i) an inherent PNR detector produces a different signal depending on whether one or two photons were absorbed by the detector, (ii) multiplexed PNR detection [152] exploits multiple single-photon detectors, and the signal consists of either one or two such detectors "clicking." An inherent PNR detector may, for example, be sensitive to the total energy deposited by the photons [153]. A second type of detector sensitive to two photons makes use of a process called "two-photon absorption" (TPA) in which one molecule can absorb two photons that arrive simultaneously and whose frequencies add up to the resonance frequency. This effect was discovered by Göppert-Mayer in 1931 [154, 155], goes through a virtual intermediate state, and has become an item of

modern interest since the realization that this TPA process is sensitive to time-frequency entanglement between the two incoming photons [156, 157, 158].

For a biological example of multiplexing, we may consider the human eye. There are about 10^8 rods, each of which is sensitive to single photons in that they can absorb one photon at a time [159]. Interestingly, the TPA process occurs in the human eye, too, where two infrared photons may give rise to the sensation corresponding to that of light in the visible range [18, 160]. In this case the detection is not strictly PNR, as the signals from two infrared photons or from one visible photon are the same.

A process related to TPA is called stepwise two-photon absorption where the first photon takes the molecule to an actual (rather than a virtual) excited state and a subsequent photon takes the molecule to an even higher lying excited state, see e.g., [161]. Taking a molecule to an excited state, however, is not yet sufficient for implementing a measurement. We also need an amplification process that produces a macroscopic signal. In the human eye a light-absorbing molecule decays from the excited state irreversibly to a metastable state, in which the shape of the molecule has changed. That change in shape triggers a chain reaction of shape changes in surrounding proteins, eventually producing (or changing) a permanent dipole moment that in turn triggers a change in a mesoscopic electric current [162], which then permanently registers the detection of the photon.

Following the example of Refs [36, 60, 64, 65] of taking inspiration from biological systems to design photo detectors (see also [163]), based on this robust photo-detection mechanism we propose and model a PNR two-photon detector consisting of a five-level molecule, as follows (see Fig. 1 and Section III for more details and reasons for choosing this particular configuration): a ground state $|F_0\rangle$

from which a photon with a frequency $\omega_\alpha \approx \omega_1 - \omega_0 =: \omega_{01}$ can induce a transition to an excited state $|F_1\rangle$, which can then irreversibly decay to a metastable state $|F_2\rangle$. In this state the molecule triggers a first amplification process that indicates and permanently registers the detection of that first photon. Subsequently, a second photon of a different frequency $\omega_\beta \approx \omega_3 - \omega_2 =: \omega_{23}$ can excite the molecule to another state $|F_3\rangle$, from which it can decay to a different metastable state $|F_4\rangle$, triggering a second (different) amplification process that indicates the detection of the second photon. The two photons must arrive sequentially rather than simultaneously for TPA.

One motivation for this work comes from recent theory efforts to find fundamental (i.e., device-independent) limits to photo detection [1, 62, 64, 65, 66, 68, 69, 71, 72]. For reasons fully explained in [69] we construct a Hamiltonian here for the *full* detection process, including the crucial amplification step. A second motivation is of a more technical nature. The theoretical description of two (or more) photons interacting with a quantum system is known to be considerably more complicated than that of just a single photon interacting with the same system [109, 113, 114, 115, 164, 165, 166, 167, 168, 169, 170]. Two types of methods have been developed to tackle this problem. One is based on a hierarchy of coupled differential equations for generalized density matrix elements [109, 113, 171] for a quantum system interacting with prescribed multi-photon pulses. The other method [114, 115] includes virtual cavities that generate the photons and is thus based on a Hamiltonian description of the quantum system *and* the photons. We refer to these two methods as the "generalized density matrix" and the "Hamiltonian" formulations, respectively. We will use both methods here, since they each have their own advantages, and we also give the

explicit equations (which seem not to have been given before) that link the two methods. Moreover, we can explain why the methods above yield expressions for scattered light and for the dynamics of the quantum system in terms of (Hilbert space) inner products that involve the temporal amplitudes of the incoming photons [172] on the one hand, and the appropriate response functions of the system on the other.

This paper is organized as follows. In Section II we first give a synopsis of some of the results, which can be understood without going into the details of the derivations. Such details are provided in the remaining Sections. In Section III we give the Hamiltonian for our 5-level molecule. Section IV describes the two different methods we used to obtain results: the generalized density matrix methods is used to obtain analytical results, while the Hamiltonian method is used to obtain numerical results. We explain why the latter method is so much easier to use for numerical calculations. Section V ends with conclusions and discusses possible extensions of our work. In the Appendix we present the transformation that unifies the two formalisms (generalized density matrix and the Hamiltonian formulation) used in the paper.

4.2. Synopsis

Since the detailed description of our system is rather involved we first give here a synopsis of the basic results without any derivations. The results presented here are quite straightforward to understand. The light-absorbing molecule at the heart of our detector is described in detail in Fig. 1.
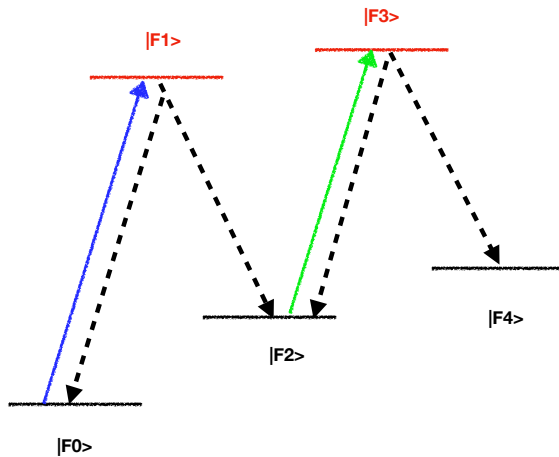
FIGURE 4.1. Model of a two-photon detector.

A light-absorbing molecule starts in the ground state $|F_0\rangle$. There are two excited states $|F_1\rangle$ and $|F_3\rangle$, indicated in red, and two metastable states $|F_2\rangle$ and $|F_4\rangle$. We assume level $|F_2\rangle$ corresponds to a shape change [while still being an electronic ground state], which down the line corresponds to a change in electric dipole moment, which in turn induces a change in a mesoscopic current or voltage (thus mimicking the process taking place in the human eye). That mesoscopic change permanently registers the detection of the first photon. The metastable state $|F_4\rangle$ corresponds to yet another change of shape, which eventually leads to a change in a dipole moment, which then in turn can change a mesoscopic current in a way that is distinct from what the molecule in state $|F_2\rangle$ accomplished. This distinct mesoscopic change then registers the second photon. The molecule can detect two photons, one "blue" photon resonant with the transition from the ground state to the first excited state, and a "green" photon resonant with the transition from $|F_2\rangle$ to the second excited state. From each of the two excited states the molecule can spontaneously decay back to state it came from or to the desired metastable state. Thus there are four decay rates, indicated from left to right by $\gamma_1 \ldots \gamma_4$, which are assumed to be more or less of the same order of magnitude. (The spontaneous transitions are indicated with dashed black lines.) On a time scale much longer than $1/\gamma_1$ the molecule resets by the metastable states decaying back to the ground state $|F_0\rangle$ (this resetting is not indicated in the figure).

4.2.1. Detection probabilities

For an incoming single-photon wave packet, the different frequency components are not all absorbed with 100% efficiency. The probabilty P_α for the

first photon, labeled α, to be detected can be written in the form

$$P_\alpha = \int d\omega \, |T_1(\omega)|^2 |u_\alpha(\omega)|^2. \tag{4.1}$$

Here $u_\alpha(\omega)$ is the Fourier component of the incoming wave packet at frequency ω and may also be referred to as its spectral amplitude. $T_1(\omega)$ is a complex transmission amplitude for the molecule to go from the initial state $|F_0\rangle$ to the desired state $|F_2\rangle$ through the intermediate excited state $|F_1\rangle$ (see Eq. (4.28) below):

$$T_1(\omega) = \frac{\sqrt{\gamma_1 \gamma_2}}{(\gamma_1 + \gamma_2)/2 - i\{\omega - \omega_{01}\}}. \tag{4.2}$$

If $\gamma_1 = \gamma_2$, the transmission probability $|T_1(\omega)|^2$ reaches a maximum of 1 at the resonance frequency ω_{01} and has a width of about γ_1. Thus, a resonant photon with a narrow width in frequency space (much less than γ_1) and whose duration is, therefore, much longer than γ_1^{-1}, can be absorbed with near-unit efficiency, exactly as was found before in Refs. [64, 65, 66].

A similar result holds for the second photon, labeled β. The only (important!) difference is that the second photon can be absorbed only when the molecule is in the state $|F_2\rangle$. Hence ideally it should arrive after photon α has been fully absorbed. In that ideal case, the conditional probability of detecting photon β (with a spectral amplitude $u_\beta(\omega)$), given that photon α was detected, is

$$P_\beta = \int d\omega |T_2(\omega)|^2 |u_\beta(\omega)|^2, \tag{4.3}$$

with

$$T_2(\omega) = \frac{\sqrt{\gamma_3 \gamma_4}}{(\gamma_3 + \gamma_4)/2 - i\{\omega - \omega_{23}\}} \tag{4.4}$$

114

a second complex transmission amplitude, describing how the molecule can transition from level $|F_2\rangle$ to level $|F_4\rangle$ through the intermediate $|F_3\rangle$ excited state.

The probability to detect both photons in the more general case when the two photons do overlap in time can be written in the form

$$P_{\alpha\&\beta} = P_\alpha P_\beta - P_{\text{overlap}}, \qquad (4.5)$$

where the (non-negative) "overlap term" will be derived and discussed in Section 4.4.1. We merely note here that the overlap term can be found analytically and is then written as a convolution involving the two spectral amplitudes $u_{\alpha,\beta}(\omega)$ and the two transmission amplitudes $T_{1,2}(\omega)$. If photon β is delayed by a time much longer than $1/\gamma_1$, then $P_{\text{overlap}} \to 0$, but if photon β entirely precedes photon α, then $P_{\text{overlap}} \to P_\alpha P_\beta$.

In Figure 2 we plot a numerical result for a case that is not optimal for two reasons. First, the widths in time of the two incoming single-photon pulses are equal to $1/(2\gamma_1)$, which is too short to be close to optimal. Second, the pulses partially overlap in time. The probability to detect both photons is then about 42%.

In Figure 3 we plot a case that shows how important the delay between the two photons is. Here photon β arrives just before photon α: while this does not affect at all the absorption (and detection) of photon α, photon β is now detected only with a very small probability of about 2%.
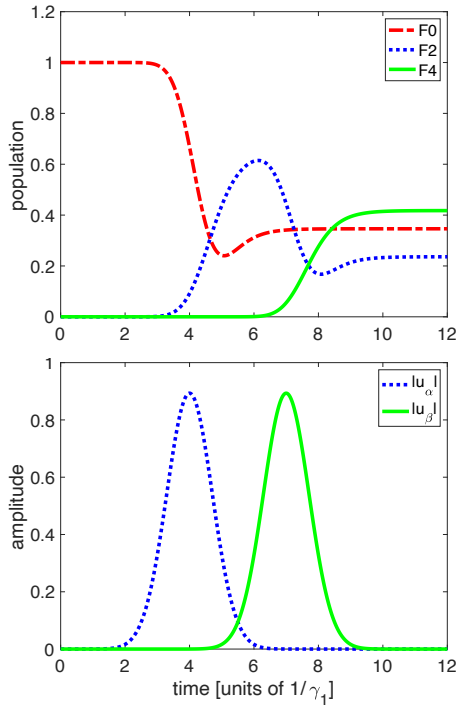
FIGURE 4.2. Top: Populations in the ground state and the two metastable states as functions of time, when two photons arrive sequentially. Bottom: the (Gaussian) amplitudes of the "blue" photon (u_α) and the "green" photon (u_β) as functions of time. We chose here $\gamma_k = \gamma_1$ for $k = 2, 3, 4$ and the time delay between the two input photons is $3/\gamma_1$

Eventually a steady state is reached, with the total population in the three lowest states adding up to 1. The steady-state population in the ground state (dot-dashed curve) is 0.346, which equals the probability to not detect any of the photons. The sum of the steady-state populations in the metastable states is .654 and equals the probability to detect the "blue" photon. The steady-state population in $|F_4\rangle$ is 0.418 and equals the probability to detect both photons.

4.2.2. Detector clicks

The generalized density matrix formalism can be used to get analytical expressions describing "clicks" of our detector in simple cases.
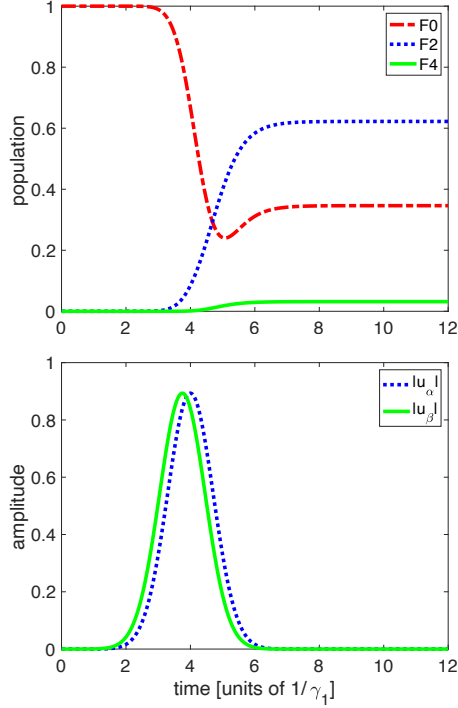
FIGURE 4.3. Top: Populations in the ground state and the two metastable states as functions of time, when the "green" photon arrives just before the "blue" photon (the time delay is $-1/(4\gamma_1)$. Bottom: the absolute values of the amplitudes $|u_\alpha|$ of the "blue" photon and $|u_\beta|$ of the "green" photon as functions of time. The probability to detect both photons is very small in this case, 0.022. The first photon is detected with the same probability (0.346) as in the previous figure.

4.2.2.1. One photon

For example, suppose for simplicity that we could measure in what state our molecule is at a specific time $T > t_0$, given that it started in the state $|F_0\rangle$ at time t_0, and suppose that we find our molecule in the state $|F_2\rangle$. This clearly would implement a measurement of the incoming photon. Thus, ignoring the second photon for now, given an expression for the population in that level as a function of time, we can write that probability at time T in the form of the Born rule as

$$P_2(T) = \mathrm{Tr}(|u_\alpha\rangle\langle u_\alpha|\Pi_1), \tag{4.6}$$

117

where $|u_\alpha\rangle\langle u_\alpha|$ is the projector onto the input single-photon wave packet of photon α, and Π_1 is a positive hermitian operator (guaranteeing that $P_2(T)$ is a real non-negative number). We can always write Π_1 in a diagonal form

$$\Pi_1 = \sum_n \lambda_n |\phi_n\rangle\langle\phi_n| \tag{4.7}$$

with λ_n real and non-negative, and with $\{|\phi_n\rangle\}$ forming an orthonormal basis of single-photon states. That means the probability $P_2(T)$ can be rewritten as

$$P_2(T) = \sum_n \lambda_n |\langle u_\alpha|\phi_n\rangle|^2. \tag{4.8}$$

The fact that the Born rule is linear in the input state (represented as a density operator or matrix) thus explains why this probability can be expressed in terms of overlaps involving the incoming single-photon wave packet [172, 173]. It also follows that $\lambda_n \leq 1$, since λ_n has the meaning of the probability that an input photon in the state $|\phi_n\rangle$ will be detected.

In our specific case we find that Π_1 is of the form

$$\Pi_1 = \int_{t_0}^{T} dt\, W_t |\phi_t\rangle\langle\phi_t| \tag{4.9}$$

where W_t is a weight per unit of time

$$W_t = \frac{\gamma_1 \gamma_2}{\gamma_1 + \gamma_2} \left[1 - \exp(-(\gamma_1 + \gamma_2)(t - t_0))\right], \tag{4.10}$$

118

and the projector projects onto a normalized single-photon state of the form

$$|\phi_t\rangle = \frac{\int_{t_0}^t dt' \exp[(\gamma_1 + \gamma_2)t'/2] \exp(i\omega_{01}(t' - t))b_1^\dagger(t')|\text{vac}\rangle}{\sqrt{\int_{t_0}^t dt' \exp[(\gamma_1 + \gamma_2)t']}} \tag{4.11}$$

where $b_1^\dagger(t)$ is the Fourier transform of $b_1^\dagger(\omega)$. (Note that we could equivalently write $t' - t$ instead of t' in the arguments of the $\gamma_{1,2}$-dependent exponentials in both numerator and denominator.) These states $|\phi_t\rangle$ are not orthogonal for different values of t and this type of nonorthogonal states also appears in the context of spectral filtering [63]. We also note that the transmission function $T_1(\omega)$ given above in Eq. (4.2) is the (properly normalized) Fourier transform of the time-dependent function —which is a Green's function—appearing in $|\phi_t\rangle$. That transmission function also determines the spectral shape of the photon emitted spontaneously by the molecule [173].

It is important to note that in Eq. (4.6) Π_1 refers only to the detector, and $|u_\alpha\rangle$ refers only to the incoming photon. Π_1 is called a POVM (Positive-Operator Valued Measure) element and fully describes the outcome of the measurement corresponding to finding the molecule in level $|F_2\rangle$ at time T. It allows us to calculate for *any* incoming photon the detection probability (4.6). In particular, it allows us in principle to infer the type of photon that is detected with the largest possible probability, by making use of the diagonal form (4.7). The largest eigenvalue $\lambda_{\max} = \max_n \lambda_n$ gives the highest possible efficiency $\eta_{\max} = \lambda_{\max}$ of detecting a single photon, and the corresponding eigenstates [there may be more than one] give the optimal single-photon states that achieve that limit.

The interpretation of

$$
\begin{aligned}
\mathrm{Tr}(\Pi_1) &= \sum_n \lambda_n = \int_{t_0}^T dt \, W_t \\
&\approx \frac{\gamma_1 \gamma_2}{\gamma_1 + \gamma_2} \left[T - t_0 - \frac{1}{\gamma_1 + \gamma_2} \right],
\end{aligned}
\tag{4.12}
$$

(where we ignored an exponentially small term in the second line) is that of a bandwidth: the effective size of the single-photon Hilbert space covered by this particular measurement outcome [62]. This bandwidth may be (much) larger than unity. For a fixed value of $\gamma_1 + \gamma_2$ the bandwidth is maximized by $\gamma_1 = \gamma_2$, an optimal "impedance-matching" condition found before in the same context of designing an optimal single-photon detector [64, 65, 66]. The bandwidth is then approximately equal to the total time the detector has been on in units of $2/\gamma_1$.

If we would be able to measure if the molecule were in state $|F_1\rangle$ at time t, then the corresponding POVM element would be proportional to a pure projector. But, since we do not know when the upper state spontaneously decayed to state $|F_2\rangle$, we do not know t, and hence we get a mixed POVM element. That is, for fixed T (when we detect the molecule to be in the state $|F_2\rangle$) there are different possibilities for time t, each with their own probability $W_t dt$. That is the interpretation of (4.9).

The idea that a quantum system absorbs a single-photon wave packet with in principle 100% efficiency if and only if it is the time-reversed version of a photon that the system would emit if it started in the final state [174, 175] does not apply so simply here, because of the presence of irreversible spontaneous decay. If we imagine we would apply a laser pulse to the $|F_1\rangle \rightarrow |F_2\rangle$ transition to induce

120

stimulated emission, then, as is well known [139, 176], that idea indeed would apply straightforwardly .

4.2.2.2. Two photons

The more interesting case of detecting the molecule in level $|F_4\rangle$ at time T signals the detection of both photons and is described by the POVM element

$$\Pi_2 = \int_{t_0}^{T} dt \int_{t_0}^{t} dt' \, W_{t'} W_{t,t'} |\phi_{t'}\rangle\langle\phi_{t'}| \otimes |\psi_{t,t'}\rangle\langle\psi_{t,t'}|, \qquad (4.13)$$

with

$$W_{t,t'} = \frac{\gamma_3 \gamma_4}{\gamma_3 + \gamma_4} \left[1 - \exp(-(\gamma_3 + \gamma_4)(t - t'))\right], \qquad (4.14)$$

and the single-photon state corresponding to the second photon is

$$|\psi_{t,t'}\rangle = \frac{\int_{t'}^{t} d\tau \exp[(\gamma_3 + \gamma_4)\tau/2] \exp(i\omega_{23}(\tau - t)) b_2^\dagger(\tau) |vac\rangle}{\sqrt{\int_{t}^{t'} d\tau \exp[(\gamma_3 + \gamma_4)\tau]}}. \qquad (4.15)$$

The prefactor W_t and the single-photon state $|\phi_t\rangle$ appearing here are exactly as defined before in (4.10) and (4.11). The time-dependent function appearing in $|\psi_{t,t'}\rangle$ is once again a Green's function, and $T_2(\omega_b)$ is its (normalized) Fourier transform.

There is a double integral over time in (4.13), each integral corresponding to an irreversible step in the detection process, which makes it uncertain at what time t we could have found the molecule in state $|F_3\rangle$ and at what earlier time $t' < t$ we could have found the molecule in $|F_1\rangle$.

We may again write down an eigenvalue equation for Π_2 [which would have to be solved numerically] and then write that POVM element in the diagonal form

$$\Pi_2 = \sum_n \mu_n |\phi_n^{(\alpha,\beta)}\rangle\langle\phi_n^{(\alpha,\beta)}|, \qquad (4.16)$$

where the projectors $|\phi_n^{(\alpha,\beta)}\rangle\langle\phi_n^{(\alpha,\beta)}|$ project onto specific pure two-photon (eigen)states, and the eigenvalues $0 \leq \mu_n \leq 1$ give the corresponding efficiencies with which those specific two-photon wave packets are detected at time T.

Like we saw for the single-photon case treated above, the bandwidth

$$\text{Tr}(\Pi_2) = \sum_n \mu_n = \int_{t_0}^{T} dt \int_{t_0}^{t} dt' \, W_{t'} W_{t,t'} \qquad (4.17)$$

is the size (dimension) of the two-photon Hilbert space covered by our detector.

4.3. The two photon absorber and its Hamiltonian

To construct the minimal absorber atom or molecule or multi-level system that can absorb two photons sequentially and produce classical outputs signaling the final state of the absorber, we consider the five level system of Figure 1 for efficient photon transduction. Some recent efforts for physically based fundamental models for photo detection assemble all parts of the process into a single fully coupled evolution problem [1, 62, 64, 65, 66, 68, 68, 69, 71, 72]. Minimal noise amplification of the absorbed photon signal has been shown to be optimally done with continuous quantum measurement [64, 65, 69]. In this scheme, the "shelving state" or the state in which the absorber produces the amplified classical readout is continuously measured. To get around the quantum Zeno effect problem with having the same state to be the photo-excited and shelving state, a three level

122

system is determined to be optimal for single photon detection [64]. Hence we use the three levels $|F_{0,1,2}\rangle$ to detect one photon.

For the two-photon detection scheme, we supplement the molecule with two more levels. The second photon can lift the molecule from state $|F_2\rangle$ into the excited state $|F_3\rangle$ which can spontaneously relax into the second shelving state $|F_4\rangle$. In the latter state the molecule triggers an amplification process which produces a noticeably different signal than that produced by the shelving state $|F_2\rangle$. The absence of a signal and the two different signals from the two levels $|F_2\rangle$ and $|F_4\rangle$ help the observer distinguish the number of photons (0, 1, or 2) absorbed by the molecule. Since the frequency of the amplified signal is independent of the input photon frequency [1], we can have different shelving states (classically) driving different oscillators of different frequencies [69]; and hence we can have distinguishable classical output signals for one or two detected photons.

We wish to calculate the dynamics of the 5-level discrete quantum system F coupled to the two continua b_1 and b_2 which contain our two input photons (with different frequencies). With $\hbar = 1$, the parts of the Hamiltonian in the Markov approximation for these coupled systems are

$$H_{sys} = \sum_{k=0}^{4} \omega_k |F_k\rangle\langle F_k|, \qquad (4.18)$$

$$H_{bath}^{1(2)} = \int d\omega\, \omega b_{1(2)}^\dagger(\omega) b_{1(2)}(\omega), \qquad (4.19)$$

$$H_{int} = -i \int d\omega \left[\sqrt{\frac{\gamma_1}{2\pi}} |F_1\rangle\langle F_0| b_1(\omega) \right.$$

$$\left. + \sqrt{\frac{\gamma_3}{2\pi}} |F_3\rangle\langle F_2| b_2(\omega) \right] + H.c. \quad . \tag{4.20}$$

This part of the Hamiltonian includes spontaneous decay back to $|F_0\rangle$ and back to $|F_2\rangle$. (The radiation field modes are fully described by four degrees of freedom. Here we fixed the quantum numbers for three of them (polarization and two transverse spatial degrees of freedom) and explicitly retain only the spectral/temporal degree of freedom.)

The next and last part of our Hamiltonian is necessary for the purpose of enabling the additional spontaneous decays of the absorber from $|F_1\rangle$ to $|F_2\rangle$ and from $|F_3\rangle$ to $|F_4\rangle$. These two transitions need to be dipole allowed and γ_2 and γ_4 determine the rates (probability per unit time) of those two processes:

$$H_{int}^1 = -i \int d\omega \left[\sqrt{\frac{\gamma_2}{2\pi}} |F_1\rangle\langle F_2| g(\omega) \right.$$

$$\left. + \sqrt{\frac{\gamma_4}{2\pi}} |F_3\rangle\langle F_4| h(\omega) \right] + H.c. \quad . \tag{4.21}$$

in terms of two additional independent (commuting) bosonic modes, described by annihilation operators $g(\omega)$ and $h(\omega)$ and their hermitian conjugates.

4.4. Two theories for photon absorption

Restriction of the number of excitations to one or two offers a workaround for the complications of the multimode nature of the interaction of propagating light with a nonlinear medium such as a two- or three-level atom. The Fock state

master equation formalism by Baragiola *et. al.* [109], and the set of generalized density matrices by Gheri *et. al.* [113] offer suitable theoretical frameworks for calculating few photon Fock state interactions with a multi-level discrete quantum system.

An alternate route for having a computationally manageable effective master equation has recently been developed by Kiilerich *et. al.* [114, 115] by restriction of the input pulse to a single time dependent mode. This approach is appealing to the problem of single photon absorption as the same physical effects of the incoming wave packet of the multimode bosonic input field is emulated. As previously formulated by Gheri *et. al.* [113], an upstream virtual cavity is introduced whose output serves as the incident field for a system under study. The incident field generated by the cavity is in a state residing in a specific wave-packet mode and all other orthogonal modes are designated the vacuum state. Since we are only interested in the input quantum state and the absorption of the photon, we only acquire the technique of *driving* with a quantum pulse from Ref. [114, 115]. The *reflected* quantum state is of no interest to us, and only the transmitted state ([66]) which quantifies the probability of absorption is required for our purpose.

The generalized density matrices framework developed by Gheri *et. al.* [113] suffices for calculating the absorption probabilities and corresponding POVMs. However, we introduce the virtual upstream cavities and formulate a Hamiltonian formulation for the entire evolution problem of photo detection (including amplification to a mesoscopic signal) that we introduced in the previous publication [69]. The Hamiltonian formulation is versatile and facilitates the calculations to be done in either the Schrödinger or the Heisenberg picture.

125

The explicit transformation between the generalized density matrices and the components of the density matrix obtained by the Hamiltonian method is presented in Appendix A.

4.4.1. Generalized Density Matrix Operators

We assume we have two unentangled single-photon wavepackets in two orthogonal modes

$$|\Psi_2\rangle = |\Psi_\alpha\rangle|\Psi_\beta\rangle, \tag{4.22}$$

where the individual photon states are defined as

$$|\Psi_{\alpha(\beta)}\rangle = \int\limits_{-\infty}^{\infty} d\omega_{a(b)} u_{\alpha(\beta)}(\omega) b_{1(2)}^\dagger(\omega)|\text{vac}\rangle. \tag{4.23}$$

$u_{\alpha(\beta)}$ is the properly normalized wave function for photon a (b). The two photons reside in the two distinct continua b_1 and b_2. (We will also use the Fourier transforms of the single-photon amplitudes, which for simplicity we denote by $u_{\alpha,\beta}(t)$.)

Following Ref. [113], we can define generalized density matrix operators for $i, j = 0, 2, \alpha, \beta$ and derive a set of coupled differential equations for them that describes the absorption of the two photons. In the following, R denotes the reservoir or bath, which includes continua other than b_1 and b_2, such as the continua g and h introduced above:

$$\rho_{i,j}(t) = \text{Tr}_R\left[U(t, t_0)\rho_S(t_0) \otimes |\Psi_i\rangle\langle\Psi_j|U^\dagger(t, t_0)\right]. \tag{4.24}$$

Here $|\Psi_0\rangle$ denotes the vacuum state $|\text{vac}\rangle$, and $|\Psi_2\rangle$, $|\Psi_\alpha\rangle$ and $|\Psi_\beta\rangle$ are the two-photon input state and the individual single-photon states introduced above. Furthermore, $\rho_S(t_0)$ is the initial state of all remaining quantum systems, including our 5-level molecule and the reservoir R. In our case, each of these generalized density matrices for fixed values of i and j is a 5x5 matrix, describing the 5 levels of our molecule.

The generalized density matrices can be expanded in a time independent complete 5x5 basis, and substitution in the evolution equations yields a set of coupled differential equations for the coefficients $\rho_{ik,jl}(t)$ of the expansion,

$$\rho_{i,j}(t) = \sum_{k,l} \rho_{ik,jl}(t)|F_k\rangle\langle F_l|. \tag{4.25}$$

These equations are given in Appendix A. The diagonal generalized density matrices (for $i = j$) have a preserved trace of 1, and off-diagonal ones have a preserved trace of 0 over the evolution [113]. (In the alternative Hamiltonian formulation shown below a single Hamiltonian (with auxiliary cavities appended) can embody the complete evolution, and a *single* density matrix (with preserved trace of 1) of size 20x20 can embody the complete dynamics [69].)

In order to simplify intermediate equations, we will absorb a time-dependent phase factor $\exp(i\omega_{01})t)$ in the definition of the single-photon amplitude $u_\alpha(t)$ for photon a and similarly a factor $\exp(i\omega_{23}t)$ in the amplitude $u_\beta(t)$ for photon b, such that both amplitudes can be considered slowly-varying if the photons are more or less on resonance with their respective transition in the molecule. End results are quoted in terms of the original amplitudes.

The evolution problem is initiated with $\rho_{00,00} = 1$ at time t_0, i.e., the molecule is in the $|F_0\rangle$ state, with any photon yet to come in. The coefficient $\rho_{\alpha2,\alpha2}$ embodies the evolution of the molecule occupation elevated to $|F_2\rangle$ state driven by just the first photon α with temporal amplitude $u_\alpha(t)$. The solution found is

$$
\rho_{\alpha2,\alpha2}(t) = \gamma_1\gamma_2 \int_{t_0}^{t} dt_1 \left[e^{-(\gamma_1+\gamma_2)t_1} \right.
$$

$$
\left. \int_{t_0}^{t_1} dt_2 e^{\frac{\gamma_1+\gamma_2}{2}t_2} u_\alpha^*(t_2) \int_{t_0}^{t_2} dt_3 e^{\frac{\gamma_1+\gamma_2}{2}t_3} u_\alpha(t_3) \right] + c.c., \tag{4.26}
$$

This result becomes especially simple when considering the steady-state, obtained by taking the limit $t \to \infty$. The result further simplifies when we take the limit $t_0 \to -\infty$ such that in principle any single-photon wave packet could be absorbed, irrespective of when it arrives. The equations in those limits are most easily solved in Fourier space, and we obtain then the same result we had obtained before in Ref. [69],

$$
\rho_{\alpha2,\alpha2}(\infty) = P_\alpha = \int d\omega \, |u_\alpha(\omega)|^2 |T_1(\omega)|^2, \tag{4.27}
$$

where

$$
T_1(\omega) = \frac{\sqrt{\gamma_1\gamma_2}}{(\gamma_1+\gamma_2)/2 - i\{\omega - (\omega_1 - \omega_0)\}} \tag{4.28}
$$

is the transmission coefficient describing the propagation of a single excitation through the Λ system [63, 66]. (This is Eq. (4.2)) of the Synopsis Section.)

$\rho_{\alpha2,\alpha2}(t)$ in Eq. 4.26 can be recast into the more informative form

$$
\rho_{\alpha2,\alpha2}(t) = \int_{t_0}^{t} dt' \left| \int_{t_0}^{t'} dt_2 \sqrt{\gamma_1\gamma_2} e^{\frac{\gamma_1+\gamma_2}{2}(t_2-t')} u_\alpha(t_2) \right|^2.
$$

$$
\tag{4.29}
$$

128

This is the form that can be used straightforwardly to obtain the expressions (4.9)–(4.11) for the POVM element Π_1. The quantity inside the integral over t' is actually γ_2 times the population in level $|F_1\rangle$ as a function of time [65].

The probability of the molecule reaching $|F_4\rangle$ state driven by the second photon β has a "nested" structure containing the expression, $\rho_{\alpha2,\alpha2}(t)$,

$$\rho_{24,24}(t) = \gamma_3\gamma_4 \int\limits_{t_0}^{t} dt_1 \left[e^{-(\gamma_3+\gamma_4)t_1} \right.$$
$$\left. \int\limits_{t_0}^{t_1} dt_2 e^{\frac{\gamma_3+\gamma_4}{2}t_2} u_\beta^*(t_2) \int\limits_{t_0}^{t_2} dt_3 e^{\frac{\gamma_3+\gamma_4}{2}t_3} u_\beta(t_3)\rho_{\alpha2,\alpha2}(t_3) \right] + c.c.$$

$$(4.30)$$

We may rewrite this expression by changing variables in the complex conjugate term and by substituting (4.29) to obtain our two-photon POVM (4.13).

As we noted in Section 4.2 the time-dependent functions appearing in the expression for $\rho_{24,24}(t)$ and other populations of quantum levels can be interpreted as Green's functions. Their (normalized) Fourier transforms act as transmission and reflection coefficients when treating this problem as a scattering problem. In our case, transmission coefficients $T_1(\omega)$ (defined above) and $T_2(\omega)$ (defined below) play the new role of determining the detection probability of photons with frequency ω in the limit of $t \to \infty$, as we saw in Eq. (4.27) and as we will show in the next subsection.

4.4.2. Overlap term

The absorption of the two photons can be completely calculated in the frequency domain. To that end, we define the Fourier transform of the population

in level $|F_1\rangle$, since we can express all quantities of interest in terms of that function. We find

$$F_1(\omega) = \frac{1}{\sqrt{2\pi}} \int dx \, T_1(\omega + x) u_\alpha(\omega + x) T_1^*(x) u_\alpha^*(x). \tag{4.31}$$

The 0-frequency component of $\sqrt{2\pi} F_1(\omega)$, equals the detection probability for the first photon $\sqrt{2\pi} F_1(0) = \int dx |u_\alpha|^2 |T_1(x)|^2 =: P_\alpha$. In the frequency domain, we then obtain the Fourier transform of $\rho_{\alpha2,\alpha2}(t)$ as

$$\rho_{\alpha2,\alpha2}(\omega) = \gamma_2 \left[iF_1(\omega) \mathrm{P}\left(\frac{1}{\omega}\right) + \pi F_1(0)\delta(\omega) \right]. \tag{4.32}$$

where P denotes the principal value. In eq. (4.30), if we replace $\rho_{\alpha2,\alpha2}(t)$ with its steady state value P_α, we get an expression identical in form to eq. (4.26) with different decay rates, and we thus can simply evaluate the result for $t \to \infty$ as the product $P_\alpha P_\beta$ with P_β given by (4.3). So, if the second photon arrives long after the first photon has been completely absorbed (and the absorber raised to the level $|F_2\rangle$), the probability of both photons being absorbed becomes the product of their individual absorption probabilities.

Therefore, we can rewrite the probability of two-photon absorption, $\rho_{24,24}(\infty)$ as a sum of two parts, one being the product of the two absorption probabilities. We name the other term P_{overlap}, since we expect the term to vanish if the second photon comes in after a delay and the two wave functions of the two photons overlap negligibly. We thus write

$$\rho_{24,24}(\infty) = P_\alpha P_\beta - P_{\mathrm{overlap}} \qquad . \tag{4.33}$$

130

After some algebra, we obtain

$$P_{\text{overlap}} = \frac{1}{2}P_\alpha P_\beta + P^{\alpha\beta} \tag{4.34}$$

where

$$
\begin{aligned}
P^{\alpha\beta} &= \frac{\gamma_2\sqrt{\gamma_3\gamma_4}}{\sqrt{2\pi}(\gamma_3+\gamma_4)} \int d\omega\, u_\beta^*(\omega)T_2(\omega) \\
&\times \int dx\, u_\beta(\omega - x)\mathrm{P}\frac{F_1(x)}{ix} + c.c.,
\end{aligned}
\tag{4.35}
$$

where P denotes the principal value. The following results are borne out in numerical simulations for different arbitrary wave shapes of the two photons that are delayed by a long time $t_d \gg 1/\gamma_1$:

$$
\begin{aligned}
P^{\alpha\beta} &\longrightarrow -\frac{1}{2}P^\alpha_{abs} P^\beta_{abs} \\
P_{\text{overlap}} &\longrightarrow 0 \\
\rho_{24,24}(\infty) &\longrightarrow P_\alpha P_\beta.
\end{aligned}
\tag{4.36}
$$

4.4.3. Hamiltonian Formulation

In a recent paper, Ref. [69], we developed a "Hamiltonian formulation" that can describe a single photon detection process in its entirety. We now adapt that formulation for the detection of two unentangled photons absorbed sequentially. The most convenient method for solving the dynamical equation set is numerical integration of the Liouvillian equation in the Hamiltonian formulation [69]. In the Hamiltonian formulation, we get a single density matrix for the entire system

that can be solved easily with well-known vectorization and Trotter decomposition techniques [177]. From the solution of the single density matrix, the generalized density matrices can be found easily with the transformation (4.50).

We introduce two auxiliary cavities with damped harmonic motion leaking one excitation each into the continuous bath modes $b_1(\omega)$ and $b_2(\omega)$. These two excitations mimic the photon wave packets in the two baths that we are trying to detect. There are two other continuous modes g and h, which are introduced only to enable the spontaneous relaxation of the molecule F. The Hamiltonian is of the
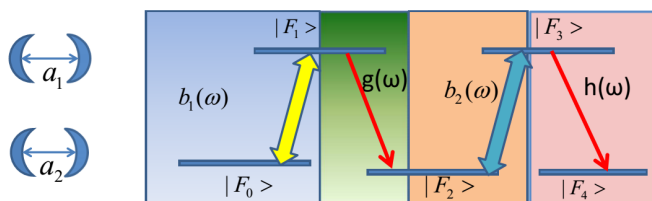
FIGURE 4.4. The cavity modes a_1 and a_2 each have one excitation to start with. These two excitations leak out into their adjacent baths (continuous modes b_1 and b_2 respectively) by designing the coupling to the baths in time, thus creating two single-photon wavecpackets. They respectively drive the $|F_0\rangle$ to $|F_1\rangle$ and $|F_2\rangle$ to $|F_3\rangle$ transitions. From the excited levels, the molecule can relax with certain probabilities either back to the state it came from or to another shelving state. The two shelving states drive two distinct amplification processes and thus produce two macroscopically distinct "classical" signals (unrelated in frequency to the incoming photons) in an output bath $d(\omega)$.

following form

$$H = H_{a_1} + H_{a_1 - b_1} + H_{b_1} + H_{a_2} + H_{a_2 - b_2} + H_{b_2}$$

$$+ H_{b_1 - F} + H_{b_2 - F} +$$

$$H_F + H_{F-g} + H_g + H_{F-h} + H_h$$

$$+ H_{F-c} + H_c + H_{c-d} + H_d. \tag{4.37}$$

The diagonal terms in the Hamiltonian give all the eigen energies of the systems. For example, for the cavities it features their resonance frequencies,

$$H_{a_{1(2)}} = \omega_{a_{1(2)}} a^{\dagger}_{1(2)} a_{1(2)}, \tag{4.38}$$

and for the continuous modes, such as g, we have

$$H_g = \int_0^{\infty} d\omega \, \omega g^{\dagger}(\omega) g(\omega), \tag{4.39}$$

and similar terms for $H_{b_1}, H_{b_2}, H_c, H_d$ and H_h. H_F is simply H_{sys} as defined before in Eq. (4.18).

The interaction between the cavities and the field modes, as well as the interaction of the photons with the molecule are mediated by the electric fields corresponding to modes b_1 and b_2. Each of the electric field operators of the modes can be expanded into plane wave basis (also their Hermitian conjugate operators). For the input fields $B_{1,2}(x, t)$, we expand

$$B_{1,2}(x, t) = \frac{1}{\sqrt{2\pi}} \int_0^{\infty} d\omega \, b_{1,2}(\omega, t) \exp(i\omega x/c). \tag{4.40}$$

The molecule is located at $x = 0$ and the cavities a_1 and a_2 are located "upstream" at $x = -c\tau_1$ and $x = -c\tau_2$ where c is the speed of light and τ_1, τ_2 are the times it takes for a photon to travel from the respective cavities to the absorber F. The cavities are coupled to the fields $B_1(x = -c\tau_1, t)$ and $B_2(x = -c\tau_2, t)$ in the manner:

$$H_{a_{1(2)}-b_{1(2)}} =$$
$$i[g^*_{1(2)}(t) a_{1(2)} B^{\dagger}_{1(2)}(-c\tau_{1(2)}, t) - g_{1(2)}(t) B_{1(2)}(-c\tau_{1(2)}, t) a^{\dagger}_{1(2)}]$$

As pointed out in previous work [69, 113, 115], the coupling of the virtual cavities to the fields can be made time dependent for the purpose of creating arbitrary photon wavepackets, and therefore the Hamiltonian formulation is completely general for the photo detection process. In this way, we can calculate the evolution of the complete system with the elements of a single density matrix, instead of the multiple generalized density matrices in eq. (4.24). All other discrete-continuum couplings are at position $x = 0$.

$$
\begin{aligned}
H_{b_{1(2)}-F} &= i\sqrt{\gamma_1} \left|F_{0(2)}\right\rangle \left\langle F_{1(3)}\right| B^\dagger_{1(2)}(x = 0, t) + H.c. \\
H_{F-g} &= i\sqrt{\gamma_2} \left|F_2\right\rangle \left\langle F_1\right| G^\dagger(x = 0, t) + H.c. \\
H_{F-h} &= i\sqrt{\gamma_4} \left|F_4\right\rangle \left\langle F_3\right| H^\dagger(x = 0, t) + H.c. \\
H_{c-d} &= i\sqrt{\Gamma} c D^\dagger(x = 0, t) + H.c.,
\end{aligned}
\tag{4.41}
$$

where the field operators $G(x, t)$ and $H(x, t)$ are defined in terms of $g(\omega)$ and $h(\omega)$ just as the field operator $B(x, t)$ is defined in Eq. (4.40) in terms of $b(\omega)$.

The amplification mechanism is embodied in the parts,

$$
\tilde{F} = \sum_{k=0,1,..,4} F_k |F_k\rangle\langle F_k|,
\tag{4.42}
$$
$$
H_{F-c} = i\tilde{F}(c - c^\dagger).
$$

The different eigenvalues of the operator $\tilde{F}$ drive a discrete quantum harmonic oscillator (another cavity, for example) with annihilation operator c by different classical driving strengths. That driven cavity mode will contain an increasing number of excitations. We assume here $F_0 = F_1 = F_3 = 0$ so that no amplification (no driving) takes place when the molecule is in the corresponding states. The

134

values for F_2 and $F_4 (\neq F_2)$ are nonzero and drive the amplification process. Excitations from the driven cavity c leak into the continuum mode $d(\omega)$, which can be observed "classically" when populated massively. Thus $d(\omega)$ contains our final "classical" signal. We will not analyze the macroscopic signal here and refer instead for further details to Ref. [69], where it is shown that this type of amplification process yields minimal noise; see also [122].

4.4.4. Invariants of motion

The Hamiltonian formalism preserves the basic idea of the photodetection process that is meant to be simulated. We can find some operators that commute with the Hamiltonian and are therefore conserved in time.

$$
\begin{aligned}
\mathcal{I}_{20} &= a_1^\dagger a_1 + \int d\omega b_1^\dagger(\omega) b_1(\omega) - |F_0\rangle\langle F_0|, \\
\mathcal{I}_{21} &= a_1^\dagger a_1 + \int d\omega b_1^\dagger(\omega) b_1(\omega) + |F_1\rangle\langle F_1| + \int d\omega g^\dagger(\omega) g(\omega), \\
\mathcal{I}_{22} &= a_2^\dagger a_2 + \int d\omega b_2^\dagger(\omega) b_2(\omega) - |F_2\rangle\langle F_2| + \int d\omega g^\dagger(\omega) g(\omega), \\
\mathcal{I}_{23} &= a_2^\dagger a_2 + \int d\omega b_2^\dagger(\omega) b_2(\omega) + |F_3\rangle\langle F_3| + \int d\omega h^\dagger(\omega) h(\omega), \\
\mathcal{I}_{24} &= |F_4\rangle\langle F_4| - \int d\omega h^\dagger(\omega) h(\omega),
\end{aligned}
$$

A conserved quantity of particular interest is $\mathcal{I}_N = \frac{1}{2}\mathcal{I}_{20} + \frac{1}{2}\mathcal{I}_{21} + \frac{1}{2}\mathcal{I}_{22} + \frac{1}{2}\mathcal{I}_{23} - \mathcal{I}_{24} + \frac{1}{2}$. The $\frac{1}{2}$ is added here to give the invariant $\mathcal{I}_N$ the meaning of the number of excitations (photons). The invariant takes the values 0,1,2 for the three cases of 0,1,2 input photons, respectively.

The values of these quantities keep track of where the excitations are and whether the photons will be detected or not. For example, an initial excitation in

the a_1 cavity means $\mathcal{I}_{20}$ maintains a value of 0 in the entire evolution. So as the eigenvalue of $a_1^\dagger a_1$ decays from 1 to 0, either the eigenvalues of both $\int d\omega b_1^\dagger(\omega)b_1(\omega)$ and $|F_0\rangle\langle F_0|$ for $t \to \infty$ are 1 (the photon was not detected) or they are both 0 (the photon was detected).

Similarly, $\mathcal{I}_{24}$ always equals 0, with an eigenvalue of 1 for both $|F_4\rangle\langle F_4|$ and $\int d\omega h^\dagger(\omega)h(\omega)$ indicating the second photon was detected, and an eigenvalue 0 indicating it was not detected (yet).

4.4.5. The Liouvillian Representation

Due to the continua in our model, the Hilbert space is infinite dimensional. However, we follow the well established practice of eliminating the continua and focus our attention on the "system Hilbert space, $\mathcal{H}_d$" (d=2×2×5=20) and are able to calculate all quantities of interest in the vector space of the linear operators, $L(\mathcal{H}_d)$ acting on the Hilbert space, $\mathcal{H}_d$. We eliminate the continua b_1, b_2, g, h and obtain our Liouvillian master equation for the system density operator, ρ_s comprised of discrete quantum systems a_1, a_2, F. Details of the exact method and validation of quantum mechanical commutation relationships can be found in the preceding paper Ref. [69]. For the absorption problem, we need not include the discrete cavity mode c. The Liouvillian master equation for the chosen discrete quantum parts of the Hamiltonian is

$$\frac{\partial}{\partial t}\rho_s = -i[H_{sys}, \rho_s] + \mathcal{D}\left[\rho_s\right]. \tag{4.43}$$

Eq. 4.43 facilitates numerical calculation in the Schrödinger picture. For a collapse operator, X, the Lindblad dissipator super-operator (a map, S: $L(\mathcal{H}_d) \to L(\mathcal{H}_d)$)

acting on the system density operator, ρ_s has the form, $\mathcal{D}_X[\rho_s] = X\rho_s X^\dagger - \frac{1}{2}\rho_s X^\dagger X - \frac{1}{2}X^\dagger X\rho_s$. For time dependent coupling of system and environment, the collapse operator take time dependent forms [114, 115]. The collapse operator embodying the decay from the upper state $\left|F_{1(3)}\right\rangle$ back to the state $\left|F_{0(2)}\right\rangle$ takes the form $X = g^*_{1(2)}(t)a_{1(2)} + \sqrt{\gamma_1}|F_{0(2)}\rangle\langle F_{1(3)}|$. A quantum jump effected by this operator indicates the corresponding photon was not detected.

The density operator in Eq. 4.43 can be expanded in the partial basis of the two virtual cavity populations, i.e. four basis states $|n, m\rangle$ with $n, m = 0, 1$ indicating the number of photons inside the cavity. This gives rise to a coupled equation set of sixteen coefficients. The complete expansion can be found in eq. 4.47. With the transformation in eq. 4.50, we get back the equation set in eq. 4.46 for the generalized density matrix operators, $\rho_{ab}(t)$ with the substitution.

$$u_{\alpha(\beta)}(t) = g^*_{1(2)}(t)e^{-\frac{1}{2}\int\limits_{t_0}^{t} dt'|g_{1(2)}(t')|^2}, \tag{4.44}$$

which is the same result as found in [114, 115]. Inversion of the relationship in eq. 4.44 gives away the method of varying the couplings $g_{1(2)}(t)$ in time so as to generate a desired photon wavepacket $u_{\alpha(\beta)}(t)$ [114, 115]

$$g_{1(2)}(t) = \frac{u^*_{\alpha(\beta)}(t)}{\sqrt{1 - \int\limits_{t_0}^{t} dt'|u_{\alpha(\beta)}(t')|^2}}. \tag{4.45}$$
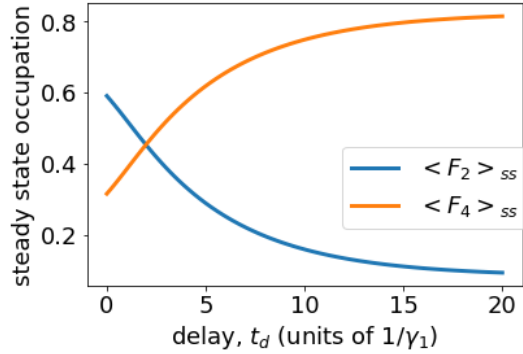
FIGURE 4.5. The steady state occupations of F_2 and F_4 level for the initial state of both cavity having one photon. Here we chose $\gamma_1 = \gamma_2 = \gamma_3 = \gamma_4$ and $\kappa_1 = \kappa_2 = \gamma_1/5$.

4.5. Results

4.5.1. Exponentially decaying $u_\alpha(t)$ and $u_\beta(t)$

With $u_\alpha(t) = \sqrt{\kappa_1}e^{-\kappa_1 t/2}\Theta(t)$ and $u_\beta(t) = \sqrt{\kappa_2}e^{-\kappa_2 t/2}\Theta(t)$, ($\Theta(t)$ being the Heaviside unit step function) either dynamical equation sets 4.46 or 4.43 as well as quantities like absorption probabilities (eq. 4.33) can be solved analytically. Through eq. 4.45, we find both couplings $g_{1(2)}(t) = \sqrt{\kappa_{1(2)}}$ to be constant in time, This is the only example which can be calculated with a time-independent system Hamiltonian and collapse operators. As discussed previously, if the two photons have significant temporal overlap, the second photon may get reflected before the first is absorbed, and the molecule may end up in $|F_2\rangle$ instead of being raised all the way to $|F_4\rangle$. If we gradually delay the second photon in time with increasing delay periods (t_d) and calculate the steady state populations in $|F_2\rangle$ and $|F_4\rangle$ from the Liouvillian equation each time, we find that with a longer delay the second photon is absorbed with higher probability (Fig. 4.5). The sum of the two populations is always $P^\alpha_{abs}(= 10/11)$, the probability of the first photon

138

being absorbed. For a delay $t_d \gg 1/\gamma_1$, the steady state occupation of the F_4 level reaches $P_{abs}^{\alpha} P_{abs}^{\beta} (= 100/121)$, as expected.

However, the delay is not the only critical determinant of the absorption probability of the second photon. (The absorption of the first photon is completely independent of the second.) The closer to P_α the occupation in $|F_2\rangle$ has risen when the second photon arrives, the more efficient the absorption of the second photon is. So, a longer width of the second photon wavefunction would also increase the efficiency of the second photon absorption. The overlap between the two photon wave functions determines the efficiency of the second photon absorption. By making κ_2 smaller we can make the second photon wave function longer in time. In Figs. 4.6 and 4.7 respectively we plot the average occupation levels of $|F_2\rangle$ and of $|F_4\rangle$ as functions of time for different values for κ_2 that make the wavefunction of the second (β) photon longer. The same colored curves from Figs. 4.6 and 4.7 add up to $P_\alpha = 10/11$ for $t \rightarrow \infty$. With the larger share of the second photon coming into the detector after the first photon has already populated the F_2 level, the probability of a successful two-photon absorption rises.

4.5.2. Gaussian $|u_\alpha(t)|^2$ and $|u_\beta(t)|^2$

We numerically calculate the two photon absorption probability, $\rho_{24,24}(\infty)$ for two real Gaussian wavefunctions with varying standard deviations and the second one delayed by different delays. The results are plotted in Fig. 4.8. A note on the numerical method is in order here. For repeated calculations with different values of the parameters, we use eq. 4.33, since it is less demanding than solving the Liouvillian equation (eq. 4.43) many times. For the numerical calculation of the principal value, we use
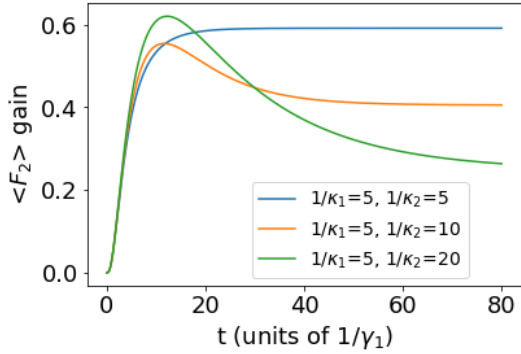
FIGURE 4.6. The occupation of the F_2 level as a function of time for an initial state of both cavities having one photon.

The decay rate κ_2 of the second cavity (which determines the width in time of the second photon) is varied. All rates γs are equal, and the rates $\kappa_{1,2}$ are given in units of γ_1. The steady-state population of $|F_2\rangle$ decreases with decreasing value of κ_2, that is, with increasing width of the second photon. The second photon moved population out of level $|F_2\rangle$.
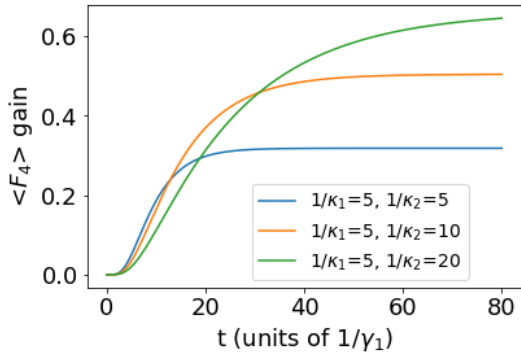
FIGURE 4.7. Same as the preceding Figure, but plotting the occupation of level F_4. Here the steady-state population of $|F_4\rangle$ increases with decreasing value of κ_2 since the second photon is more effective at moving population from $|F_2\rangle$ to $|F_4\rangle$.

$$P\left(\frac{1}{\omega}\right) = \frac{1}{2}\left(\frac{1}{\omega - i\epsilon} + \frac{1}{\omega + i\epsilon}\right),$$

and use a sufficiently small ϵ.

Curiously, we find that the efficiency plot is symmetric in their standard deviations for any given delay. The efficiency for a standard deviation σ_1 for

140

photon α and standard deviation σ_2 for photon β for a given time delay t_d is the same as for standard deviations σ_2 for photon α and σ_1 photon β. The probability of the second photon absorption improves a lot as the delay is increased. For some delays there is a peak efficiency for a certain standard deviation and falls off slightly with even longer standard deviations.

FIGURE 4.8. $\rho_{24,24}(\infty)$ plotted on the vertical z-axis against the standard deviations of the α and β photons plotted on the two axes on the horizontal plane for (a) no time delay, (b) $1/\gamma_1$,(c) $3/\gamma_1$, and (d) $5/\gamma_1$ delays (of the means/centres of the waveshape) of the second photon, β.

4.5.3. Gaussian $|u_\alpha(t)|^2$ and exponentially decaying $u_\beta(t)$

For completeness we also consider the "mixed" case of one Gaussian wave packet (for the first photon) and an exponentially decaying wave packet (for the second photon). The results are plotted in Fig. 4.9 As long as the two photon wavefunctions overlap, we get a decrease in the $\rho_{24,24}(\infty)$ value with increasing the standard deviation of the α photon. Increase in κ or decrease in the time constant of the β photon increases P_{abs}^β and is responsible for larger $\rho_{24,24}(\infty)$.
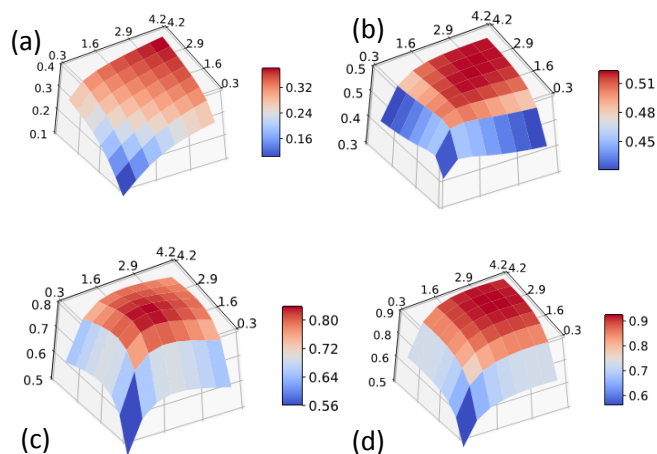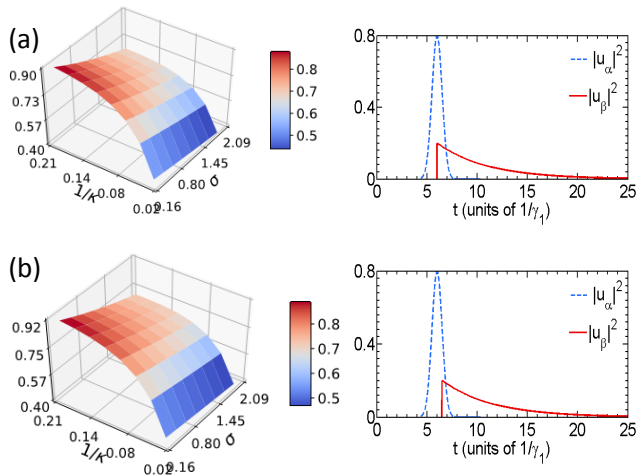
FIGURE 4.9. $\rho_{24,24}(\infty)$ plotted on the vertical z-axis against the standard deviations of the α photon Gaussian waveshape on the x axis and the inverse of the rate constant (κ) of the β photons plotted on the y axis for (a) no time delay, (b) $0.5/\gamma_1$ delay (delay between the mean of the Gaussian and the onset of the β photon waveshape).

4.6. Conclusions

We developed a fully quantum-mechanical model for a photon-number resolving detector that can detect up to two photons by extending the model of Ref. [69] to a five-level molecule. Moreover, we used two different methods for treating the interaction of two photons with a quantum system—the methods developed by [113] and [109] on the one hand, and by [114, 115] on the other—and provided the explicit connection between the two. The former method allowed us to obtain several analytical results in Section 4.2 that characterize our detector, the latter method is very well suited for numerical calculations, as shown in Section 4.5.

The model developed in [69] followed the lead by Refs. [60, 64, 65] in taking inspiration from visual systems appearing in biology. It is an open question whether our current extension of that model can be found in nature as well: in

particular, whether the specific *step-wise* two-photon absorption process we studied here occurs in the human eye, just as *simultaneous* two-photon absorption does occur [160].

We note two extensions of our work that may be interesting. The first extension of our model is to another type of five-level molecule that would detect just one photon, but it would be sensitive to polarization. From the initial state we could either reach an excited state $|F_1\rangle$ (as in our actual model) but also an alternative excited state $|F_{1'}\rangle$ (for an orthogonally polarized photon), which would then decay to a different metastable state $|F_{2'}\rangle$. If the signal produced in the latter state is distinguishable from that produced by $|F_2\rangle$, then this molecule would perform a polarization-sensitive single-photon measurement. It is known that some animals (insects, fish, birds) did develop polarization vision, see, e.g. Ref. [178].

Second, we focused here on the case of two distinguishable input photons, with different frequencies. The case of two overlapping frequencies (relevant when the two molecular transitions would have nearly equal transition frequencies) would reveal two additional features. Both input photons would be able to drive the two transitions, and the final expression for the two-photon absorption amplitude would contain two terms, corresponding to two different time orders in which the "first" and "second" photon could be absorbed. Those two terms may interfere destructively. That type of effect is certainly interesting but known [63, 179]. Moreover, the POVM element would involve projections onto *entangled* two-photon input states, like it does for standard two-photon absorption [156].

4.7. Emulating Photon wavepackets with Auxiliary Cavities

We outline the systematic process of deriving the transformations between the generalized density matrix operators and coefficients (in the expansion in eq. 4.47) in the Hamiltonian formulation. Unlike Gheri et al, we do not introduce a detuning of the auxiliary cavities for the emulation of the generalized density matrix equations (Refs. [114, 115] did not either). Gheri et al addressed the mapping for the problem of photons (one or few) in a single continuum. For the problem of two photons residing in two continua (or even more complex scenarios), the procedure outlined here can find the mapping between the two formalisms (generalized density matrix operator and Hamiltonian formulation) systematically. The generalized density matrix equations found for the system described in sections III and IV are

$$\dot{\rho}_{2,2}(t) = \mathcal{L}\{\rho_{2,2}\}(t) + [\sqrt{\gamma_3}u_\beta(t)[\rho_{\alpha2}(t), |F_3\rangle\langle F_2|(t_0)]$$

$$+\sqrt{\gamma_1}u_\alpha(t)[\rho_{\beta2}(t), |F_1\rangle\langle F_0|(t_0)] + H.c.]$$

$$\dot{\rho}_{\alpha,2}(t) = \mathcal{L}\{\rho_{\alpha,2}\}(t) - \sqrt{\gamma_3}u_\beta^*(t)[\rho_{\alpha,\alpha}, |F_2\rangle\langle F_3|(t_0)] +$$

$$\sqrt{\gamma_1}u_\alpha(t)[\rho_{0,2}, |F_1\rangle\langle F_0|(t_0)] - \sqrt{\gamma_1}u_\alpha^*(t)[\rho_{\alpha,\beta}, |F_0\rangle\langle F_1|(t_0)]$$

$$\dot{\rho}_{\beta,2}(t) = \mathcal{L}\{\rho_{\beta,2}\}(t) - \sqrt{\gamma_1}u_\alpha^*(t)[\rho_{\beta,\beta}, |F_0\rangle\langle F_1|(t_0)] +$$

$$\sqrt{\gamma_3}u_\beta(t)[\rho_{0,2}, |F_3\rangle\langle F_2|(t_0)] - \sqrt{\gamma_3}u_\beta^*(t)[\rho_{\beta,\alpha}, |F_2\rangle\langle F_3|(t_0)]$$

$$\dot{\rho}_{\alpha,\alpha}(t) = \mathcal{L}\{\rho_{\alpha,\alpha}\}(t) - \sqrt{\gamma_1}u_\alpha(t)\left[|F_1\rangle\langle F_0|(t_0), \rho_{0,\alpha}(t)\right]$$

$$+\sqrt{\gamma_1}u_\alpha^*(t)\left[|F_0\rangle\langle F_1|(t_0), \rho_{\alpha,0}(t)\right]$$

$$\dot{\rho}_{\beta,\beta}(t) = \mathcal{L}\{\rho_{\beta,\beta}\}(t) - \sqrt{\gamma_3}u_\beta(t)\left[|F_3\rangle\langle F_2|(t_0), \rho_{0,\beta}(t)\right]$$

$$+\sqrt{\gamma_3}u_\beta^*(t)\left[|F_2\rangle\langle F_3|(t_0), \rho_{\beta,0}(t)\right]$$

$$\dot{\rho}_{\alpha,\beta}(t) = \mathcal{L}\{\rho_{\alpha,\beta}\}(t) - \sqrt{\gamma_1}u_\alpha(t)\left[|F_1\rangle\langle F_0|(t_0), \rho_{0,\beta}(t)\right]$$

$$+\sqrt{\gamma_3}u_\beta^*(t)\left[|F_2\rangle\langle F_3|(t_0), \rho_{\alpha,0}(t)\right]$$

$$\dot{\rho}_{0,2}(t) = \mathcal{L}\{\rho_{0,2}\}(t)$$

$$-\sqrt{\gamma_3}u_\beta^*(t)[\rho_{0,\alpha}, |F_2\rangle\langle F_3|(t_0)] - \sqrt{\gamma_1}u_\alpha^*(t)[\rho_{0,\beta}, |F_0\rangle\langle F_1|(t_0)]$$

$$\dot{\rho}_{0,\alpha}(t) = \mathcal{L}\{\rho_{0,\alpha}\}(t) + \sqrt{\gamma_1}u_\alpha^*(t)[\rho_{0,0}, |F_0\rangle\langle F_1|(t_0)]$$

$$\dot{\rho}_{0,\beta}(t) = \mathcal{L}\{\rho_{0,\beta}\}(t) + \sqrt{\gamma_3}u_\beta^*(t)[\rho_{0,0}, |F_2\rangle\langle F_3|(t_0)]$$

$$\dot{\rho}_{0,0}(t) = \mathcal{L}\{\rho_{0,0}\}(t) \tag{4.46}$$

$\mathcal{D}$ is the Lindblad dissipator superoperator and its explicit form depends on the number and nature of the baths coupled to the system. Due to the coupling of the total of four continua, we get four collapse operators for the Lindblad dissipator superoperator, $\mathcal{D}$, namely $\sqrt{\gamma_1}|F_0\rangle\langle F_1|$, $\sqrt{\gamma_2}|F_2\rangle\langle F_1|$, $\sqrt{\gamma_3}|F_2\rangle\langle F_3|$, and

$\sqrt{\gamma_4}|F_4\rangle\langle F_3|$. The density matrix in the Hamiltonian formulation can be expanded in the complete basis (time dependence restricted to the expansion coefficients):

$$\rho(t) =$$

$$\tilde{\rho}_{2,2}(t)|0,0\rangle\langle 0,0| + \tilde{\rho}_{\alpha,\alpha}(t)|0,1\rangle\langle 0,1| + \tilde{\rho}_{\beta,\beta}(t)|1,0\rangle\langle 1,0|$$

$$+\tilde{\rho}_{\beta,2}(t)|1,0\rangle\langle 0,0| + \tilde{\rho}_{0,\alpha}(t)|1,1\rangle\langle 0,1|$$

$$+\tilde{\rho}_{2,\beta}(t)|0,0\rangle\langle 1,0| + \tilde{\rho}_{\alpha,0}(t)|0,1\rangle\langle 1,1|$$

$$+\tilde{\rho}_{\alpha,2}(t)|0,1\rangle\langle 0,0| + \tilde{\rho}_{0,\beta}(t)|1,1\rangle\langle 1,0|$$

$$+\tilde{\rho}_{2,\alpha}(t)|0,0\rangle\langle 0,1| + \tilde{\rho}_{\beta,0}(t)|1,0\rangle\langle 1,1|$$

$$+\tilde{\rho}_{0,0}(t)|1,1\rangle\langle 1,1| + \tilde{\rho}_{0,2}(t)|1,1\rangle\langle 0,0| + \tilde{\rho}_{2,0}(t)|0,0\rangle\langle 1,1|$$

$$+\tilde{\rho}_{\beta,\alpha}(t)|1,0\rangle\langle 0,1| + \tilde{\rho}_{\alpha,\beta}(t)|0,1\rangle\langle 1,0| \tag{4.47}$$

Here a state $|n,m\rangle$ for $n,m \in \{0,1\}$ indicates the number of photons in the two cavities, respectively. Since we start the cavities with one photon each, an input photon in mode α or β will correspond to a cavity state $|n,m\rangle$ with $n = 0$ or $m = 0$ respectively (the photons have leaked out of their cavities). The F-operators in the Hamiltonian and Lindbladian of eq. 4.43 act on the expansion coefficients, $\tilde{\rho}_{i,j}(t)$ and the cavity mode annihilation a_1, a_2 operators act on the basis elements $|n,m\rangle$. Using the expansion, eq. 4.47 in eq. 4.43, we get a set of coupled differential equations for the 16 coefficients. For example, the two

coefficients, $\tilde{\rho}_{\beta,2}(t)$ and $\tilde{\rho}_{0,\alpha}$ have the coupled equations,

$$\dot{\tilde{\rho}}_{\beta,2}(t) = \left(\mathcal{D}_{\sqrt{\gamma_1}|F_0\rangle\langle F_1|} + \mathcal{D}_{\sqrt{\gamma_2}|F_2\rangle\langle F_1|} + \mathcal{D}_{\sqrt{\gamma_3}|F_2\rangle\langle F_3|}\right.$$

$$\left. +\mathcal{D}_{\sqrt{\gamma_4}|F_4\rangle\langle F_3|}\right)\tilde{\rho}_{\beta,2}(t) - \frac{1}{2}|g_2(t)|^2\left[\tilde{\rho}_{\beta,2}\right] + |g_1(t)|^2\tilde{\rho}_{0,\alpha}(t)$$

$$+g_1(t)\sqrt{\gamma_1}\left[|F_0\rangle\langle F_1|, \tilde{\rho}_{\beta,\beta}(t)\right] - g_2(t)\sqrt{\gamma_3}\left[\tilde{\rho}_{\beta,\alpha}, |F_2\rangle\langle F_3|\right]$$

$$-g_2^*(t)\sqrt{\gamma_3}\left[|F_3\rangle\langle F_2|, \tilde{\rho}_{0,2}(t)\right] \tag{4.48}$$

$$\dot{\tilde{\rho}}_{0,\alpha}(t) = \left(\mathcal{D}_{\sqrt{\gamma_1}|F_0\rangle\langle F_1|} + \mathcal{D}_{\sqrt{\gamma_3}|F_2\rangle\langle F_3|}\right.$$

$$\left. -|g_1(t)|^2 - \frac{1}{2}|g_2(t)|^2\right)\tilde{\rho}_{0,\alpha}$$

$$+g_1(t)\sqrt{\gamma_1}\left[|F_0\rangle\langle F_1|, \tilde{\rho}_{0,0}(t)\right] \tag{4.49}$$

The following transformation from the tilde operators gives us back the set of differential equations in eq. 4.46 with the generalized density matrix operators defined previously in eq. 4.24. This comes with the substitutions in eq. 4.45.

$$\rho_{0,0}(t) = \tilde{\rho}_{0,0}(t)e^{\int dt(|g_1(t)|^2+|g_2(t)|^2)}$$

$$\rho_{\alpha,\alpha}(t) = \left[\tilde{\rho}_{\alpha,\alpha}(t) + \tilde{\rho}_{0,0}(t)\right]e^{\int dt|g_1(t)|^2}$$

$$\rho_{\beta,\beta}(t) = \left[\tilde{\rho}_{\beta,\beta}(t) + \tilde{\rho}_{0,0}(t)\right]e^{\int dt|g_2(t)|^2}$$

$$\rho_{2,2} = \left[\tilde{\rho}_{2,2} + \tilde{\rho}_{\alpha,\alpha}(t) + \tilde{\rho}_{\beta,\beta}(t)\right]$$

$$\rho_{0,\alpha}(t) = \tilde{\rho}_{0,\alpha}(t)e^{\int dt(|g_1(t)|^2+\frac{1}{2}|g_2(t)|^2)}$$

$$\rho_{\beta,2}(t) = \left[\tilde{\rho}_{\beta,2}(t) + \tilde{\rho}_{0,\alpha}(t)\right]e^{\int dt\frac{1}{2}|g_2(t)|^2}$$

$$\rho_{0,\beta}(t) = \tilde{\rho}_{0,\beta}(t)e^{\int dt(\frac{1}{2}|g_1(t)|^2+|g_2(t)|^2)}$$

$$\rho_{\alpha,2}(t) = \left[\tilde{\rho}_{\alpha,2}(t) + \tilde{\rho}_{0,\beta}(t)\right]e^{\int dt\frac{1}{2}|g_1(t)|^2}$$

$$\rho_{\alpha,\beta} = \tilde{\rho}_{\alpha,\beta}e^{\int dt\frac{1}{2}(|g_1(t)|^2+|g_2(t)|^2)}$$

$$\rho_{0,2}(t) = \tilde{\rho}_{0,2}(t)e^{\int dt\frac{1}{2}(|g_1(t)|^2+|g_2(t)|^2)} \tag{4.50}$$

The coefficients in eq. 4.47 can actually be given the meaning of a density matrix element with their usual meaning. The Hamiltonian formulation helps us write the density operator with trace of 1 that embodies all the generalized density operators in eq. 4.46 (the diagonal(off-diagonal) ones each have a preserved trace of 1(0) each).

CHAPTER V

CONCLUSIONS

We talk about two kinds of amplifications. The first kind is the one Bohr remarked on, classical measurements of a microscopic quantum observable need to be the outcome of an irreversible amplification from it. The second kind are specific unitary (reversible) evolutions of quantum mechanical operators with explicit gains and noise additions. Quantum measurement theories cannot completely eliminate the need for an interpretative process in the end of the quantum mechanical process of the amplification. We do have answers to a number of puzzles in the measurement process. Quantum mechanical decoherence can be used to explain and interpret quantum measurement process in most parts. As progress continues in quantum measurement theories, it behoves us to push the efforts to write fundamental models and theories for technological platforms like single photon detectors using our best understanding of nature at the time.

This dissertation accomplishes the task of embodying the entire process of single/few photon detection with Hamiltonians as well as outlines the procedure for analysing absorption probabilities. A few well known Hamiltonians are discussed. The mechanism and physics inherent in these Hamiltonians are well understood from cavity Quantum Electro-Dynamics. As such the methodology described can serve as a guideline for designing photon detectors and their amplification characteristics. The models are capable of depicting the entire evolution composed of absorption, amplification and measurement. This is an improvement over the status quo Hamiltonian description of single photon detectors which discusses definite models for absorption stage only. A number

of Hamiltonians are discussed that can implement a wide range of quantum amplification processes and measurement interpretations in the theoretical frameworks known today. The measurement section is described with classicality of large macroscopic signals. But it is compatible with the modern theory of measurement induced decoherence and readily adaptable to quantum Darwinism and emergence of classical objective reality theories.

Hamiltonians readily ensure preservation of bosonic canonical commutation and fermionic canonical anticommutation relationships. Photon absorptions leading the evolution into a macroscopic number of bosonic excitations in a mode or macroscopic number of atoms or spins excited or generated can be modelled with known Hamiltonian models that are explicitly compliant with quantum mechanical evolution requirements. Bonus features like models with dissipative phase transitions can make our models further protected against non-ideal realizations. The macroscopic excitations generation gives us an output quantum mechanical operator amplified with minimal noise contribution added. The other desired attribute of near-perfect absorption is built in the absorber molecule in all cases.

The absorber molecule can be designed with the near-perfect absorption design into a five level atom that can absorb the two photons sequentially. The versatility of our Hamiltonian formulation is verified by the model and suitability of computations. The model can be adapted to implement polarization sensitive single photon detection capability. The POVM elements show rich structure. If the two photons have somewhat close central frequencies, the photons become less distinguishable and the POVM elements involve projectors into entangled photon pairs and connects with the standard two photon absorber physics.

On a more fundamental physics front, we get exciting new prospects of device level modelling of modern quantum measurement theory and interpretations. Theories of decoherence and quantum Darwinism can be incorporated and more profound quantum measurement processes could be conceptualized. Going beyond a single photon detection problem alone, the more general problem of amplifying microscopic quantum mechanical observables into objective reality can be touched upon. Concrete models of generating macroscopic number of excitations or large signal amplitudes in a quantum mechanical evolution can benefit the modern evolution of the ideas of the quantum measurement problem.

APPENDIX A

HEISENBERG PICTURE EVOLUTION OF OPERATORS

Knowing the Hamiltonian essentially indicates knowing the input-output relationship for the amplification evolution, as it comes down to the formal solution of the Heisenberg equation of motion. The density matrix evolves accordingly in the Schrödinger equation [180],

$$\rho(t) = U(t)\rho(0)U^\dagger(t), \ \rho(t) = \rho(0); \qquad \text{Schrödinger picture} \qquad (A.1)$$

$$A(t) = U^\dagger(t)A(0)U(t), \ A(t) = A(0); \qquad \text{Heisenberg picture} \qquad (A.2)$$

$$U(t) = \mathcal{T}exp\left(-i\int_0^t H(t')dt'\right), \qquad (A.3)$$

where $\mathcal{T}$ is the Dyson time-ordering operator. The decomposition of the output operator in terms of the input operators tells us the gain of the amplification as well as noise operators and their contributions. From the point of view of amplification, computation of eq. (A.2) is of paramount importance. Computation of eq. (A.2), even with convergent series expansions, can answer the important question of which operators (signal and noise) do and do not contribute to the output signal operator. Now we look at methodical ways of counting or enlisting the operators that should arise in the decomposition of an output operator.

There are methods of solving eq. (A.1) in the Schrödinger picture with series expansions. For an explicitly time dependent Hamiltonian (time dependent in the Schrödinger as well as Heisenberg picture), the evolution operator in eq. (A.3) can

be expanded in a Dyson series [180],

$$U(t) = \mathcal{T} exp\left(-i \int_0^t H(t')dt'\right)$$

$$= \mathbf{1} - i \int_0^t dt_1 H(t_1) + \frac{(-1)^2}{2!} \int_0^t dt_1 \int_0^{t_1} dt_2 H(t_1)H(t_2) + ...$$

The Hamiltonian does not necessarily commute at different times, i.e.

$[H(t_1), H(t_2)] \neq 0$, and the time ordering operator ensures $t_1 \geq t_2 \geq t_3 \geq t_4....$

Average Hamiltonian Theory (AHT) ([180]) and Magnus expansion ([181])

tries to calculate an average solution for a certain time T [182],

$$U(t = T) = \mathcal{T} exp\left(-i \int_0^t H(t')dt'\right) = e^{-iH_{avg}T} \qquad (A.4)$$

$$\text{with } H_{avg} = \sum_{j=0} H^j$$

$$H^{(0)} = \frac{1}{T} \int_0^T dt_1 H(t_1), \quad H^{(0)} = \frac{1}{T}\frac{i}{2!} \int_0^T dt_1 \int_0^{t_1} dt_2 [H(t_1), H(t_2)]$$

Therefore, the computation of the operator at some point in time T, can be

facilitated through

$$A(t) = U^\dagger(t)A(0)U(t) = e^{iH_{avg}T}A(0)e^{-iH_{avg}T} \qquad (A.5)$$

For a Hamiltonian constant in time (in the Schrödinger picture), we trivially have

the same form for the evolution of an operator in the Heisenberg picture, from eq.

(A.2)

$$A(t) = U^\dagger(t)A(0)U(t) = e^{iHT}A(0)e^{-iHT} \qquad (A.6)$$

Now, H_{avg} needs to be calculated for each T. And later we see an approximate evaluation of an operator evolved till T with H_{avg} to a given order in T. So, numerically the expansion to be mentioned soon is not very useful for Hamiltonians with explicit time dependence. But the expansion into powers of T still gives us the structure of evolution and an approximate magnitude for $A(t)$ at T.

With labels indicating the picture a operator is represented in, we write out

$$U(t) = e^{-iHt/\hbar}$$

$$A_H(t) = U^\dagger(t) A_S U(t) \tag{A.7}$$

$$\frac{d}{dt} A_H(t) = \frac{i}{\hbar}[H, A_H(t)], \tag{A.8}$$

where H is understood to be a Hamiltonian constant in time (in the spirit of eq. (A.5) and eq. (A.6)).

A.1. Open system dynamics as a homomorphism for operators

Structure preserving maps in algebra and group theory are called Homomorphism. Fermionic and Bosonic creation and annihilation operators generate CAR (Canonical Anticommutation Relation) and CCR (Canonical Anticommutation Relation) algebras respectively. Interactions of two level and three level atoms can be represented by the two and three dimensional representation of SU(2) and SU(3) Algebra respectively. The irreversible transduction of photons can be emulated with the quantum mechanical rulebook where the system evolution is tracked disregarding the evolution of the environmental degrees of freedom. Mathematically it amounts to eliminating the

bath operators in favour of system operators. However, all quantum mechanical rules hold in the back of our minds in the description with the all operators and variables kept track of.

$$[AB]_H (t) = e^{iHt/\hbar} A_S e^{-iHt/\hbar} e^{iHt/\hbar} B_S e^{-iHt/\hbar} = A_H(t) B_H(t) \tag{A.9}$$

A simple reflection of the Heisenberg evolution of operators eq. (A.9) demands that the calculated system operator dynamics when appended with the bath operators we have integrated out must preserve its structure. Mathematically, it is equivalent of a homomorphism. And therefore CCR, CAR, SU(3) etc. algebra are expected to be preserved fully in the evolution in the complete space of 'system+bath' operators. With the bath coupling for Bosonic operators, the following general form can be found which with a condition of the white noise correlations ($[b_{in}(t), b_{in}^\dagger(t')] = \delta(t - t')$) for the input field operator, $b_{in}(t)$ always conform to Bosonic commutation relations [183].

$$a(t) = a(t_0) exp[-(i\omega_a + \frac{\gamma}{2})(t - t_0)] - \sqrt{\gamma} \int_{t_0}^{t} dt' b_{in}(t') exp[-(i\omega_a + \frac{\gamma}{2})(t - t')], \quad t > t_0 \tag{A.10}$$

Eq. (A.9) ensures the preservation of commutation relationships in the Heisenberg picture at the same time,

$$[A_H(t), B_H(t)] = A_H(t)B_H(t) - B_H(t)A_H(t)$$

$$= e^{iHt/\hbar}A_S e^{-iHt/\hbar} e^{iHt/\hbar}B_S e^{-iHt/\hbar} - e^{iHt/\hbar}B_S e^{-iHt/\hbar} e^{iHt/\hbar}A_S e^{-iHt/\hbar}$$

$$= e^{iHt/\hbar}A_S B_S e^{-iHt/\hbar} - e^{iHt/\hbar}B_S A_S e^{-iHt/\hbar}$$

$$= e^{iHt/\hbar}\left(A_S B_S e^{-iHt/\hbar} - B_S A_S e^{-iHt/\hbar}\right)$$

$$= e^{iHt/\hbar}\left(A_S B_S - B_S A_S\right)e^{-iHt/\hbar}$$

$$= e^{iHt/\hbar}\left([A_S, B_S]\right)e^{-iHt/\hbar}$$

$$= [A_S, B_S]_H(t)$$

is the Heisenberg evolution of the commutator in the Schrödinger picture operators.

A.2. A Complete Basis

The linear space of operators associated with the Hilbert space of $\{|n_a\rangle \otimes |F_j\rangle\}$ is L(S). A complete basis for L(S) is succinctly written as $\{|q\rangle\langle p|\}$. The time evolution of each element,$|q\rangle\langle p|$ of the basis can facilitate the calculation of correlation function of interest in the system.[184] $|q\rangle\langle p|$ can be written out more explicitly,

$$|q\rangle\langle p| = |n_q, F_q\rangle\langle n_p, F_p|$$

Since any given operator (for example $|F_1\rangle\langle F_1|$ or $\hat{a}$) can be written out in the basis at $t = t_0$, knowing the time evolution of all $|q\rangle\langle p|(t)$ produces the

time evolution of the operator. The evolving operator will have components along different static basis elements, $|k\rangle\langle l|(t_0)$. The time varying component, i.e. coefficient of $|q\rangle\langle p|(t)$ along $|k\rangle\langle l|(t_0)$ is C_{kl}^{qp}.

$$|q\rangle\langle p|(t) = \sum_{k,l} C_{k,l}^{qp}(t)|k\rangle\langle l|(t_0) \tag{A.11}$$

The coefficients, $C_{k,l}^{qp}(t)$ can have interesting physical interpretations in problems like photodetection and amplification [69].

A.2.1. Evolution of basis elements, $(|j\rangle\langle i|)(t)$ in L(S)

Any operator in the linear space of operators acting on Hilbert space, H can be expanded in terms of basis elements $(|j\rangle\langle i|)(t)$. Their dynamics can be a powerful computational tool in the calculation of quantities of interest. We recount some of the equations from ref. [184]. The density matrix, $\rho = Tr_E(\rho_{SE})$, obeys the linear master equation,

$$\frac{d}{dt}\rho_{ij}(t) = \sum_{i',j'} M_{ij,i'j'}\rho_{i',j'}(t) \tag{A.12}$$

Now,

$$Tr_S\{\rho(t)|j\rangle\langle i|(t_0)\} = Tr_S\{\rho(t_0)(|j\rangle\langle i|)(t)\}$$

$$\implies \rho_{ij}(t) = Tr_S\{\rho(t_0)(|j\rangle\langle i|)(t)\} = \langle(|j\rangle\langle i|)(t)\rangle$$

$$\implies \rho_{ij}(t) = \langle(|j\rangle\langle i|)(t)\rangle \tag{A.13}$$

Now, the identity,

$$\langle A(t) \rangle = \sum_{ij} \rho_{ij}(t_0) A_{ji}(t) = \sum_{ij} \rho_{ij}(t) A_{ji}(t_0) = Tr\rho A$$

$$\langle (|j\rangle\langle i|)(t) \rangle = \sum_{ij} \rho_{ij}(t) |j\rangle\langle i|_{ji}(t_0) = \sum_{ij} \rho_{ij}(t_0) |j\rangle\langle i|_{ji}(t)$$

(A.14)

For the case, $|j\rangle\langle i|_{ji}(t_0) = \delta_{r,i}\delta_{c,j}$ ad $\rho_{ij}(t_0) = \delta_{r,i}\delta_{c,j}$,

$$(\rho_{ij}(t))_S = (|j\rangle\langle i|(t))_H$$

Consequently, if the master equation is,

$$\frac{d}{dt}\rho_{ij}(t) = \sum_{ij,i'j'} M_{ij,i'j'} \rho_{i',j'}(t) \tag{A.15}$$

we can use eq. (A.13) to write,

$$\frac{d}{dt}\langle (|j\rangle\langle i|)(t) \rangle = \sum_{ij,i'j'} M_{ij,i'j'} \rho_{i',j'}(t) \tag{A.16}$$

Eq. (A.16) is written only to be corrected with the noise operators so as to satisfy the commutation relations,

$$\frac{d}{dt}\langle (|j\rangle\langle i|)(t) \rangle = \sum_{ij,i'j'} M_{ij,i'j'} \rho_{i',j'}(t) + F_{ij}(t) \tag{A.17}$$

A.3. Expansion of evolving operators in orders of time

Equations (A.7) and (A.8) enable us to write an operator evolving in time at a particular time with evolution operators having constant Hamiltonians. We

158

define the notation,

$$[H, A_S] = A_S^H \qquad [H, A_H(t)] = A_H^H(t)$$

$$[H, [H, A_S]] = A_S^{HH} \qquad [H, [H, A_H(t)]] = A_H^{HH}(t)$$

$$[H, [H, [H, A_S]]] = A_S^{HHH} \qquad [H, [H, [H, A_H(t)]]] = A_H^{HHH}(t)$$

....

The solution of eq. (A.8) is,

$$A_H(t) = \frac{i}{\hbar} \int_0^t [H, A_H(t_1)] dt_1 \tag{A.18}$$

Of course, we can substitute the integral for $A_H(t)$ in the right hand side, as many times as we wish,

$$A_H(t) = \frac{i}{\hbar} \int_0^t [H, A_H(t_1)] dt_1 \tag{A.19}$$

$$A_H(t) = \left(\frac{i}{\hbar}\right)^2 \int_0^t \int_0^{t_1} [H, [H, A_H(t_2)]] dt_2 dt_1 \tag{A.20}$$

$$A_H(t) = \left(\frac{i}{\hbar}\right)^3 \int_0^t \int_0^{t_1} \int_0^{t_2} [H, [H, [H, A_H(t_3)]]] dt_3 dt_2 dt_1 \tag{A.21}$$

In the notation chosen,

$$A_H(t) = \frac{i}{\hbar} \int_0^t A_H^H(t_1) dt_1$$

$$A_H(t) = \left(\frac{i}{\hbar}\right)^2 \int_0^t \int_0^{t_1} A_H^{HH}(t_2) dt_2 dt_1$$

$$A_H(t) = \left(\frac{i}{\hbar}\right)^3 \int_0^t \int_0^{t_1} \int_0^{t_2} A_H^{HHH}(t_3) dt_3 dt_2 dt_1$$

A.3.1. Expansion in unevolving Schrödinger operators

Continuing from eq. (A.7),

$$A_H(t) = e^{iHt/\hbar} A_S e^{-iHt/\hbar}$$

$$= 1 + \left(\frac{it}{\hbar}\right)[H, A_S] + \frac{1}{2!}\left(\frac{it}{\hbar}\right)^2 [H,[H,A_S]] + \frac{1}{3!}\left(\frac{it}{\hbar}\right)^3 [H,[H,[H,A_S]]] + \text{(A.22)}$$

$$= 1 + \left(\frac{it}{\hbar}\right) A_S^H + \frac{1}{2!}\left(\frac{it}{\hbar}\right)^2 A_S^{HH} + \frac{1}{3!}\left(\frac{it}{\hbar}\right)^3 A_S^{HHH} + ...$$

$$= \sum_{n=0}^{\infty} \frac{1}{n!}\left(\frac{it}{\hbar}\right)^n A_S^{H^n} + \mathcal{E}(t^{n+1}) \tag{A.23}$$

Eq. (A.23) can be verified citing identities in literature [185],

$$e^{\tau A_1} B e^{-\tau A_1} = B + [A_1, B]\tau + ... + [A_1, ..., [A_1, B]...]\frac{\tau^{p-1}}{(p-1)!} + O(\tau^p) \tag{A.24}$$

where the error term, explicitly is,

$$O(\tau^p) = \int_0^\tau d\tau_2 e^{(\tau-\tau_2)A_1} [A_1, ..., [A_1, B]...]e^{-(\tau-\tau_2)A_1} \frac{\tau_2^{p-1}}{(p-1)!} \tag{A.25}$$

160

Therefore, the error term in eq. (A.23) would be

$$\mathcal{E}(t^{n+1}) = \left(\frac{i}{\hbar}\right)^{p+1} \int\limits_0^{it/\hbar} dt_2 e^{\frac{i}{\hbar}(t-t_2)H}[H,...,[H,A_S]...]e^{-\frac{i}{\hbar}(t-t_2)H}\frac{t_2^p}{p!} \qquad (A.26)$$

A.4. Binomial Expansion

The terms in the expansion eq. (A.23) resemble a binomial expansion,

$$A_S^{H^n} = (H - A_S)^n = \sum_{r=0}^{n} \binom{n}{r}(-1)^r H^{n-r} A_S^r \qquad (A.27)$$

For example, the term, $A_S^{H^4}$ in the expansion of eq. (A.23),

$$A_S^{H^4} = A_S^{HHHH} = [H,[H,[H,[H,A_S]]]]$$

$$= HHHHA_S - 4HHHA_SH + 6HHA_SHH - 4HA_SHHH + A_SHHHH$$

The calculation of $A_S^{H^n}$ terms completely enumerates all the possible time stationary Schrödinger operators that can show up in the closed system evolution of a an operator.

A.5. Example time independent Hamiltonian: A Cavity mode Driving a 2LS

The cavity mode will be assumed to have a maximum occupation of 1. The driven system is a Two-Level System (TLS) with the two levels, F_0 and F_1(F_1 is

higher in energy).

$$H(t) = H = H_{sys}(t) + H_{int}(t), \text{ an invariant of time}$$

$$H_{sys}(t) = \hbar\omega_a a^\dagger(t)a(t) - \hbar\delta_{0,1}|F_0\rangle\langle F_0|(t) + \hbar\int\limits_{-\infty}^{\infty} d\omega|\omega|b^\dagger(\omega,t)b(\omega,t)$$

$$H_{int}(t) = i\hbar\int\limits_{-\infty}^{\infty} d\omega\kappa_1(\omega)\left(b^\dagger(\omega,t)a(t) - a^\dagger(t)b(\omega,t)\right)$$

$$+i\hbar\int\limits_{-\infty}^{\infty} d\omega\kappa_2(\omega)\left(b^\dagger(\omega,t)|F_0\rangle\langle F_1|(t)e^{-i\omega\tau} - |F_1\rangle\langle F_0|(t)b(\omega,t)e^{i\omega\tau}\right)$$

$H_{sys}(t)$ or $H_{int}(t)$ are not invariants of time; but their sum is.

Integrating the equation of motion for $b(\omega,t)$, the bath mode annihilation operator can be found to be,

$$b(\omega,t) = b_0(\omega)e^{-i\omega(t-t_0)} + \int\limits_{t_0}^{t} dt'\left[\sqrt{\frac{\kappa}{2\pi}}a(t')e^{-i\omega(t-t')} + \sqrt{\frac{\gamma_1}{2\pi}}|F_0\rangle\langle F_1|(t')e^{-i\omega(t-t'+\tau)}\right] \quad (A.28)$$

$H_{int}(t)$ is necessarily time dependent, H is the only operator which can be taken to be conserved in time. Substitution of eq. (A.28) can give the $H_{int}(t)$.

$$H_{int}(t) = i\hbar\sqrt{\kappa\gamma_1}\left(a^\dagger(t-\tau)|F_0\rangle\langle F_1|(t) - |F_1\rangle\langle F_0|(t)a(t-\tau)\right)$$

$$+i\hbar\sqrt{\kappa}\left(b_{in}^\dagger(t)a(t) - a^\dagger(t)b_{in}(t)\right) + i\hbar\sqrt{\gamma_1}\left(b_{in}^\dagger(t-\tau)|F_0\rangle\langle F_1|(t) - |F_1\rangle\langle F_0|(t)b_{in}(t-\tau)\right) \quad (A.29)$$

$H_{sys}(t)$ can be evaluated at $t = t_0$, substituting eq. (A.28) for $t = t_0$,

$$H_{sys}(t_0) = \hbar\omega_a a^\dagger(t_0)a(t_0) - \hbar\delta_{0,1}|F_0\rangle\langle F_0|(t_0) + \hbar\int\limits_{-\infty}^{\infty} d\omega|\omega|b_0^\dagger(\omega)b_0(\omega)$$

162

The quantity, $\hbar \int_{-\infty}^{\infty} d\omega |\omega| b_0^\dagger(\omega) b_0(\omega)$ is a constant and do not contribute to any dynamical coupling between operators evolving in time in the Heisenberg picture.

Taking that last number to be zero, we have our Hamiltonian, (ignoring the delay, τ)

$$H = H(t_0) = H_{sys}(t_0) + H_{int}(t_0)$$

$$= \hbar\omega_a a^\dagger(t_0)a(t_0) - \hbar\delta_{0,1}|F_0\rangle\langle F_0|(t_0) + i\hbar\sqrt{\kappa\gamma_1}\left(a^\dagger(t_0)|F_0\rangle\langle F_1|(t_0) - |F_1\rangle\langle F_0|(t_0)a(t_0)\right)$$

$$+i\hbar\sqrt{\kappa}\left(b_{in}^\dagger(t_0)a(t_0) - a^\dagger(t_0)b_{in}(t_0)\right) + i\hbar\sqrt{\gamma_1}\left(b_{in}^\dagger(t_0)|F_0\rangle\langle F_1|(t_0) - |F_1\rangle\langle F_0|(t_0)b_{in}(t_0)\right) \quad (A.30)$$

A.5.1. Matrix representation of a system Hamiltonian

Making open system dynamics explicitly unitary (conforming to quantum mechanical rules) requires tracting the bath operators and a combinatorial counting problem that may be facilitated by graph theoretical algorithms. Konig digraphs can be a very useful representation for matrices and matrix multiplication [186]. For a closed system evolution problem without bath contributions Konig digraph methods can be formulated most straightforwardly. Our H will be,

$$H = \hbar\omega_a a^\dagger(t_0)a(t_0) - \hbar\delta_{0,1}|F_0\rangle\langle F_0|(t_0) + i\hbar\sqrt{\kappa\gamma_1}\left(a^\dagger(t_0)|F_0\rangle\langle F_1|(t_0) - |F_1\rangle\langle F_0|(t_0)a(t_0)\right)$$

In the rotating frame defined by,

$$U(t) = exp\left\{i\hbar\omega_a a^\dagger a - i\hbar\delta_{0,1}|F_0\rangle\langle F_0|\right\},$$

the Hamiltonian would be even more compact,

$$H = i\hbar\sqrt{\kappa\gamma_1}\left(a^\dagger(t_0)|F_0\rangle\langle F_1|(t_0) - |F_1\rangle\langle F_0|(t_0)a(t_0)\right)$$

In the basis $\{|n_a\rangle \otimes |F_j\rangle\}$,

$$H = i\hbar\sqrt{\kappa\gamma_1} \begin{bmatrix} 0 & 0 & 0 & 0 & 0 & 0 \\ 0 & 0 & 0 & -1 & 0 & 0 \\ 0 & 0 & 0 & 0 & 0 & 0 \\ 0 & 1 & 0 & 0 & 0 & 0 \\ 0 & 0 & 0 & 0 & 0 & 0 \\ 0 & 0 & 0 & 0 & 0 & 0 \end{bmatrix} \tag{A.31}$$

A.5.2. Weighted Konig Digraph

Hamiltonian matrices are always Hermitian, so they would necessarily have directed edges going in both directions between two nodes (weighted by complex conjugate numbers). We choose the following Hamiltonian (chosen to be more stuffy than the one in eq. (A.31)) to demonstrate the method. The elements of the Hamiltonian are taken to be -1 for simplicity.

$$H = \begin{bmatrix} \Delta_1 & 0 & 0 & -t_h & 0 & -t_h \\ 0 & 0 & 0 & 0 & 0 & 0 \\ 0 & 0 & 0 & 0 & 0 & 0 \\ -t_h & 0 & 0 & \Delta_4 & 0 & -t_h \\ 0 & 0 & 0 & 0 & 0 & 0 \\ -t_h & 0 & 0 & -t_h & 0 & \Delta_6 \end{bmatrix} \tag{A.32}$$

Now for the calculation of some $C_{k,l}^{qp}(t)$ (in eq. (A.11)), for example, $C_{6,4}^{61}(t)$, we have to calculate all the different contribution from t-powers from the closed walks from 6 to 4 (k to l). For the coefficient of t^n, we find the weight of all walks
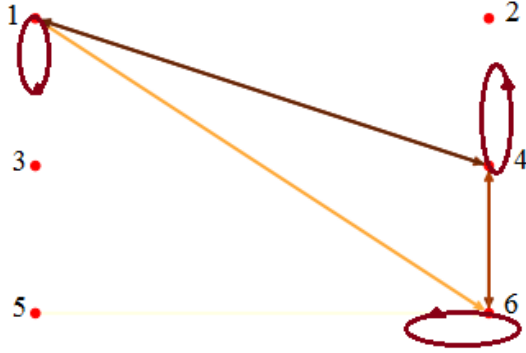
FIGURE A.1. The Digraph (brown edges) for the Hamiltonian in eq. (A.32) along with the edge $|6\rangle\langle1|$ (orange). The edge 1-6 of the Hamiltonian is not shown (or is hidden under the edge $|6\rangle\langle1|$). The edges have arrows on both ends (bidirectional edges or two edges) because of the hermiticity of the matrix.

of length (n+1) from the node k to l (in fig. (A.2)). If $|6\rangle\langle1|$ appears multiple times (if only the Hamiltonian has that edge itself), we have multiple permutations to be summed; each time with a factor of $(-1)^m$; m is the serial (starting from 1, $m \in N$) of the edge $|6\rangle\langle1|$ in the composite (cascaded) graph (fig. (A.2)). The general relationship is,

$$C_{k,l}^{qp}(t) = \delta_{k,l} + \sum_{n=1}^{\infty} \frac{1}{n!} \left(\frac{i}{\hbar}\right)^n t^n (-1)^m W_{kl}^{n+1}$$

$$W_{kl}^{n-1} = \text{Weight of the walks of length (n+1)}$$

from k to l through the edge p $\rightarrow$ q

m = the serial of the edge p $\rightarrow$ q in the walk, $m \in N$

If i=j, and there is a self-loop at vertex i, the walk must include that loop (as an edge) at a serial in the walk.

Fig. (A.2) makes the method more obvious; however the weighted Konig di-graph (fig. (A.1)) of the Hamiltonian is all we need for the calculation of any $C_{k,l}^{pq}(t)$ coefficient.
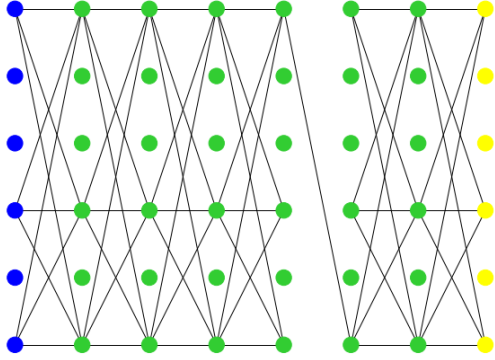
FIGURE A.2. The composite graph (ref. [186]) for $H^4|6\rangle\langle 1|H^2$ (The arrows of the graph-edges not shown). H is from eq. (A.32)

The QuTiP ([187]) function mesolve is used for calculating the expectation value of any operator in L(S) in the open system evolution. However, it operates on exponentiating matrices and runs into memory problems for large Hilbert space sizes. Knowledge of all $|q\rangle\langle p|(t)$ calculated through algorithms of graph theory might make it possible to calculate these expectation values for very very large system dimensions with known error terms.

The coefficients $C_{k,l}^{qp}(t)$ can be calculated recursively. Here is a pseudo code expressing this idea.

Algorithm 1: Recursive function program for A(t)

Input: A(t_0), H, N(max^m order of t)

Output: A(t)

1 Initialize n to 1

2   A(t) = recursive function(n).

3 Recursive function(n):

4 Step 0: Set A^n to 0. m to 1.

5 Step 1: take the product C = HH..A ..HHH of length (n+1) with A at the serial of m.

6 Step 2. Add $(-1)^m C$ to A^n.

7   if m < N:

8   m → m+1.

9   goto Step 1.

10   else:

11       $A(t_0) \to A(t_0) + (it/\hbar)^n A^n$

12 Step 3:

13   if n < N: resursive function(n+1)

14   else: return $A(t_0)$

APPENDIX B

AMPLIFICATION MECHANISMS AND HAMILTONIANS

We have discussed a quantum amplification mechanism implemented with a driven quantum Harmonic oscillator. We now contemplate a host of other cavity-QED Hamiltonians that can implement such amplification mechanisms.

Ref. [122] discusses a class of nonlinear amplifiers that add a single noise mode for the amplification evolution.

$$\hat{a}_{out} = g\hat{f}_{in} + \hat{b}_{in} \tag{B.1}$$

$\hat{f}_{in}$ is the quantum mode carrying the signal and $\hat{b}_{in}$ is the added noise mode. It was facilitated with the interaction Hamiltonian,

$$\hat{H}_I = -i\kappa \left(\hat{f}^\dagger \hat{b} - \hat{f}\hat{b}^\dagger \right) \tag{B.2}$$

The input-output transformaton is achieved with a normal operator $\hat{f}_{in}$ (an operator that commutes with its adjoint). In fact f need not be a modal operator, it can be a qubit operator such as $|0\rangle\langle 1| - |1\rangle\langle 0|$ which is normal but non-Hermitian. Therefore a qubit population operator such as $\hat{\sigma}_z$ can be measured with minimum noise addition.

Ref. [122] summarizes modern techniques in qubit readout techniques with the single interaction Hamiltonian in eq. (B.2). Conditional displacement of an oscillator based on the occupation of a qubit is exploited in some nondemolition measurements of qubits [188, 189, 190]. Fundamentally, the oscillation frequency of a cavity mode is dynamically modulated by the occupation of the qubit. The

Langevin equation of the cavity mode reads [189],

$$\dot{\hat{a}} = -i\frac{1}{2}\tilde{g}_z\hat{\sigma}_z - \frac{1}{2}\kappa\hat{a} - \sqrt{\kappa}\hat{a}_{in} \tag{B.3}$$

The input-output boundary condition reads,

$$\hat{a}_{out} = \hat{a}_{in} + \sqrt{\kappa}\hat{a} \tag{B.4}$$

The mean of the output is,

$$\alpha_{out} = \langle\hat{a}_{out}\rangle = -\frac{i\tilde{g}_z}{\sqrt{\kappa}}\langle\hat{\sigma}_z\rangle\left[1 - e^{-\frac{1}{2}\kappa t}\right] \tag{B.5}$$

The homodyne detection of the output signal corresponds to the measurement operator, $\hat{M}(\tau)$, (τ being the integration time and ϕ_h the homodyne angle).

$$\hat{M}(\tau) = \sqrt{\kappa}\int_0^\tau dt\left[\hat{a}_{out}^\dagger(t)e^{i\phi_h} + \hat{a}_{out}(t)e^{-i\phi_h}\right] \tag{B.6}$$

For long measurement times, the signal to Noise Ratio (SNR) grows as square root of time [189, 190]. The interaction Hamiltonian is a special case of the general relationship in eq. (B.2).

The amplification mechanism formulated in chapters 3 and 4 are different from the one in [122] in the sense that they include the projector into a third Hilbert space,

$$\hat{a}_{out} = g\hat{n}_{in} \otimes |\psi_0\rangle\langle\psi_0| + \hat{b}_{in} \tag{B.7}$$

$|\psi_0\rangle\langle\psi_0| = |F_2\rangle\langle F_2|$ in the single photon model. The shelving state $|F_2\rangle$ drives the amplification process. Since the operator, $|\psi_0\rangle\langle\psi_0|$ commutes with the

measurement Hamiltonian, it counts as a Quantum Non Demolition (QND) observable. In chapter 4, it was established that to project onto photon wavepackets, the temporal shape of the occupation of the absorber levels are necessary. We now consider physical amplification mechanisms where such quantum signals (carried by a projector operator) can be amplified into large quantum signals carried by a large number of spins or atoms. Readout techniques for such large quantum signals into classical signals may enable us to learn the growing occupation levels in the shelving state within the liberties of quantum mechanics.

The projector operator of the shelving state $|\psi_0\rangle\langle\psi_0|$ can be used in other cavity-QED Hamiltonians to achieve the desired change in some parameter value that will drive an amplification. A driven version of the *Jaynes-Cummings model* can lead to a coherent state steady state ([191]). Therefore, we are able to use the model for amplification of a change in a parameter, μ caused by an absorbed photon.

$$\dot{\rho} = \mathcal{L}\rho = -i[\tilde{H}_{dJC}, \rho] + \mathcal{D}_{\sqrt{\kappa_d}d}\rho + \mathcal{D}_{\sqrt{\kappa_{\tau_z}}\tau_z}\rho$$

$$\tilde{H}_{dJC} = \frac{1}{2}(\Delta - \omega_a)(1 + \tau_z) + \lambda(\tau^+ d + \tau^- d^\dagger) + \mu(t)(\tau^+ + \tau^-) \qquad \text{(B.8)}$$

$$\mu(t) = \mu|\psi_0\rangle\langle\psi_0|(t) \qquad \text{(B.9)}$$

For, $\mu > \lambda$, as the shelving state grows its occupation, we get to the coherent state (with amplitude μ/λ, ([191])) steady state for the cavity mode. $\tilde{H}_{dJC}$ is written in a rotating frame, ω_a is the angular frequency of the ac field driving the qubit τ_z, τ are the Pauli spin operators representing a two level atom. The steady state of the cavity mode, $\hat{d}$ would be our pointer state. The Heisenberg picture evolution of

$|\psi_0\rangle\langle\psi_0|(t)$ is unchanged if terms are added to the Hamiltonian that it commutes with. And the evolution of other operators can be calculated from the Hamiltonian $\tilde{H}_{dJC}$ in eq. B.8.

The detuning of different photon signal can lead to different steady state occupation of the absorber atom. In fact, the switching between distinct steady states brought about by varying the detuning across certain critical value was utilized to fashion a quantum transducer in a Kerr resonator.[192] There are a host of *non-linear Kerr models* where the steady-states are Schrödinger cat states of coherent states [193]. These systems involve the physics of driven-dissipative phase transitions [194]. The heightened susceptibilities of the degrees of freedom of a system close to a critical point has long been investigated for applications in metrology, estimation and sensing[195, 196]. First order phase transitions have also attracted much attention in schemes for amplifying weak signals.[71].

B.1. From master equation to rate equation

Dicke Hamiltonian describes the dynamics of a two level atom/ qubit coupled to a single mode of electromagnetic cavity mode.

$$H_{Dicke} = \omega_0 S_z + \omega a^\dagger a + \lambda(a + a^\dagger)(\sigma^+ + \sigma^-)$$

The Jaynes Cummings Hamiltonian discards terms far from resonance,

$$H_{JC} = \omega_0 S_z + \omega a^\dagger a + \lambda(a\sigma^+ + a^\dagger \sigma^-)$$

The emission from the qubit and the populations are found to be discrete in time (in a single shot measurement) and can be calculated with the quantum

trajectory method. However, the solutions and measurement signals can both be continuous (solutions from the master equation approach) for an ensemble of qubits driven and decaying identically. Such a system is described by the Tavis-Cummings Hamiltonian, where N qubits are coupled identically to a single electromagnetic cavity mode.

$$H_{TC} = \omega_0 J_z + \omega a^\dagger a + \frac{\lambda}{\sqrt{N}}(a + a^\dagger)(J^+ + J^-)$$

The collective spin-operators abide by the SU(2) algebra just like the individual spin operators [125, 182, 197, 198].

$$J_i = \sum_{j=1}^{N} \sigma_i^j, \ i = x, y, z;$$

$$J_\pm = \sum_{j=1}^{N} \sigma_\pm^j = \sum_{j=1}^{N} \left(\sigma_x^j \pm i\sigma_y^j\right) = J_x \pm iJ_y$$

$$[J_x, J_y] = iJ_z, \ [J_y, J_z] = iJ_x, \ [J_z, J_x] = iJ_y$$

$$[J_z, J_\pm] = \pm J_\pm, \ [J_+, J_-] = 2J_z \tag{B.10}$$

The simultaneous eigenstates of $\mathbf{J}^2$ and J_z are called Dicke states. With $\hbar = 1$,

$$\mathbf{J}^2|j, m\rangle = j(j+1)|j, m\rangle$$

$$J_z|j, m\rangle = m|j, m\rangle$$

$$J_\pm|j, m\rangle = \sqrt{(j \mp m)(j \pm m + 1)}|j, m\rangle$$

where $j \leq N/2$, and $|m| \leq j$, j,m multiples of half-integers for spin-1/2 particles. $j_{min} = 0$ for even M (number of TLS) and 1/2 for odd N.

The Dicke states are permutationally symmetric quantum superpositions of spin tensor product states with the same number of excited and unexcited spins.

$$|j, m = k - \frac{N}{2}\rangle = \frac{1}{\sqrt{\binom{N}{k}}} \sum_p |j_1, 1\rangle...|j_k, 1\rangle|j_{k+1}, 0\rangle...|j_N, 0\rangle \qquad \text{(B.11)}$$

$$= \frac{1}{\sqrt{\binom{N}{k}}} \mathcal{S}\left[|e\rangle^{\otimes k} \otimes |g\rangle^{(N-k)}\right] \qquad \text{(B.12)}$$

The Symmetrization operator $\mathcal{S}$ enlists all permutations with the same number of excited ($|e\rangle$) and unexcited ($|g\rangle$) spins in the sum. The Dicke states with j=N/2 are called the symmetric Dicke states.

Quantum information can transfer from a system to the monitoring environment. While single-shot measurements yield a discrete in time quantum jumps, an ensemble of atoms under the same drive and coupling can accumulate temporal shapes of "click"s that are sufficiently continuous or smooth. The populations of the master equation's density operator becomes state populations in a rate equation. If the environment does not distinguish between individual spins, the dynamics is split into individual symmetric subspaces evolving separately. The populations may be labeled by the z-component of the Spin operators m, and we get a rate equation model for the state populations, $p_m = \rho_{m,m}$.

$$\frac{d}{dt}p_m = -\Gamma_{m \to m \pm 1}p_m + \Gamma_{m-1 \to m}p_{m-1} + \Gamma_{m+1 \to m}p_{m+1}$$

if the population transfer with state of m is limited to states with $m \pm 1$. The symmetries (such as collective spin operator interactions only) in the meter-environment Hamiltonian also facilitates Decoherence Free Subspaces (DFS) that can protect against environmental errors [182].

B.1.1. The observable $|\psi_0\rangle\langle\psi_0|$

The "generalized Dicke model" of ref. [199] shows utility in engineering arbitrary Dicke states in the steady state.

$$H_{gen.\ Dicke} = \omega_0 J_z + \omega a^\dagger a + \frac{\lambda}{\sqrt{N}}(a + a^\dagger)(J^+ + J^-) + \frac{U}{N}J_z a^\dagger a \qquad \text{(B.13)}$$

We propose a scheme for amplifying a monotonically increasing amplitude of a occupation operator through the transformation in eq. (B.7).

$$H_{gen.\ Dicke\ pd} = \omega_0 J_z + \omega a^\dagger a + \frac{\lambda}{\sqrt{N}}(a + a^\dagger)(J^+ + J^-) + |\psi_0\rangle\langle\psi_0|\frac{U}{N}J_z a^\dagger a \qquad \text{(B.14)}$$

Since $|\psi_0\rangle\langle\psi_0|$ commutes with $H_{gen.Dickepd}$, it's equation of motion is not changed with the addition of the "meter" spin ensemble. Therefore the solution for $|\psi_0\rangle\langle\psi_0|(t)$ we obtained before still holds. For any of the collective spin operators, $J_* \in \{J_x, J_y, J_z, J^+, J^-\}$, we get the Heisenberg equation of motion,

$$\frac{d}{dt}J_* = i\left[H_{gen.\ Dicke\ pd}, J_*\right] \qquad \text{(B.15)}$$

The derived equations of motion would be exactly the same ones as the ones derived from the following Hamiltonian,

$$H_{gen.\ Dicke\ spin} = \omega_0 J_z + \omega a^\dagger a + \frac{\lambda}{\sqrt{N}}(a + a^\dagger)(J^+ + J^-) + \frac{U(t)}{N}J_z a^\dagger a \qquad \text{(B.16)}$$

where, $U(t) = U|\psi_0\rangle\langle\psi_0|(t)$.

$$\dot{\rho} = -\frac{i}{\hbar}[H, \rho] + \frac{\gamma_\downarrow}{2}\mathcal{L}_{J_-}[\rho] + \frac{\gamma_\Phi}{2}\mathcal{L}_{J_z}[\rho] + \frac{\gamma_\uparrow}{2}\mathcal{L}_{J_+}[\rho] \tag{B.17}$$

As long as the master equation has system Hamiltonian and collapse operators only in terms of collective operators J_x, J_y, J_z, J_+, J_- and the system was initialized in a symmetric Dicke state the evolution is confined to the (N+1) symmetric Dicke states. For a closed system evolution (without any bath coupling), we can solve the Schrödinger equation itself instead of eq. (B.17),

$$i\frac{d}{dt}|\psi\rangle(t) = H_{gen.\ Dicke\ spin}(t)|\psi\rangle(t) \tag{B.18}$$

since it is computationally much less demanding. However, decoherence must be introduced for the purpose of measurement as discussed in chapter 1. The closed system results can serve as a guiding measure and are easier to compute.

B.1.2. Measurement Models

A macroscopic number of spins/atoms/qubits may cause a discernible classical signal. But to be more precise about the measurement model, there must be a transfer of information from the "meter" (quantum system) to the environment. Our meter here is a large number of spins. The model would require introduction of decoherence to be a viable model for measurement. If only collective emission (or other collective operators) are considered, the Hilbert space size can be restricted to (N+1). It still is a sizeable and time-costing job computationally.

B.1.2.1. Model 1

As discussed in ref. [182], in the semiclassical approach to Nuclear Magnetic Resonance (NMR) physics, the spin magnetization model is quantum mechanical and the NMR detection coil is treated semi-classically. So with the variation of the spin magnetic field calculated from the quantum mechanical Dicke model, we can calculate the emf induced in the coil,

$$emf = -\frac{d}{dt}\int \hat{B}_1.\vec{M}(t)d\Omega \tag{B.19}$$

B.1.2.2. Model 2

The weak measurement model introduced in ref. [182] can serve as a method to extract the classical readout $\langle J_z \rangle(t)$. While strong measurement model demands the $\langle J_z \rangle(t)$ value to be repeated in measurements done in quick succession, it does not necessarily happen in the weak measurement model. In fact, in the weak measurement model, the measurement device is less precise and the spin ensemble collapses to a few manifolds of m centred around m_0. The conditional probability distribution $p(\mathbf{m}|m_0)$ is a distribution with mean m and width w. The POVM elements, $E_m = \mathscr{M}^\dagger \mathscr{M}$ is written as,

$$E_m = \sum_{l=-N/2}^{l=N/2} D(m,l)\Pi_l \tag{B.20}$$

In one model,

$$D(m,l) = \left(1/\sum_k e^{-\frac{(k-l)^2}{2w^2}}\right) e^{-\frac{(m-l)^2}{2w^2}} \tag{B.21}$$

If w is taken to be vanishingly small, $D(m, l)$ becomes a delta function, $\delta(m - l)$. More details of the weak measurement model can be found in ref. [182].

B.1.2.3. Machine Learning/Deep Learning Algorithms

Given that measurement models can be found that enables us to learn the temporal shape of $\langle J_z \rangle(t)$, we still have to determine the theoretical shape of U(t) or $\psi_0 \rangle \langle \psi_0 |(t)$ that produced it. Modern Machine learning and Deep Learning algorithms are one of doing that. A large number of theoretical $\langle J_z \rangle(t)$ and the corresponding U(t) can be derived from the theory and used to train. Experimentally observed $\langle J_z \rangle(t)$ can lead us to the corresponding U(t).

B.1.3. Fermionic Quantum Amplification

Inverse of the **Jordan-Wigner transformation** and the transformation itself are clever ways of adorning a spin with fermionic statistics and vice-versa.

$$\sigma_j^+ = e^{-i\pi \sum_{k=1}^{j-1} a_k^\dagger a_k} a_j^\dagger, \quad \sigma_j^+ = e^{-i\pi \sum_{k=1}^{j-1} a_k^\dagger a_k} a_j^\dagger, \quad \sigma_j^z = 2a_j^\dagger a_j - 1 \tag{B.22}$$

Instead of measuring $\langle J_z \rangle(t)$, the problem can be mapped mapped to a problem of counting fermions i.e. the number of fermions changing in time would indicate the source U(t)'s temporal profile.

B.1.4. Single mode amplification

Ref. [1] paper concluded that amplifying in a single mode will outperform multi-mode amplification. So, a collective mode of a large number of fermions or

spins would have superior signal to noise characteristic performance over multi-mode amplifiers.

B.2. New class of Phase Preserving Linear Amplification

Very recently, from ref. [121], we have learnt of new phase preserving linear amplifiers (which are not simulable by linear parametric amplifiers). Hamiltonians can be found for achieving these new kinds of phase preserving linear amplifiers.

$$\frac{d}{dt}\hat{a} = (\kappa_\uparrow - \kappa_\downarrow)\,\hat{a}^\dagger\hat{a}^\dagger\hat{a}\hat{a} + 2\kappa_\uparrow\hat{a}$$

We find the Hamiltonian,

$$H_{nl} = \frac{i}{3}(\kappa_\uparrow - \kappa_\downarrow)\,\hat{a}^\dagger\hat{a}^\dagger\hat{a}^\dagger\hat{a}\hat{a} + 2i\kappa_\uparrow\hat{a}^\dagger\hat{a}$$

B.3. Quantum Darwinism

Quantum states are understood to be fragile against measurement (they collapse to eigenstates) or even the smallest leak of information that necessarily 'reprepare's it in states consistent with the leaked information [200]. The measurement and amplification models discussed in this dissertation use it to advantage. The eigenstates of the bosonic annihilation operator (the coherent states) in the case of collecting the excitations in the mode d (leaked from mode c), or the eigenstate of the z-component of the collective spin operator are singled out, among other states while the system leaks out information about itself. Phase relations between eigenstates or these "pointer" states are destroyed. Decoherence

solves the puzzle of non-observationality of quantum superposition in measurement theory [200].

The second part of the measurement problem, the emergence of objective reality, is explainable in the setting of 'Quantum Darwinism' as well. In the coupled evolution of the system, $\mathcal{S}$ and environment, $\mathcal{E}$; information about $\mathcal{S}$ is accumulated in $\mathcal{E}$. Although in the numerical result presented, $\mathcal{E}$ is 'traced out' and is inaccessible, our observers (plural) are eavesdropping on it, None of whom need to access the entire $\mathcal{E}$. Only fragments of $\mathcal{E}$ suffice to reveal the eigenstates they need to observe. This is how classical objective reality may emerge. The eigenstates mentioned are capable of producing multiple informational offspring or inserting multiple record into $\mathcal{E}$ at a robust rate. The proliferation of information throughout $\mathcal{E}$, enables our observers (plural) to collect it from shards and pieces of $\mathcal{E}$ and agree about the observations.

The models in this dissertation chooses system states robust against environmental decoherence as both the 'meter' states for the absorber molecule and 'einselected' (environment induced superselected) pointer states amenable to classical readouts. Coherent states of bound cavity modes and Dicke states are shown to be suitable choices for that purpose.

B.4. Code Repository

Some code examples of amplification and measurement ideas can be found in [201].

REFERENCES CITED

[1] Tzula B Propp and S J van Enk. On nonlinear amplification: Improved quantum limits for photon counting. *Opt. Express*, 27(16):23454–23463, 2019.

[2] Maximilian A Schlosshauer. *Decoherence: and the quantum-to-classical transition.* Springer Science & Business Media, 2007.

[3] Alastair IM Rae. *Quantum physics: illusion or reality?* Cambridge University Press, 2004.

[4] Wojciech Hubert Zurek. Quantum theory of the classical: quantum jumps, bornâĂŹs rule and objective classical reality via quantum darwinism. *Philosophical Transactions of the Royal Society A: Mathematical, Physical and Engineering Sciences*, 376(2123):20180107, 2018.

[5] Selig Hecht, Simon Shlaer, and Maurice Henri Pirenne. Energy, quanta, and vision. *Journal of General Physiology*, 25(6):819–840, 1942.

[6] Foster Rieke and Denis A Baylor. Single-photon detection by rod cells of the retina. *Reviews of Modern Physics*, 70(3):1027, 1998.

[7] Jonathan N Tinsley, Maxim I Molodtsov, Robert Prevedel, David Wartmann, Jofre Espigulé-Pons, Mattias Lauwers, and Alipasha Vaziri. Direct detection of a single photon by humans. *Nature communications*, 7(1):1–9, 2016.

[8] Edward N Pugh Jr. The discovery of the ability of rod photoreceptors to signal single photons. *Journal of General Physiology*, 150(3):383–388, 2018.

[9] Daisuke Takeshita, Lina Smeds, and Petri Ala-Laurila. Processing of single-photon responses in the mammalian on and off retinal pathways at the sensitivity limit of vision. *Philosophical Transactions of the Royal Society B: Biological Sciences*, 372(1717):20160073, 2017.

[10] Jürgen Reingruber, Johan Pahlberg, Michael L Woodruff, Alapakkam P Sampath, Gordon L Fain, and David Holcman. Detection of single photons by toad and mouse rods. *Proceedings of the National Academy of Sciences*, 110(48):19378–19383, 2013.

[11] Greg D Field and Fred Rieke. Mechanisms regulating variability of the single photon responses of mammalian rod photoreceptors. *Neuron*, 35(4):733–747, 2002.

[12] Rebecca M Holmes, Michelle M Victora, Ranxiao Frances Wang, and Paul G Kwiat. Testing the limits of human vision with quantum states of light: past, present, and future experiments. In *Advanced Photon Counting Techniques XII*, volume 10659, page 1065903. International Society for Optics and Photonics, 2018.

[13] Michelle Victora, Rebecca M Holmes, R Frances Wang, and Paul G Kwiat. Measuring temporal integration in human vision with single photons. In *Frontiers in Optics*, pages FW3A–4. Optical Society of America, 2016.

[14] Rebecca Holmes. Seeing single photons. *Physics World*, 29(12):28, 2016.

[15] Rebecca M Holmes, Bradley G Christensen, Whitney Street, Cory Alford, R Frances Wang, and Paul G Kwiat. Determining the lower limit of human vision using a single-photon source. In *Quantum Information and Measurement*, pages QTu2A–2. Optical Society of America, 2014.

[16] Edward N Pugh Jr and TD Lamb. Amplification and kinetics of the activation steps in phototransduction. *Biochimica et Biophysica Acta (BBA)-Bioenergetics*, 1141(2-3):111–149, 1993.

[17] L Stryer, JL Tymoczko, and JM Berg. Biochemistry 5th ed freeman. *WH and Company*, 41, 2002.

[18] Grazyna Palczewska, Frans Vinberg, Patrycjusz Stremplewski, Martin P Bircher, David Salom, Katarzyna Komar, Jianye Zhang, Michele Cascella, Maciej Wojtkowski, Vladimir J Kefalov, et al. Human infrared vision is triggered by two-photon chromophore isomerization. *Proceedings of the National Academy of Sciences*, 111(50):E5445–E5454, 2014.

[19] Fundamental limits of photon detection (detect). URL `https://www.darpa.mil/program/fundamental-limits-of-photon-detection`.

[20] Tzula B Propp. *Fundamental Limits to Single-Photon Detection*. PhD thesis, University of Oregon, 2020.

[21] Hans G. Dehmelt. Monoion oscillator as potential ultimate laser frequency standard. *IEEE transactions on instrumentation and measurement*, (2): 83–87, 1982.

[22] D. J. Wineland, J. C. Bergquist, Wayne M. Itano, and R. E. Drullinger. Double-resonance and optical-pumping experiments on electromagnetically confined, laser-cooled ions. *Opt. Lett.*, 5(6):245–247, 1980.

[23] JC Bergquist, Randall G Hulet, Wayne M Itano, and DJ Wineland. Observation of quantum jumps in a single atom. *Phys. Rev. Lett.*, 57(14): 1699, 1986.

[24] M. D. Eisaman, J. Fan, A. Migdall, and S. V. Polyakov. Invited review article: Single-photon sources and detectors. *Review of Scientific Instruments*, 82(7): 071101, 2011.

[25] Robert H. Hadfield. Single-photon detectors for optical quantum information applications. *Nature Photonics*, 3(12):696–705, 2009. ISSN 1749-4885, 1749-4893.

[26] Christopher J Chunnilall, Ivo Pietro Degiovanni, Stefan Kück, Ingmar Müller, and Alastair G Sinclair. Metrology of single-photon sources and detectors: a review. *Optical Engineering*, 53(8):081910, 2014.

[27] GS Buller and RJ Collins. Single-photon generation and detection. *Measurement Science and Technology*, 21(1):012002, 2009.

[28] Alan Migdall, Sergey V Polyakov, Jingyun Fan, and Joshua C Bienfang. *Single-photon generation and detection: physics and applications*. Academic Press, 2013.

[29] Kristine M. Rosfjord, Joel K. W. Yang, Eric A. Dauler, Andrew J. Kerman, Vikas Anant, Boris M. Voronov, Gregory N. Goltsman, and Karl K. Berggren. Nanowire single-photon detector with an integrated optical cavity and anti-reflection coating. *Opt. Express*, 14(2):527, 2006.

[30] Kristen A. Sunter and Karl K. Berggren. Optical modeling of superconducting nanowire single photon detectors using the transfer matrix method. *Appl. Opt*, 57(17):4872, 2018. ISSN 1559-128X, 2155-3165.

[31] F Marsili, Varun B Verma, Jeffrey A Stern, S Harrington, Adriana E Lita, Thomas Gerrits, Igor Vayshenker, Burm Baek, Matthew D Shaw, and Richard P Mirin. Detecting single infrared photons with 93 percent system efficiency. *Nat. Photonics*, 7(3):210, 2013.

[32] Emma E. Wollman, Varun B. Verma, Andrew D. Beyer, Ryan M. Briggs, B. Korzh, Jason P. Allmaras, F. Marsili, Adriana E. Lita, R. P. Mirin, and S. W. Nam. Uv superconducting nanowire single-photon detectors with high efficiency, low noise, and 4 k operating temperature. *Optics Express*, 25(22): 26792–26801, 2017.

[33] G. N. Gol'tsman, O. Okunev, G. Chulkova, A. Lipatov, A. Semenov, K. Smirnov, B. Voronov, A. Dzardanov, C. Williams, and Roman Sobolewski. Picosecond superconducting single-photon optical detector. *Applied Physics Letters*, 79(6):705–707, 2001.

[34] Boris Korzh, Qing-Yuan Zhao, Jason P. Allmaras, Simone Frasca, Travis M. Autry, Eric A. Bersin, Andrew D. Beyer, Ryan M. Briggs, Bruce Bumble, Marco Colangelo, Garrison M. Crouch, Andrew E. Dane, Thomas Gerrits, Adriana E. Lita, Francesco Marsili, Galan Moody, Cristián Peña, Edward Ramirez, Jake D. Rezac, Neil Sinclair, Martin J. Stevens, Angel E. Velasco, Varun B. Verma, Emma E. Wollman, Si Xie, Di Zhu, Paul D. Hale, Maria Spiropulu, Kevin L. Silverman, Richard P. Mirin, Sae Woo Nam, Alexander G. Kozorezov, Matthew D. Shaw, and Karl K. Berggren. Demonstration of sub-3 ps temporal resolution with a superconducting nanowire single-photon detector. *Nature Photonics*, 14(4):250–255, 2020.

[35] Elisha S Matekole, Hwang Lee, and Jonathan P Dowling. Limits to atom-vapor-based room-temperature photon-number-resolving detection. *Phys. Rev. A*, 98(3):033829, 2018.

[36] François Léonard, Michael E Foster, and Catalin D Spataru. Prospects for bioinspired single-photon detection using nanotube-chromophore hybrids. *Scientific reports*, 9(1):1–13, 2019.

[37] James S. Allen. The detection of single positive ions, electrons and photons by a secondary electron multiplier. *Phys. Rev.*, 55:966–971, 1939.

[38] Bayarto K Lubsandorzhiev. On the history of photomultiplier tube invention. *Nuclear Instruments and Methods in Physics Research Section A: Accelerators, Spectrometers, Detectors and Associated Equipment*, 567(1): 236–238, 2006.

[39] Jun-ichi nishizawa: Engineer, sophia university special professor (interview), 2011.

[40] GA Morton. Photon counting. *Applied Optics*, 7(1):1–10, 1968.

[41] RE Simon, AH Sommer, JJ Tietjen, and BF Williams. New high-gain dynode for photomultipliers. *Applied Physics Letters*, 13(10):355–356, 1968.

[42] A Peacock, P Verhoeve, N Rando, A Van Dordrecht, BG Taylor, C Erd, MAC Perryman, R Venn, J Howlett, DJ Goldie, et al. Single optical photon detection with a superconducting tunnel junction. *Nature*, 381(6578): 135–137, 1996.

[43] A Peacock, P Verhoeve, N Rando, A Van Dordrecht, BG Taylor, C Erd, MAC Perryman, R Venn, J Howlett, DJ Goldie, et al. On the detection of single optical photons with superconducting tunnel junction. *Journal of applied physics*, 81(11):7641–7646, 1997.

[44] B Cabrera, RM Clarke, P Colling, AJ Miller, S Nam, and RW Romani. Detection of single infrared, optical, and ultraviolet photons using superconducting transition edge sensors. *Applied Physics Letters*, 73(6): 735–737, 1998.

[45] Adriana E Lita, Brice Calkins, LA Pellouchoud, Aaron Joseph Miller, and S Nam. Superconducting transition-edge sensors optimized for high-efficiency photon-number resolving detectors. In *Advanced Photon Counting Techniques IV*, volume 7681, page 76810D. International Society for Optics and Photonics, 2010.

[46] A. W. Lightstone, R. J. McIntyre, and P. P. Webb. Iia-1 avalanche photodiodes for single photon detection. *IEEE Transactions on Electron Devices*, 28(10): 1210–1210, 1981. ISSN 1557-9646.

[47] Francesco Ceccarelli, Giulia Acconcia, Angelo Gulinatti, Massimo Ghioni, Ivan Rech, and Roberto Osellame. Recent advances and future perspectives of single-photon avalanche diodes for quantum photonics applications. *Advanced Quantum Technologies*, 4(2):2000102, 2021.

[48] Deepak Sethu Rao, Thomas Szkopek, Hans Daniel Robinson, Eli Yablonovitch, and Hong-Wen Jiang. Single photoelectron trapping, storage, and detection in a one-electron quantum dot. *Journal of Applied Physics*, 98(11):114507, 2005.

[49] Mary A Rowe, EJ Gansen, Marion Greene, RH Hadfield, TE Harvey, MY Su, Sae Woo Nam, RP Mirin, and D Rosenberg. Single-photon detection using a quantum dot optically gated field-effect transistor with high internal quantum efficiency. *Applied physics letters*, 89(25):253505, 2006.

[50] BE Kardynał, SS Hees, AJ Shields, C Nicoll, I Farrer, and DA Ritchie. Photon number resolving detector based on a quantum dot field effect transistor. *Applied physics letters*, 90(18):181114, 2007.

[51] C Kurtsiefer et al. Quantum optics devices. *Lecture Notes, Les Houches Singapore, Centre for Quantum Technologies*, 2009.

[52] EJ Gansen, Mary A Rowe, MB Greene, Danna Rosenberg, Todd E Harvey, MY Su, RH Hadfield, Sae Woo Nam, and Richard P Mirin. Photon-number-discriminating detection using a quantum-dot, optically gated, field-effect transistor. *Nature Photonics*, 1(10):585–588, 2007.

[53] Pieter Kok, William J Munro, Kae Nemoto, Timothy C Ralph, Jonathan P Dowling, and Gerard J Milburn. Linear optical quantum computing with photonic qubits. *Reviews of modern physics*, 79(1):135, 2007.

184

[54] Prem Kumar, Paul Kwiat, Alan Migdall, Sae Woo Nam, Jelena Vuckovic, and Franco NC Wong. Photonic technologies for quantum information processing. *Quantum Information Processing*, 3(1):215–231, 2004.

[55] Adriana E. Lita, Aaron J. Miller, and Sae Woo Nam. Counting near-infrared single-photons with 95% efficiency. *Optics Express*, 16(5):3032, 2008.

[56] Christine Silberhorn. Detecting quantum light. *Contemporary Physics*, 48(3):143–156, 2007.

[57] Leaf A Jiang, Eric A Dauler, and Joshua T Chang. Photon-number-resolving detector with 10 bits of resolution. *Physical Review A*, 75(6):062325, 2007.

[58] Aleksander Divochiy, Francesco Marsili, David Bitauld, Alessandro Gaggero, Roberto Leoni, Francesco Mattioli, Alexander Korneev, Vitaliy Seleznev, Nataliya Kaurova, Olga Minaeva, et al. Superconducting nanowire photon-number-resolving detector at telecommunication wavelengths. *Nature Photonics*, 2(5):302–306, 2008.

[59] Daryl Achilles, Christine Silberhorn, Cezary Śliwa, Konrad Banaszek, and Ian A Walmsley. Fiber-assisted detection with photon number resolution. *Optics letters*, 28(23):2387–2389, 2003.

[60] Steve M Young, Mohan Sarovar, and François Léonard. Design of high-performance photon-number-resolving photodetectors based on coherently interacting nanoscale elements. *ACS Photonics*, 7(3):821–830, 2020.

[61] Nam Mai Phan, Mei Fun Cheng, Dmitri A. Bessarab, and Leonid A. Krivitsky. Interaction of fixed number of photons with retinal rod cells. *Phys. Rev. Lett.*, 112:213601, 2014.

[62] S J van Enk. Photodetector figures of merit in terms of povms. *Journal of Physics Communications*, 1(4):045001, 2017.

[63] S J van Enk. Time-dependent spectrum of a single photon and its positive-operator-valued measure. *Phys. Rev. A*, 96(3):033834, 2017.

[64] Steve M Young, Mohan Sarovar, and François Léonard. Fundamental limits to single-photon detection determined by quantum coherence and backaction. *Phys. Rev. A*, 97(3):033836, 2018.

[65] Steve M Young, Mohan Sarovar, and François Léonard. General modeling framework for quantum photodetectors. *Phys. Rev. A*, 98(6):063835, 2018.

[66] Tzula B. Propp and S. J. van Enk. Quantum networks for single photon detection. *Phys. Rev. A*, 100:033836, Sep 2019. doi: 10.1103/PhysRevA.100.033836. URL `https://link.aps.org/doi/10.1103/PhysRevA.100.033836`.

[67] NJ Harmon and ME Flatte. Theory of single photon detection by a photoreceptive molecule and a quantum coherent spin center. *arXiv preprint arXiv:1906.01800*, 2019.

[68] Tzula B Propp and Steven J van Enk. How to project onto an arbitrary single-photon wave packet. *Physical Review A*, 102(5):053707, 2020.

[69] Saumya Biswas and SJ van Enk. Heisenberg picture of photodetection. *Physical Review A*, 102(3):033705, 2020.

[70] Saumya Biswas and SJ van Enk. Detecting two photons with one molecule. *arXiv preprint arXiv:2108.00498*, 2021.

[71] Li-Ping Yang and Zubin Jacob. Quantum critical detector: amplifying weak signals using discontinuous quantum phase transitions. *Opt. Express*, 27(8): 10482–10494, 2019.

[72] Li-Ping Yang and Zubin Jacob. Engineering first-order quantum phase transitions for weak signal detection. *J. Appl. Phys.*, 126(17):174502, 2019.

[73] Li-Ping Yang, Chinmay Khandekar, Tongcang Li, and Zubin Jacob. Single photon pulse induced transient entanglement force. *New Journal of Physics*, 22(2):023037, 2020.

[74] Juan Pablo Llinas, Michelle A Hekmaty, A Alec Talin, and FrancÌğois LeÌĄonard. Origami terahertz detectors realized by inkjet printing of carbon nanotube inks. *ACS Applied Nano Materials*, 3(3):2920–2927, 2020.

[75] Kevin Bergemann and Francois Leonard. Giga-gain at room temperature in functionalized carbon nanotube phototransistors based on a nonequilibrium mechanism. *ACS nano*, 14(8):10421–10427, 2020.

[76] Catalin D Spataru and François Léonard. Quantum dynamics of single-photon detection using functionalized quantum transport electronic channels. *Physical Review Research*, 1(1):013018, 2019.

[77] Catalin D Spataru and François Léonard. Nanoscale functionalized superconducting transport channels as photon detectors. *Physical Review B*, 103(13):134512, 2021.

186

[78] Yang Zhang, Yang Wu, Xiaoxin Wang, Lei Ying, Rahul Kumar, Zongfu Yu, Eric R. Fossum, Jifeng Liu, Gregory Salamo, and Shui-Qing Yu. Detecting single photons using capacitive coupling of single quantum dots. *ACS Photonics*, 5(5):2008–2021, 2018.

[79] Saman Jahani, Li-Ping Yang, AdriÃąn Buganza Tepole, Joseph C. Bardin, Hong X. Tang, and Zubin Jacob. Probabilistic vortex crossing criterion for superconducting nanowire single-photon detectors. *Journal of Applied Physics*, 127(14):143101, 2020.

[80] Roy J Glauber. The quantum theory of optical coherence. *Phys. Rev.*, 130(6): 2529, 1963.

[81] PL Kelley and WH Kleiner. Theory of electromagnetic field measurement and photoelectron counting. *Physical Review*, 136(2A):A316, 1964.

[82] Marlan O. Scully and Willis E. Lamb. Quantum theory of an optical maser. III. Theory of photoelectron counting statistics. *Phys. Rev.*, 179(2):368, 1969.

[83] Albert Einstein. Strahlungs-Emission und ÂŋAbsorption nach der Quantentheorie. *Deutsche Physikalische Gesellschaft*, 18:318–323, 1916.

[84] Paul Adrien Maurice Dirac. The quantum theory of the emission and absorption of radiation. *Proceedings of the Royal Society of London. Series A, Containing Papers of a Mathematical and Physical Character*, 114(767): 243–265, 1927.

[85] E. Wigner. Einige folgerungen aus der schrÃűdingerschen theorie fÃijr die termstrukturen. *Zeitschrift fÃijr Physik*, 43(9-10):624–652, September 1927.

[86] J. R. Oppenheimer. Note on the theory of the interaction of field and matter. *Physical Review*, 35(5):461–477, 1930.

[87] Enrico Fermi. Quantum theory of radiation. *Rev. Mod. Phys.*, 4:87–132, 1932.

[88] F. Bloch and A. Nordsieck. Note on the radiation field of the electron. *Physical Review*, 52(2):54–59, 1937.

[89] V. F. Weisskopf. On the self-energy and the electromagnetic field of the electron. *Physical Review*, 56(1):72–85, 1939.

[90] S. Tomonaga. On a relativistically invariant formulation of the quantum theory of wave fields. *Progress of Theoretical Physics*, 1(2):27–42, 1946.

[91] Julian Schwinger. Quantum electrodynamics. i. a covariant formulation. *Physical Review*, 74(10):1439–1461, 1948.

[92] R. P. Feynman. Space-time approach to quantum electrodynamics. *Physical Review*, 76(6):769–789, 1949.

[93] Daniel A. Steck. *Quantum and Atom Optics,*. Available online at http://steck.us/teaching, revision 0.12.3, 25 October 2018.

[94] Marlan O Scully and M Suhail Zubairy. Quantum optics, 1999.

[95] Roy J Glauber. *Quantum theory of optical coherence: selected papers and lectures.* John Wiley & Sons, 2007.

[96] Roy J Glauber. Coherent and incoherent states of the radiation field. *Physical Review*, 131(6):2766, 1963.

[97] R. Hanbury Brown and R. Q. Twiss. A test of a new type of stellar interferometer on sirius. *Nature*, 178(4541):1046–1048, 1956.

[98] L. Mandel. Fluctuations of photon beams: The distribution of the photo-electrons. *Proceedings of the Physical Society*, 74(3):233–243, 1959.

[99] Bernard Yurke and John S. Denker. Quantum network theory. *Phys. Rev. A*, 29(3):1419, 1984.

[100] M. Ueda. Probability-density-functional description of quantum photodetection processes. *Quantum Opt.: J. Eur. Opt. Soc. B*, 1:131, 01 1999.

[101] D. I. Schuster, Andreas Wallraff, Alexandre Blais, L. Frunzio, R.-S. Huang, J. Majer, S. M. Girvin, Schoelkopf, and RJ. ac Stark shift and dephasing of a superconducting qubit strongly coupled to a cavity field. *Phys. Rev. Lett.*, 94 (12):123602, 2005.

[102] Aashish A Clerk, Michel H Devoret, Steven M Girvin, Florian Marquardt, and Robert J Schoelkopf. Introduction to quantum noise, measurement, and amplification. *Rev. Mod. Phys.*, 82(2):1155, 2010.

[103] L. Mandel and E. Wolf. *Optical Coherence and Quantum Optics.* Cambridge University Press, 2nd edition, 1995. ISBN 0521417112.

[104] Howard J Carmichael. *Statistical methods in quantum optics 2: Non-classical fields.* Springer Science & Business Media, 2009.

[105] U Gavish, B Yurke, and Y Imry. Generalized constraints on quantum amplification. *Physical review letters*, 93(25):250601, 2004.

[106] E.T. Jaynes and F.W. Cummings. Comparison of quantum and semiclassical radiation theories with application to the beam maser. *Proceedings of the IEEE*, 51(1):89–109, 1963.

[107] Robin L Hudson and Kalyanapuram R Parthasarathy. Quantum ito's formula and stochastic evolutions. *Communications in mathematical physics*, 93(3): 301–323, 1984.

[108] MD Srinivas. Quantum theory of continuous measurements. In *Quantum Probability and Applications to the Quantum Theory of Irreversible Processes*, pages 356–364. Springer, 1984.

[109] Ben Q Baragiola, Robert L Cook, Agata M Brańczyk, and Joshua Combes. N-photon wave packets interacting with an arbitrary quantum system. *Physical Review A*, 86(1):013811, 2012.

[110] Wilhelm von Waldenfels. Ito solution of the linear quantum stochastic differential equation describing light emission and absorption. In *Quantum probability and applications to the quantum theory of irreversible processes*, pages 384–411. Springer, 1984.

[111] Martin B Plenio and Peter L Knight. The quantum-jump approach to dissipative dynamics in quantum optics. *Reviews of Modern Physics*, 70(1): 101, 1998.

[112] Howard M Wiseman and Gerard J Milburn. *Quantum measurement and control*. Cambridge university press, 2009.

[113] Klaus M Gheri, Klaus Ellinger, Thomas Pellizzari, and Peter Zoller. Photon-wavepackets as flying quantum bits. *Fortschritte der Physik: Progress of Physics*, 46(4-5):401–415, 1998.

[114] Alexander Holm Kiilerich and Klaus Mølmer. Input-output theory with quantum pulses. *Phys. Rev. Lett.*, 123(12):123604, 2019.

[115] Alexander Holm Kiilerich and Klaus Mølmer. Quantum interactions with pulses of radiation. *Physical Review A*, 102(2):023717, 2020.

[116] C W Gardiner. Driving a quantum system with the output field from another driven quantum system. *Phys. Rev. Lett.*, 70(15):2269, 1993.

[117] Crispin W Gardiner and MJ Collett. Input and output in damped quantum systems: Quantum stochastic differential equations and the master equation. *Phys. Rev. A*, 31(6):3761, 1985.

[118] Bernard Yurke, Samuel L McCall, and John R Klauder. Su (2) and su (1, 1) interferometers. *Physical Review A*, 33(6):4033, 1986.

[119] Carlton M Caves. Reframing su (1, 1) interferometry. *Advanced Quantum Technologies*, 3(11):1900138, 2020.

[120] Norman F Ramsey. A molecular beam resonance method with separated oscillating fields. *Physical Review*, 78(6):695, 1950.

[121] Andy Chia, Michal Hajdušek, R Nair, Rosario Fazio, Leong Chuan Kwek, and Vlatko Vedral. Phase-preserving linear amplifiers not simulable by the parametric amplifier. *Physical Review Letters*, 125(16):163603, 2020.

[122] Jeffrey M Epstein, K Birgitta Whaley, and Joshua Combes. Quantum limits on noise for a class of nonlinear amplifiers. *Physical Review A*, 103(5):052415, 2021.

[123] Jonathan Kohler, Justin A Gerber, Emma Deist, and Dan M Stamper-Kurn. Simultaneous retrodiction of multimode optomechanical systems using matched filters. *Physical Review A*, 101(2):023804, 2020.

[124] Christian F Roos. Ion trap quantum gates with amplitude-modulated laser beams. *New Journal of Physics*, 10(1):013002, 2008.

[125] Serge Haroche and J-M Raimond. *Exploring the quantum: atoms, cavities, and photons*. Oxford university press, 2006.

[126] Claude Cohen-Tannoudji, Jacques Dupont-Roc, and Gilbert Grynberg. *Photons and Atoms-Introduction to Quantum Electrodynamics*. 1997.

[127] Claude Fabre and Nicolas Treps. Modes and states in quantum optics. *Reviews of Modern Physics*, 92(3):035005, 2020.

[128] UM Titulaer and RJ Glauber. Density operators for coherent fields. *Physical Review*, 145(4):1041, 1966.

[129] Benjamin Brecht, Dileep V Reddy, Christine Silberhorn, and Michael G Raymer. Photon temporal modes: a complete framework for quantum information science. *Physical Review X*, 5(4):041017, 2015.

[130] Michael G Raymer and Ian A Walmsley. Temporal modes in quantum optics: then and now. *Physica Scripta*, 95(6):064002, 2020.

[131] Li-Ping Yang and Zubin Jacob. Quantum structured light: Non-classical spin texture of twisted single-photon pulses. *arXiv preprint arXiv:2102.13248*, 2021.

[132] Dietrich Leibfried, Rainer Blatt, Christopher Monroe, and David Wineland. Quantum dynamics of single trapped ions. *Reviews of Modern Physics*, 75(1): 281, 2003.

[133] O Castaños, S Cordero, R López-Peña, and E Nahmad-Achar. Single and collective regimes in three-level systems interacting with a one-mode electromagnetic field. In *Journal of Physics: Conference Series*, volume 512, page 012006. IOP Publishing, 2014.

[134] Stephen Barnett and Paul M Radmore. *Methods in theoretical quantum optics*, volume 15. Oxford University Press, 2002.

[135] Andrzej Veitia and Steven J van Enk. Testing the context-independence of quantum gates. *arXiv preprint arXiv:1810.05945*, 2018.

[136] Jay Gambetta, Alexandre Blais, David I Schuster, Andreas Wallraff, L Frunzio, J Majer, Michel H Devoret, Steven M Girvin, and Robert J Schoelkopf. Qubit-photon interactions in a cavity: Measurement-induced dephasing and number splitting. *Physical Review A*, 74(4):042318, 2006.

[137] Crispin W Gardiner. Quantum noise. *Springer series in synergetics*, 1991.

[138] Yimin Wang, Jiří Minář, Lana Sheridan, and Valerio Scarani. Efficient excitation of a two-level atom by a single photon in a propagating mode. *Physical Review A*, 83(6):063842, 2011.

[139] Alexey V Gorshkov, Axel André, Michael Fleischhauer, Anders S Sørensen, and Mikhail D Lukin. Universal approach to optimal photon storage in atomic media. *Physical review letters*, 98(12):123601, 2007.

[140] Joel KW Yang, Andrew J Kerman, Eric A Dauler, Vikas Anant, Kristine M Rosfjord, and Karl K Berggren. Modeling the electrical and thermal response of superconducting nanowire single-photon detectors. *IEEE transactions on applied superconductivity*, 17(2):581–585, 2007.

[141] JJ Renema, R Gaudio, Q Wang, Z Zhou, A Gaggero, F Mattioli, R Leoni, D Sahin, MJA De Dood, A Fiore, et al. Experimental test of theories of the detection mechanism in a nanowire superconducting single photon detector. *Phys. Rev. Lett.*, 112(11):117604, 2014.

[142] S Frasca, B Korzh, M Colangelo, D Zhu, AE Lita, JP Allmaras, EE Wollman, VB Verma, AE Dane, E Ramirez, et al. Determining the depairing current in superconducting nanowire single-photon detectors. *Phys. Rev. B*, 100(5): 054520, 2019.

[143] Carlton M Caves. Quantum limits on noise in linear amplifiers. *Phys. Rev. D*, 26(8):1817, 1982.

[144] John E Hall. *Guyton and Hall textbook of medical physiology e-Book*. Elsevier Health Sciences, 2010.

[145] Xinjian Zhou, Thomas Zifer, Bryan M Wong, Karen L Krafcik, François Léonard, and Andrew L Vance. Color detection using chromophore-nanotube hybrid devices. *Nano letters*, 9(3):1028–1033, 2009.

[146] Warren Nagourney, Jon Sandberg, and Hans Dehmelt. Shelved optical electron amplifier: Observation of quantum jumps. *Phys. Rev. Lett.*, 56(26): 2797, 1986.

[147] Howard J Carmichael. *Statistical methods in quantum optics 1: master equations and Fokker-Planck equations*. Springer Science & Business Media, 2013.

[148] F Dimer, B Estienne, AS Parkins, and HJ Carmichael. Proposed realization of the dicke-model quantum phase transition in an optical cavity qed system. *Phys. Rev. A*, 75(1):013804, 2007.

[149] Eric M Kessler, Geza Giedke, Atac Imamoglu, Susanne F Yelin, Mikhail D Lukin, and J Ignacio Cirac. Dissipative phase transition in a central spin system. *Phys. Rev. A*, 86(1):012116, 2012.

[150] HJ Carmichael. Breakdown of photon blockade: A dissipative quantum phase transition in zero dimensions. *Phys. Rev. X*, 5(3):031028, 2015.

[151] Johannes M Fink, András Dombi, András Vukics, Andreas Wallraff, and Peter Domokos. Observation of the photon-blockade breakdown phase transition. *Phys. Rev. X*, 7(1):011012, 2017.

[152] MJ Fitch, BC Jacobs, TB Pittman, and JD Franson. Photon-number resolution using time-multiplexed single-photon detectors. *Physical Review A*, 68(4):043814, 2003.

[153] Danna Rosenberg, Adriana E Lita, Aaron J Miller, and Sae Woo Nam. Noise-free high-efficiency photon-number-resolving detectors. *Physical Review A*, 71(6):061803, 2005.

[154] Maria Goppert-Mayer. Uber elementarakte mit zwei quantensprungen. *Ann. Phys.*, 9:273–295, 1931.

[155] Maria Göppert-Mayer. Elementary processes with two quantum transitions. *Annalen der Physik*, 18(7-8):466–479, 2009.

[156] Hong-Bing Fei, Bradley M Jost, Sandu Popescu, Bahaa EA Saleh, and Malvin C Teich. Entanglement-induced two-photon transparency. *Physical review letters*, 78(9):1679, 1997.

[157] Michael G Raymer, Tiemo Landes, Markus Allgaier, Sofiane Merkouche, Brian J Smith, and Andrew H Marcus. How large is the quantum enhancement of two-photon absorption by time-frequency entanglement of photon pairs? *Optica*, 8(5):757–758, 2021.

[158] Dmitry Tabakaev, Matteo Montagnese, Geraldine Haack, Luigi Bonacina, J-P Wolf, Hugo Zbinden, and RT Thew. Energy-time-entangled two-photon molecular absorption. *Physical Review A*, 103(3):033701, 2021.

[159] Haruhisa Okawa and Alapakkam P Sampath. Optimization of single-photon response transmission at the rod-to-rod bipolar synapse. *Physiology*, 22(4): 279–286, 2007.

[160] Pablo Artal, Silvestre Manzanera, Katarzyna Komar, Adrián Gambín-Regadera, and Maciej Wojtkowski. Visual acuity in two-photon infrared vision. *Optica*, 4(12):1488–1491, 2017.

[161] Yoichi Kobayashi, Katsuya Mutoh, and Jiro Abe. Stepwise two-photon absorption processes utilizing photochromic reactions. *Journal of Photochemistry and Photobiology C: Photochemistry Reviews*, 34:2–28, 2018.

[162] John E Hall and Michael E Hall. *Guyton and Hall textbook of medical physiology e-Book*. Elsevier Health Sciences, 2020.

[163] Herman CH Chan, Omar E Gamel, Graham R Fleming, and K Birgitta Whaley. Single-photon absorption by single photosynthetic light-harvesting complexes. *Journal of Physics B: Atomic, Molecular and Optical Physics*, 51 (5):054002, 2018.

[164] Tao Shi, Darrick E Chang, and J Ignacio Cirac. Multiphoton-scattering theory and generalized master equations. *Physical Review A*, 92(5):053834, 2015.

[165] Anders Nysteen, Philip Trøst Kristensen, Dara PS McCutcheon, Per Kaer, and Jesper Mørk. Scattering of two photons on a quantum emitter in a one-dimensional waveguide: exact dynamics and induced correlations. *New Journal of Physics*, 17(2):023030, 2015.

[166] Yu Pan, Daoyi Dong, and Guofeng Zhang. Exact analysis of the response of quantum systems to two-photons using a qsde approach. *New Journal of Physics*, 18(3):033004, 2016.

[167] Ben Q Baragiola and Joshua Combes. Quantum trajectories for propagating fock states. *Physical Review A*, 96(2):023819, 2017.

[168] William Konyk and Julio Gea-Banacloche. One-and two-photon scattering by two atoms in a waveguide. *Physical Review A*, 96(6):063826, 2017.

[169] Hemlin Swaran Rag and Julio Gea-Banacloche. Two-level-atom excitation probability for single-and n-photon wave packets. *Physical Review A*, 96(3): 033817, 2017.

[170] Anita Dąbrowska, Gniewomir Sarbicki, and Dariusz Chruściński. Quantum trajectories for a system interacting with environment in n-photon state. *Journal of Physics A: Mathematical and Theoretical*, 52(10):105303, 2019.

[171] BR Mollow. Pure-state analysis of resonant light scattering: Radiative damping, saturation, and multiphoton effects. *Physical Review A*, 12(5):1919, 1975.

[172] Alexandre Roulet and Valerio Scarani. Solving the scattering of n photons on a two-level atom without computation. *New Journal of Physics*, 18(9): 093035, 2016.

[173] Philipp Müller, Tristan Tentrup, Marc Bienert, Giovanna Morigi, and Jürgen Eschner. Spectral properties of single photons from quantum emitters. *Physical Review A*, 96(2):023861, 2017.

[174] Magdalena Stobińska, Gernot Alber, and Gerd Leuchs. Perfect excitation of a matter qubit by a single photon in free space. *EPL (Europhysics Letters)*, 86 (1):14007, 2009.

[175] Michael G Raymer, Dileep V Reddy, Steven J van Enk, and Colin J McKinstrie. Time reversal of arbitrary photonic temporal modes via nonlinear optical frequency conversion. *New Journal of Physics*, 20(5): 053027, 2018.

[176] Luigi Giannelli, Tom Schmit, Tommaso Calarco, Christiane P Koch, Stephan Ritter, and Giovanna Morigi. Optimal storage of a single photon by a single intra-cavity atom. *New Journal of Physics*, 20(10):105009, 2018.

[177] Granade, Christopher E. *Characterization, Veriﬁᾰᾳcation and Control for Large Quantum Systems*. PhD thesis, 2015. URL `http://hdl.handle.net/10012/9217`.

[178] Gábor Horváth, Amit Lerner, and Nadav Shashar. *Polarized light and polarization vision in animal sciences*, volume 2. Springer, 2014.

[179] CA Schrama, G Nienhuis, HA Dijkerman, C Steijsiger, and HGM Heideman. Destructive interference between opposite time orders of photon emission. *Physical review letters*, 67(18):2443, 1991.

[180] U Haeberlen and JS Waugh. Coherent averaging effects in magnetic resonance. *Physical Review*, 175(2):453, 1968.

[181] Wilhelm Magnus. On the exponential solution of differential equations for a linear operator. *Communications on pure and applied mathematics*, 7(4): 649–673, 1954.

[182] Razieh Annabestani. Collective dynamics in nmr and quantum noise. 2016.

[183] Crispin Gardiner, Peter Zoller, and Peter Zoller. *Quantum noise: a handbook of Markovian and non-Markovian quantum stochastic methods with applications to quantum optics*. Springer Science & Business Media, 2004.

[184] Philip Daniel Blocher, Serwan Asaad, Vincent Mourik, Mark AI Johnson, Andrea Morello, and Klaus Mølmer. Measuring out-of-time-ordered correlation functions without reversing time evolution. *arXiv preprint arXiv:2003.03980*, 2020.

[185] Nathan Wiebe and Shuchen Zhu. A theory of trotter error. *Physical Review X*, 11(011020):26, 2021.

[186] Richard A Brualdi and Dragos Cvetkovic. *A combinatorial approach to matrix theory and its applications*. CRC press, 2008.

[187] J Robert Johansson, Paul D Nation, and Franco Nori. Qutip: An open-source python framework for the dynamics of open quantum systems. *Computer Physics Communications*, 183(8):1760–1772, 2012.

[188] Joni Ikonen, Jan Goetz, Jesper Ilves, Aarne Keränen, Andras M Gunyho, Matti Partanen, Kuan Y Tan, Dibyendu Hazra, Leif Grönberg, Visa Vesterinen, et al. Qubit measurement by multichannel driving. *Physical review letters*, 122(8):080503, 2019.

[189] Nicolas Didier, Jérôme Bourassa, and Alexandre Blais. Fast quantum nondemolition readout by parametric modulation of longitudinal qubit-oscillator interaction. *Physical review letters*, 115(20):203601, 2015.

[190] S Touzard, A Kou, NE Frattini, VV Sivak, S Puri, A Grimm, L Frunzio, S Shankar, and MH Devoret. Gated conditional displacement readout of superconducting qubits. *Physical review letters*, 122(8):080502, 2019.

[191] Michael J Kastoryano and Mark S Rudner. Topological transport in the steady state of a quantum particle with dissipation. *Physical Review B*, 99 (12):125118, 2019.

[192] Toni L Heugel, Matteo Biondi, Oded Zilberberg, and R Chitra. Quantum transducer using a parametric driven-dissipative phase transition. *Physical review letters*, 123(17):173601, 2019.

[193] Fabrizio Minganti, Nicola Bartolo, Jared Lolli, Wim Casteels, and Cristiano Ciuti. Exact results for schrödinger cats in driven-dissipative systems and their feedback control. *Scientific reports*, 6(1):1–8, 2016.

[194] Wim Casteels, Rosario Fazio, and Christiano Ciuti. Critical dynamical properties of a first-order dissipative phase transition. *Physical Review A*, 95 (1):012128, 2017.

[195] Paolo Zanardi, Matteo GA Paris, and Lorenzo Campos Venuti. Quantum criticality as a resource for quantum estimation. *Physical Review A*, 78(4): 042105, 2008.

[196] Katarzyna Macieszczak, Mădălin Guţă, Igor Lesanovsky, and Juan P Garrahan. Dynamical phase transitions as a resource for quantum enhanced metrology. *Physical Review A*, 93(2):022103, 2016.

[197] Andrei B Klimov and Sergei M Chumakov. *A group-theoretical approach to quantum optics: models of atom-field interactions*. John Wiley & Sons, 2009.

[198] Nathan Shammah, Shahnawaz Ahmed, Neill Lambert, Simone De Liberato, and Franco Nori. Open quantum systems with local and collective incoherent processes: Efficient numerical simulations using permutational invariance. *Physical Review A*, 98(6):063815, 2018.

[199] Stuart J Masson and Scott Parkins. Extreme spin squeezing in the steady state of a generalized dicke model. *Physical Review A*, 99(2):023822, 2019.

[200] Wojciech Hubert Zurek. Quantum darwinism. *Nature physics*, 5(3):181–188, 2009.

[201] Amplification and measurement code repository. URL
https://github.com/sbisw002/Amplification-and-Measurement.